CR 62060

A STUDY OF DYNAMICS OF MAGMA EXTRUSION AND INVESTIGATION OF VOLCANIC VAPOR

report to

NASA MANNED SPACECRAFT CENTER
ADVANCED SPACECRAFT TECHNOLOGY DIVISION
HOUSTON, TEXAS 77058

CONTRACT NAS9-5839

GPO PRICE $ _____

CFSTI PRICE(S) $ _____

Hard copy (HC) 3.00

Microfiche (MF) .65

ff 653 July 65

Arthur D. Little, Inc.

A STUDY OF DYNAMICS OF MAGMA EXTRUSION AND INVESTIGATION OF VOLCANIC VAPOR

Final Report To

NASA Manned Spacecraft Center
Advanced Spacecraft Technology Division
Houston, Texas 77058
Attention: David S. McKay/ET33
Contract No.NAS9-5839

Prepared By

Arthur D. Little, Inc.
15 Acorn Park
Cambridge, Massachusetts

Robert K. McConnell, Jr. Leslie A. McClaine Ronald V. Allen

C-68231

July 1967

ABSTRACT

The work done under Contract NAS9-5839, which is described in this report, represents a continuation of the program to develop a quantitative model for igneous activity which is consistent with terrestrial observations and which is suitable for extrapolation to the moon. This study was initiated under contract NAS9-3449 and much of the earlier work has been reported by McConnell, et al. (1967).

In this report the heat flow model is revised to incorporate and to obtain consistency with the information relating to continental drift, terrestrial heat flow, and crustal and mantle structure. The implications of this model for mantle composition are considered.

Much of the available geochemical data for tholeiitic magmas is reviewed and a hypothesis consistent with the data is developed which interprets the observed terrestrial variations in magma composition in terms of the depth of origin of the magma. Implications of this hypothesis relating to the composition of the earth's mantle are discussed.

It is concluded that if the moon has the same composition as the one inferred for the earth's mantle, early volcanism is almost inevitable. In this case the primary melts are predicted to be similar to submarine basalts or basaltic achondrites. On the other hand, if recent lunar volcanism can be demonstrated, it would seem to imply that the composition of the moon is different from that of the earth's mantle. Some implications of these differences are discussed.

Data gathered to date for use in development of a quantitative model for magma approaching the surface is presented. Included are the results of literature reviews and experimental studies on gases dissolved in magmas, the volatility of basalt, and "smoke" particles derived from condensation of volcanic vapors.

Progress to date on magma chamber mechanics and the mobilization of ash flows is discussed. The report is concluded with a preliminary presentation of the implications of the findings for lunar exploration efforts and with suggestions for further work.

TABLE OF CONTENTS

TABLE OF CONTENTS (Cont.)

TABLE OF CONTENTS (Cont.)

LIST OF FIGURES

LIST OF FIGURES (Cont.)

LIST OF FIGURES (Cont.)

LIST OF TABLES

LIST OF TABLES (Cont.)

I. INTRODUCTION

As a result of our studies under the previous contract (NAS9-3449), "The Effect of the Lunar Environment on Magma Generation, Migration, and Crystallization," we concluded that, if radiative thermal conductivity was not excessive, most reasonable theoretical models of the moon's composition require a period of intense volcanic activity with sudden onset and approximately exponential decline. On the basis of the melting behavior of a basalt-dunite mixture, we proposed a mechanism for sudden generation of magma and discussed the factors controlling the migration of this magma through a dike, formation of magma chambers, and the deposition of volatile species on the moon's surface. In conclusion, we recommended that the most critical areas where further work was required to insure productive lunar exploration were: determination of the radiative component of thermal conductivity for model rock types at high temperatures; experimental and theoretical studies to determine the interaction of volatiles of the melt, with particular emphasis on the rheological properties; and theoretical study of the dynamics of eruption using experimental data on the behavior of the volatiles. We also pointed out the importance of further experimental work on direct determinations of the melting relationships of basalt and dunite mixtures as a function of pressure.

Under contract NAS9-3840 we undertook to measure radiative conductivity at high temperatures. The report of that work, including a description of the apparatus, the results of preliminary measurements, and recommendations for the required further work has already been submitted. In this report we describe our progress in the study of the dynamics of magma extrusion and the investigations of volcanic vapors.

Our initial efforts under the present contract (NAS9-5839) to study extrusion mechanics seemed to indicate that the problems of mechanics were somehow very closely related to the composition of the primary melt. This of course has been known to volcanologists for a long time; however, we were surprised by the extent to which minor compositional differences between magmas apparently corresponded to differences in surface behavior.

Rather than simply assume the qualitative relationship "more acidic volcanos behave more explosively than more basic volcanos" and then try to rationalize observations of surface behavior on this assumption, it seemed to us that a more profitable way to attack the problem would be to continue the approach of the previous study which has proven so successful. We therefore first attempted to determine which observed differences could be explained by partial melting of "pyrolite" under different conditions of pressure and temperature and which would require a source of different compositions. We believed that once compositional differences could be related to source conditions it would be much easier to predict the type of behavior to be expected under lunar conditions.

In order to gain the necessary understanding of the compositional differences which seems to be so strongly related to the extrusion mechanics, we studied the generation of magmas from two different points of view. On the one hand we sought to interpret the existing evidence for conditions of generation of basaltic magmas from measurements of terrestrial heat flow, structure, seismic evidence for crustal and upper mantle structure, and viscosity considerations. Simultaneously, we examined the data on major and trace element compositional differences between the various types of magmas in an attempt to relate them to melting behavior and to partition coefficients of the various elements.

As a result of this phase of the study we came to the following conclusions:

1. Modified chondritic ratios of the elements may be more consistent with upper mantle and lunar compostion than "terrestrial ratios."

2. The pressure at which magma is generated can be estimated from the chemical composition of the melt. We believe that lunar primary basalts are more likely to resemble "submarine" type basalts, which we believe originate at a depth of about 100 km rather than Hawaiian basalts which originate somewhat shallower if the source compositions are the same.

3. We believe most terrestrial andesites and more acidic magmas are derived from remelting of basalt or other crustal materials and hence are not likely to occur on the moon.

4. The only acid melts we expect will be found on the moon will represent the final fraction of liquid remaining after the crystallization of a basaltic magma.

5. The equilibrium heat flow from the moon may be somewhat different than calculated using our original model or the models employed by most other people who have investigated the moon's thermal history. We first interpreted this as being consistent both with the Shoemaker's interpretations that lunar crater counts imply very recent volcanism and with our own measurements which indicate that radiative transfer may not be as important as previously expected.

6. We now believe that if lunar volcanism is continuing to the present day it will imply a lunar composition different from that of the earth's mantle.

In our previous report the importance of the volatile species in the melt was emphasized. Their influence in controlling the viscosity of the melt has long been known and the viscosity in turn controls the manner in which magmas move when they near the surface. In addition, volcanic vapors provide an energy source for many types of eruptive activity, and hence it is important to know the amount present at any time in order to calculate the subsequent behavior of a magma chamber. Volatiles have also been postulated as the agents for mobilizing terrestrial ash flows, and although in this report we indicate that other mechanisms may also be important, they can be the only significant factor if ash flows are to exist on the moon. Volatile species liberated by subsurface melts provide a method for strong upward fractionation of a number of elements and in the previous report we postulated that condensation of these vapors on the lunar surface might contribute to the formation of a fine particulate veneer. If the chemical characteristics of this fine material are sufficiently different from fragmented rocks they could provide a diagnostic test for the presence of volcanic activity.

For a number of reasons including the above, an investigation of volcanic vapor was considered to be one of the major purposes of this investigation. Our studies were concentrated along two lines: experimental measurements of vaporization from basaltic magmas and detailed examination of smokes and particulate matter collected in the Surtsey area. Both of these studies confirmed the importance of vaporization phenomena. The experimental studies indicated that 90% or greater of the material condensed from basaltic vapors is Na_2O with small quantities of silicon, aluminum, and barium also present. Analyses of the smokes collected from Surtsey confirmed that they could only result from condensation of vapors and provided evidence that the vaporization process also provides a mechanism for concentration of nickel and chromium.

Our studies of magma extrusion included both theoretical and experimental modeling. To examine some limiting conditions for explosive eruptions, we restricted our models to simple ones which included only gas phases in the chamber; nevertheless, we believe we have demonstrated to our satisfaction that violent explosive eruptions can only take place once cones and/or craters have developed. To extend these models to more detailed analyses of eruptive activity, one must consider the distribution of volatiles between the vapor and the melt and the rate at which equilibrium can be re-established after each eruption. With the data now available on vaporization phenomena, it should be possible to make the necessary extension to include realistic mixtures of vapor and melt. If the eruption characteristics remain consistent with terrestrial observations, then it seems reasonable to expect that lunar volcanics can be used to infer the nature of subsurface magma chambers there. We also carried out a number of experiments on gelatin models in an attempt to confirm the necessity of doubling the pressure before eruption takes place. While these experiments showed the necessity for a pressure increase, difficulties associated with the presence of stress concentrators resulting from the emplacement of the chamber made it difficult to assess the exact amount necessary. In addition to their value as a test for pressure doubling hypothesis, the experiments using gelatin have provided a great deal of insight into the events taking place beneath a volcano. Among our conclusions from this work are:

1. Tabular dikes are formed as a result of an initial fracture where no opening to the surface is available.

2. The length of the dike is usually comparable to the depth from the source.

3. Initial eruptions from a dike will take place along a long fissure; however, once free access to the surface is gained, eruption sites will be concentrated along low impedence channels, and only a limited number will persist.

4. The direction of dikes is very strongly controlled by anisotropic elastic properties or pre-existing stress conditions and hence alignment of eruption fissures as a result of tectonic stresses is to be expected.

All of the above conclusions from the work on gelatin models would seem to be in accordance with observations of actual volcanic activity.

Because of the great deal of interest which has been paid recently to the possible presence of ash flows on the surface of the moon, we devoted a great deal of attention to trying to understand their mechanics. We were particularly troubled by a number of observations of thin, high velocity flows, which seemed to be inconsistent with mobilization completely controlled by fluidization processes. We therefore examined several different hypotheses such as the effect of very small particle size in an attempt to remove some of the inconsistencies. While this latter effect at first seemed promising it required the presence of more very fine particles than observed. Finally we came to the conclusion that some of the discrepancies can be eliminated by postulating that thin high velocity terrestrial ash flows are levitated as a result of aerodynamic lift developed over the front of the flow. This mechanism of mobilization of course would not take place on the moon.

Although it has not been possible within the scope of the present year's work to fit all of the aspects of magma extrusion into a coherent pattern, it is clear that the evidence for such a pattern is now emerging

and that continuation of a present line of approach should make it possible to infer a great deal more quantitative information about igneous activity than has been previously available from the surface products. Even from our current knowledge we can make a few predictions.

Eruption is as much a function of the size, shape and depth of burial of the chamber as it is of the viscosity of the magma. Small gas-rich chambers at relatively shallow depths are the only kind that can erupt explosively.

Condensed vapor species of diagnostic compositions are an important constituent of terrestrial volcanic smokes. Even when intermixed with lunar rock fragments derived from other sources the two types of material may be distinguishable.

The length of fissures from which melt is emitted provides an indication of the depth to the chamber. Periodicity of eruptions can be predicted in some and perhaps many classes of eruptions.

II. REVISION OF HEAT FLOW MODEL

The model for the composition and radioactive heat sources in the previous report was derived under the assumption that there is no convective movement in the earth's mantle. As the evidence for highly developed near-surface movement of the earth's crust and mantle is becoming overwhelming, we have attempted to see whether any significant change in the original compositional model would be necessary.

A. MODEL

As a start we considered the simple model shown in Figure II-1 which divides the earth into three portions, an inner rigid lower mantle, a soft deformable upper mantle or asthenosphere of uniform viscosity and a rigid "crust" or lithosphere. If we let the thickness of the oceanic and continental lithosphere be h_{ol} and h_{cl}, respectively, and the thickness of the oceanic and continental asthenosphere be h_{oa} and h_{ca}, respectively, then for isostatic equilibrium to prevail

$$\rho_{ol}\, h_{ol} + \rho_{oa}\, h_{oa} = \rho_{cl}\, h_{cl} + \rho_{ca}\, h_{ca} \qquad \text{(II-1)}$$

We then assume that:

1. Except at the mid-Atlantic ridge the entire crust and mantle are moving with a velocity v_c towards the west.

2. The chemical composition of the deep mantle is similar to that of the upper mantle.

3. A heat flow of Q_{om} watts/cm^2 °C is flowing from the deep mantle into the upper mantle.

4. No material transport is taking place across this boundary.

5. The earth's departure from isostatic equilibrium is not increasing so the mass flow towards the east under the crust must exactly equal the westward flow of the crust.

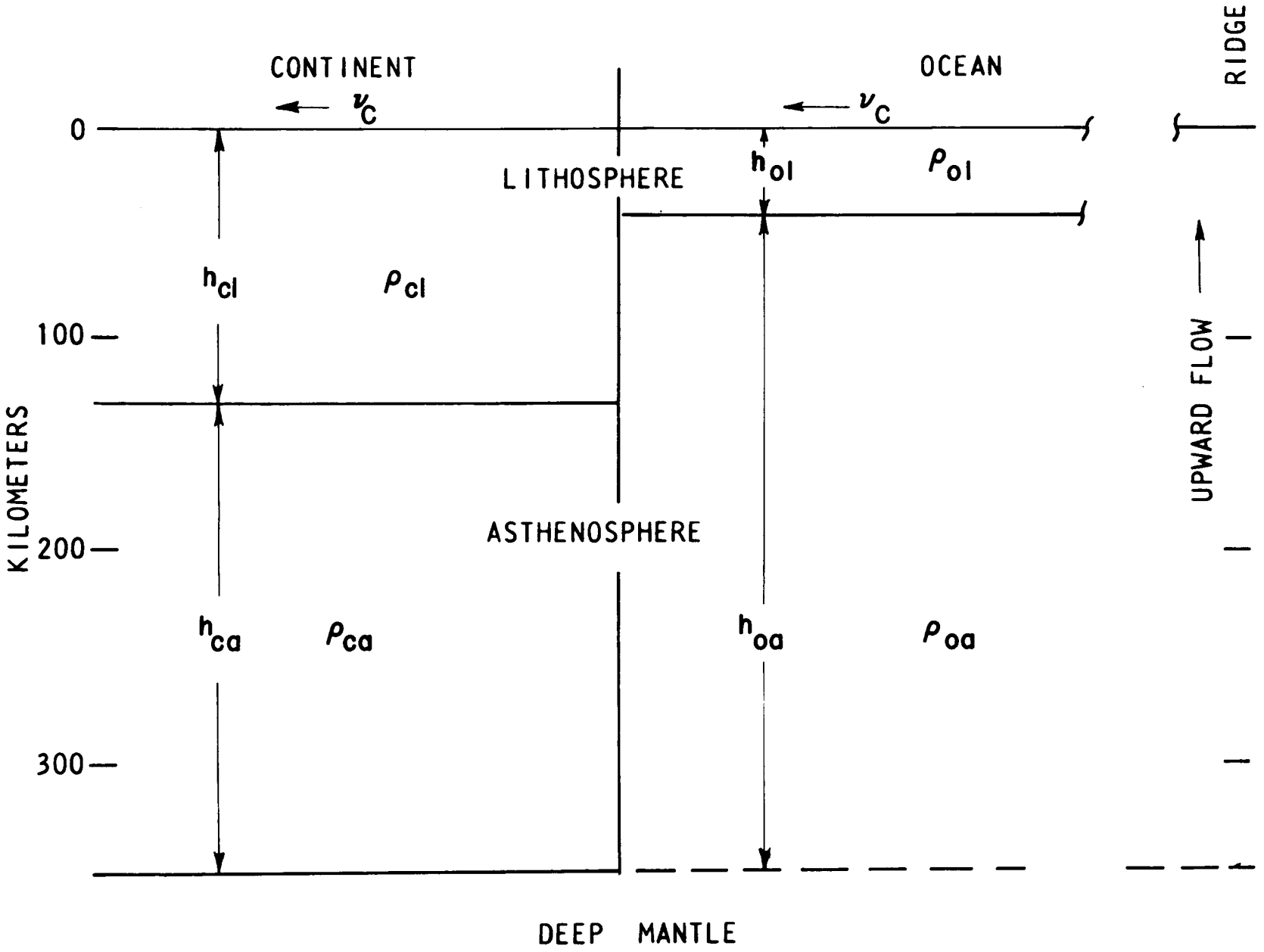

FIGURE II-1 MODEL FOR TERRESTRIAL MANTLE CONVECTION USED FOR HEAT FLOW CALCULATIONS

6. A plane drawn vertically through the crest of the mid-Atlantic ridge is a plane of symmetry near which much of the upward flow is concentrated.

B. CRUSTAL AND MANTLE STRUCTURE

To estimate the material flow pattern we must first obtain an estimate of the thickness of the rigid crustal layer and of the lower mantle layers both under the ocean and under the continents. Our data for this, which comes from seismic evidence, relaxation time, and heat flow data, is summarized for the continental layer and oceanic layers in Figure II-2.

Although the existence of the upper mantle low velocity zone has been known for many years and its possible significance as a site for most deformation in the upper mantle has been suggested by many geophysicists, recent seismic evidence suggests pronounced structural differences may exist between suboceanic and subcontinental mantle (Toksoz, Chinnery, and Anderson, 1967). By analyzing the data from Love and Rayleigh waves over different paths these authors conclude:

1. The model which fits the continental data best would have a region of low shear wave velocity which decreases abruptly between 125 and 140 km and does not increase again until 350 km.

2. Under the ocean a similar layer exists which starts at 40 km, has its lowest velocities between 85 and 125 km and then shows no significant velocity increase until 300 km.

It is important to note that the depth to the top of the region where Toksoz, et al., infer the shear velocity decrease under the shield area coincides very closely with the value of 120 km estimated for the depth to the top of the low viscosity layer under the Fennoscandian shield from postglacial uplift data (McConnell, 1965,1967). We therefore would suggest that, under shield areas at least, the effective top of the deforming layer be taken to lie about 120 km.

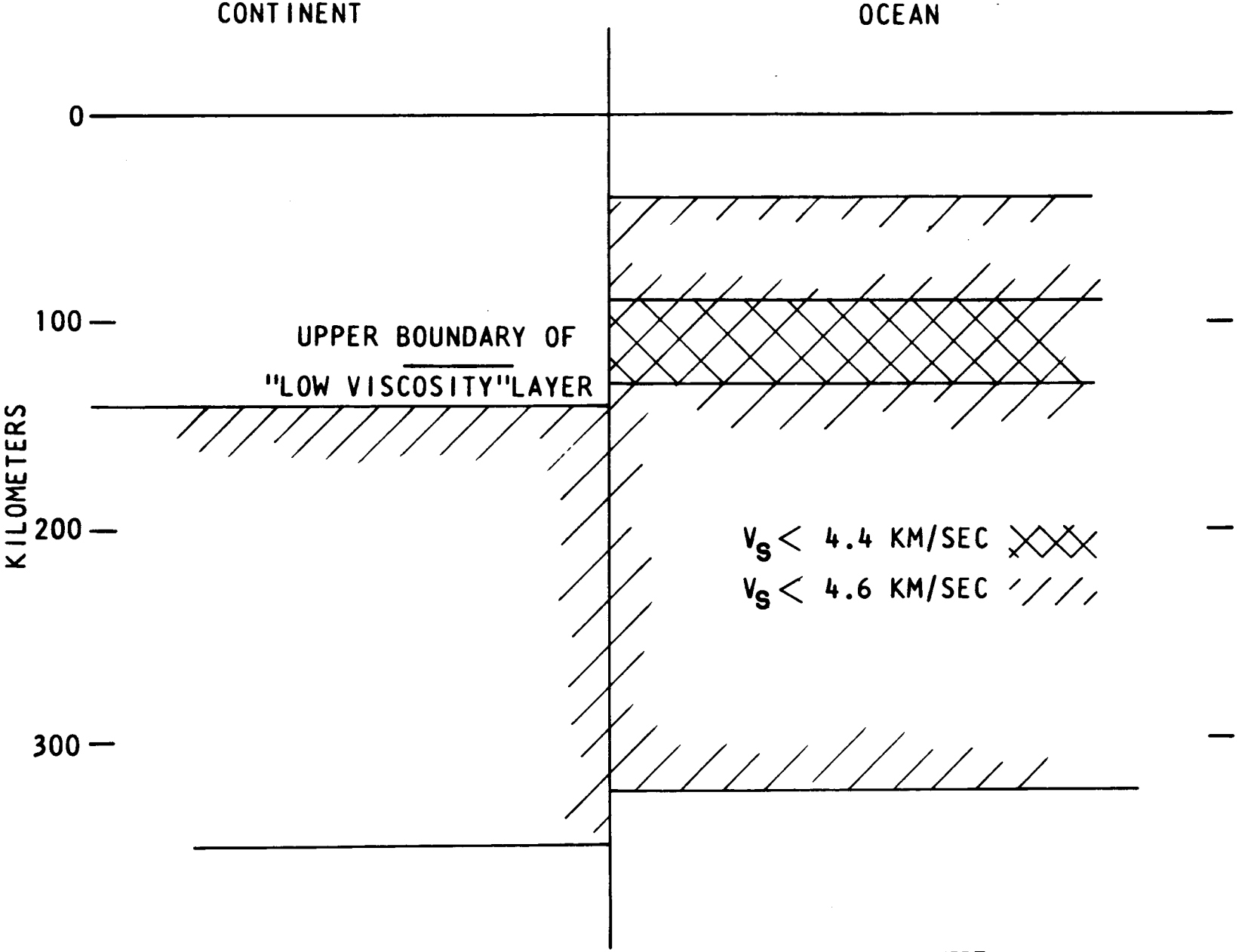

FIGURE II-2 INFERRED BOUNDARIES IN MANTLE COMPARED WITH POSSIBLE SOURCES OF BASALT MAGMAS SUGGESTED IN CHAPTER III

Although no direct evidence on flow properties is yet available under the oceans, if we take the low shear velocity to be a good indicator of low viscosity, we would infer the top of the low viscosity layer to occur near 40 km with the very softest region between 75 and 125 km, and with continued abnormally low viscosity down at least below 300 km.

In principle, heat flow data may also be used to estimate the upper limit of the low viscosity region. When the heat flow, thermal conductivity, and distribution of radioactive heat sources are known, the temperature may be calculated as a function of depth and compared with predicted melting relationships to see when the melting curve is most closely approached. As various estimates of thermal conductivity at appropriate temperatures differ by as much as a factor of 3, and the experimental program to measure conductivities was terminated before we were able to obtain any data on olivines, this approach is not particularly reliable. However, we can show that if the melting temperature is closely approached somewhere between 50 and 100 km, the thermal conductivities deduced from the heat flow data are not in conflict with those observed experimentally.

Figure II-3 shows the estimated solidus temperature of "pyrolite" as a function of depth in the earth as discussed in our previous report. If melts are generated somewhere in the region between 40 and 150 km, this would imply that when the first small fraction of melt forms the average thermal gradient to the depth of melting is between 28°/km and 10°/km. For an average heat flow of 6.3μ watts/cm^2 these values would correspond to thermal conductivities of 2.2×10^{-2} and 6.3×10^{-2} watts/cm °C, respectively. These values are entirely consistent with the lower end of the range normally postulated for mantle rocks at high temperatures.

C. DRIFT RATES

Having established a starting model for the boundaries dividing the soft regions of the mantle from the more rigid portions, we must select appropriate velocities for the current continental drift and ocean floor spreading rates before attempting to estimate the amount of heat which is not related to convection. By examination of the magnetic anomalies,

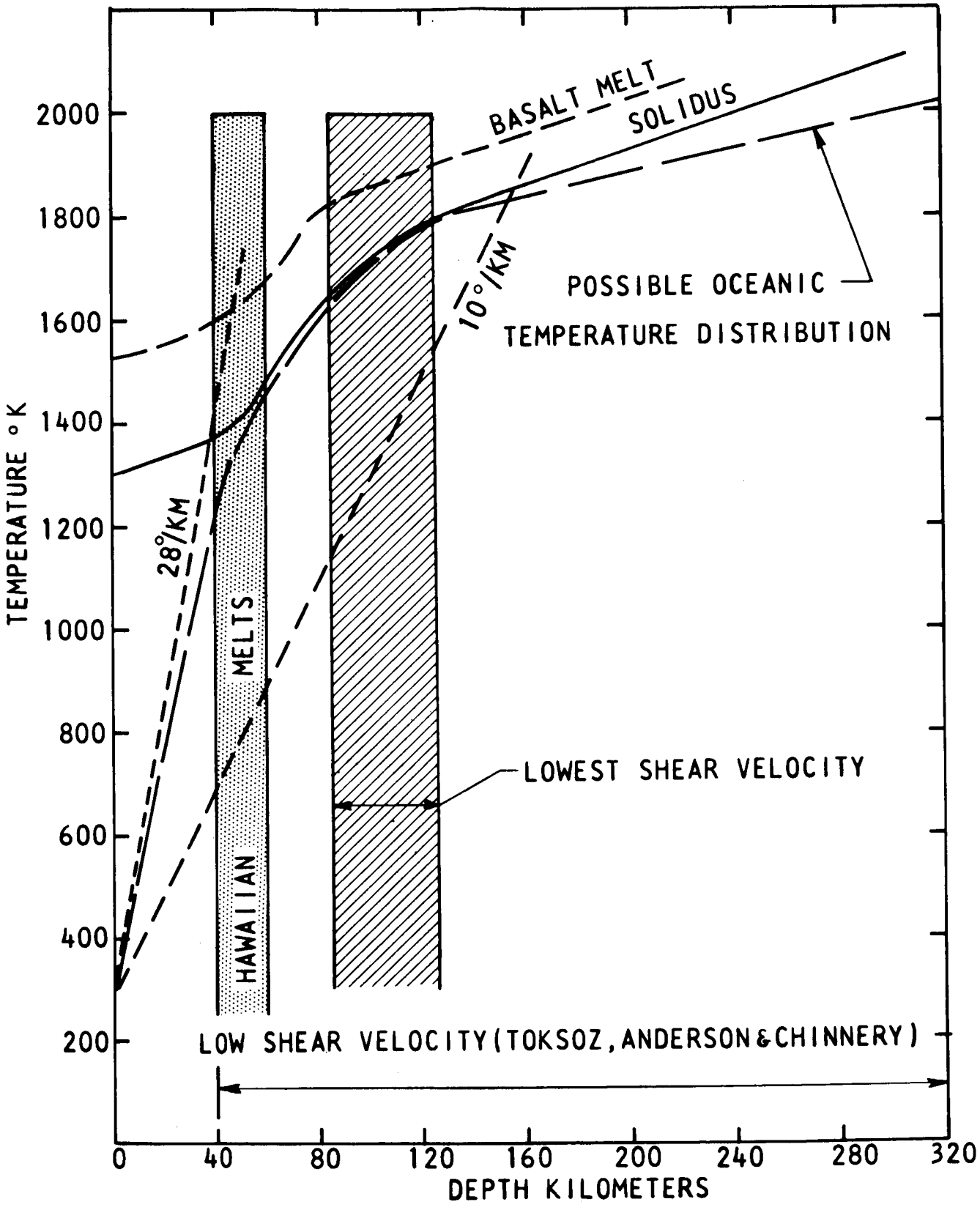

FIGURE II-3 COMPARISON OF HIGH TEMPERATURES AND THERMAL GRADIENTS WITH LOW SHEAR VELOCITY REGIONS IN OCEANIC MANTLE

Vine (1966) suggests an average rate of spreading relative to the center of the mid-Atlantic ridge of 1.5 cm/year in the South Atlantic and 1 cm/year near the Reykjanes ridge. We shall take a value of 1.25 for our initial calculations to represent some sort of an average westward drift rate for the western Atlantic crust and assume for the moment that this also represents the current drift rate for North American relative to the mid-Atlantic ridge. If the spreading rate at the ridge and the continental drift rate are the same, then it is easy enough to calculate the volume of material moving westward for any given thickness of rigid crust (Figure II-4). To maintain a constant degree of isostatic equilibrium the eastward mass flow within the asthenosphere must everywhere equal the westward mass flow within the lithsphere. We may take average densities for the different parts of the model to be 3.2 for the continental lithosphere, 3.3 for the oceanic lithosphere, 3.4 for the very low shear wave region of the oceanic upper mantle and 3.5 for the remainder of the upper mantle above 300 km.

D. INTERPRETATION OF MODEL IN TERMS OF HEAT FLOW DATA

When we compare theoretical heat flow for the model in terms with observed heat flow measurements, it becomes clear that serious deficiencies exist in the model. Using a fairly sophisticated computational approach Langseth, et al.(1966), have shown that a convective model is not consistent with currently assumed estimates for heat flow in the absence of convection. Even using a much cruder approach this discrepancy is easily demonstrated by showing the incompatibility between the total heat liberated by a reasonable steady-state drift model and that actually observed over the Atlantic ocean. The model we shall use to demonstrate this incompatibility is shown in Figure II-5.

Let Q_{om} be total heat per unit length of ridge flowing from the deep mantle.

Q_{oa} be total heat per unit length from the asthenosphere.

Q_{o} be total heat per unit length into ocean bottom.

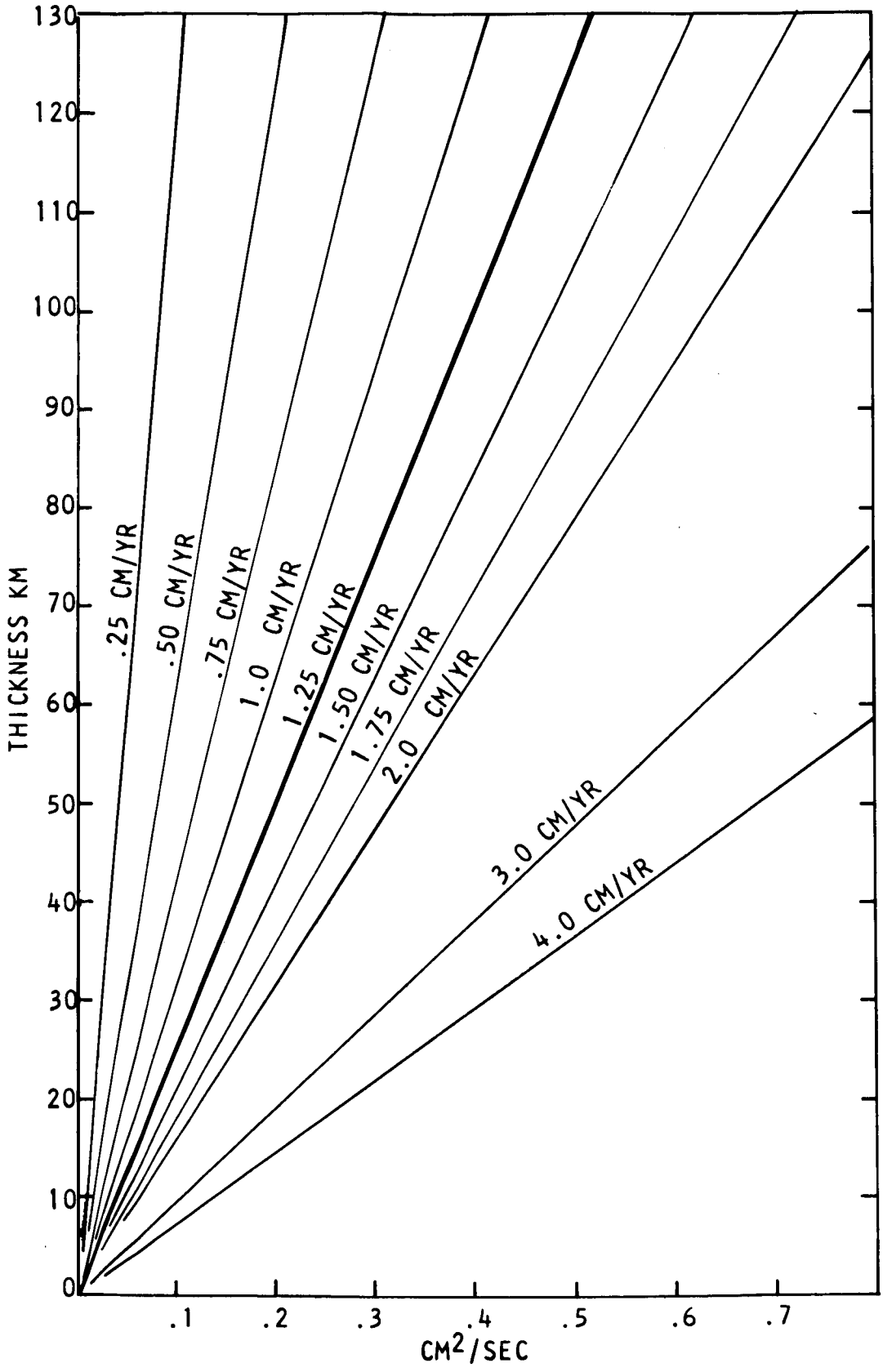

FIGURE II-4 LAYER THICKNESS AS A FUNCTION OF FLOW VOLUME FOR DIFFERENT DRIFT RATES

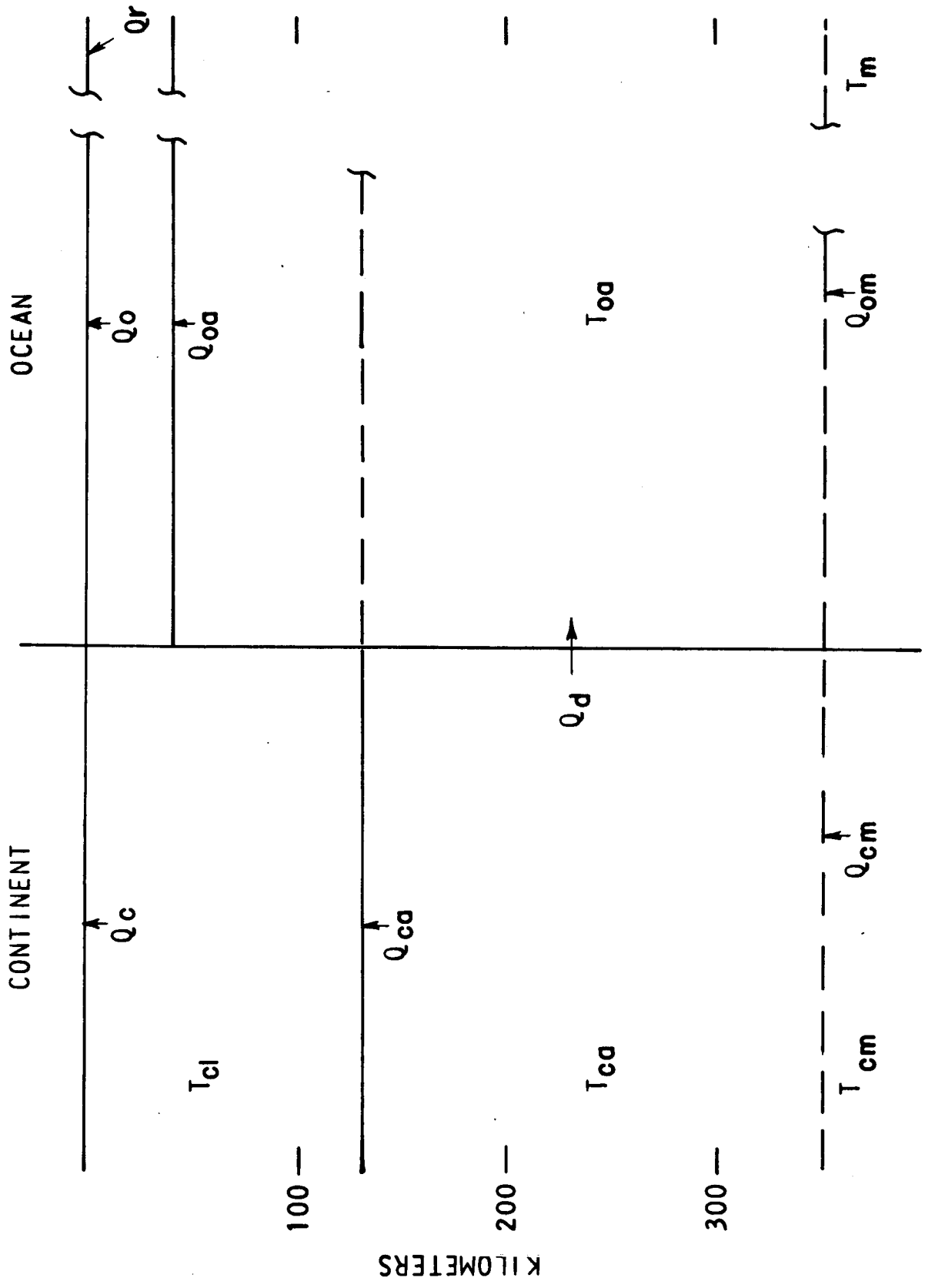

FIGURE II-5 HEAT FLOW MODEL FOR CONVECTING PLANET

Let Q_{cm}, Q_{ca}, and Q_c be equivalent heat flows beneath the continents.

Let Q_d be heat carried from subcontinental to suboceanic mantle as a result of convection liberated by formation of new ocean floors.

Q_r be heat liberated near the ridge by upward material transport, which may or may not be detected by heat flow measurements.

Let us also represent the average temperatures of each region in the steady state situation as

$$T_{om},\ T_{oa},\ T_{ol},\ T_{cm},\ T_{ca},\ T_{cl},\ \text{and for}$$

the moment assume

$$T_{oa} = T_{ca} \equiv T_a \qquad \text{(II-2)}$$

$$T_{ol} = T_{cl} \equiv T_l$$

We may now write for the steady state situation

$$Q_o = Q_d + Q_{om} + \Delta Q_o \qquad \text{(II-3)}$$

where ΔQ_o is amount of heat being generated in the oceanic mantle and crust.

By trying to estimate each of these quantities for the line at 40°N latitude in the western Atlantic using the drift rates and crustal thicknesses discussed above, a number of contradictions become apparent.

1. Measured Oceanic Heat Flow

Because of the sparsity of data and the approximations involved in the model it would seem sufficient to estimate the heat flow Q_c by multiplying the estimate of Langseth, et al., for the average Atlantic heat flux of 5.60μ watts/cm^2 (1.34 calories/cm^2 sec) by the distance from

the crest of the mid-Atlantic ridge to the continental shelf along the parallel 40°N latitude, which is approximately 42° at 8.5×10^6 cm/degree or 3.6×10^8 cm to yield $Q_o = 2.0 \times 10^3$ watts/cm.

2. Heat Liberated at Mid-Atlantic Ridge

It is important to estimate the excess heat at the ridge for two reasons: to show that it is small when compared with the total flow over the Atlantic; and to show that it is compatible with the model we are using to estimate the flow Q_{om} in the absence of convection.

To show that the ridge heat flow is small one may use the estimates of Langseth, et al.(1966) and Langseth (personal communication) that the total heat flow over the crest province of the ridge is of the order of 12 μ watts/cm^2, an excess of about 6.4 μ watts over the normal flow. Over a distance of 100 km from the ridge crest this would represent a total of about 120 watts of heat/cm of ridge length or 64 watts of excess heat. Thus the excess heat over the ridge represents something of the order of 3% of the total oceanic heat flow over the region in question and is insignificant compared with the total flow.

In spite of the small size of the ridge flow, it can easily be shown to be of the same order as the heat liberated during the formation of a basaltic crust. To make this comparison we note that formation of such crust 5 km thick, with a density of 3, at a rate of 1.25 cm per year would correspond to the generation of about 5.9×10^{-2} grams per cc per second. Generation of this crust would perturb the normal heat flow in several ways; in the first place, an amount of energy equal to the heat liberated upon cooling of the basalt would be brought directly to the surface bypassing the normal conductive mechanism. In addition, some heat would be lost to the sides of the fissure through which the melt was traveling as a result of conduction to the walls. Our work on mechanics of magma migration discussed in the previous report indicates that this heat loss to the walls should almost exactly balance the gravitational potential energy. In addition to each of these factors acting to increase the heat flow there will be a decrease in the conductive flow as a result of energy required to melt basalt at the point of its origin.

If we take a "normal" heat flow to be 5.6 μ watts/square cm, then the total normal heat flow over 100 km of width would be 56 watts/cm. At 5.9×10^{-2} grams/cm/sec of basalt liberated this would correspond to normal flow of 950 joules/gram of basaltic crust.

The specific heat of basalt should be about the same as "pyrolite" which we have estimated in our previous report to be about 1.1 joules/gram °C, i.e., about 1375 joules over the temperature range from 0 to 1250°C or 81 watts/cm over the ridge width at the above extrusion rate.

We have estimated the heat of fusion at the surface of basaltic magma to be about 300 joules/gram and at pressures of 30 kb to be about 750 joules/gram. These two values correspond to 18 and 44 watts/cm of ridge length, respectively. The former would act to increase the measured heat flow while the latter would tend to decrease it.

The gravitational energy for melt coming from a depth of about 100 km with a density difference of 10% would amount to about 100 joules/gram at 5.9×10^{-2} grams/cm/sec. The gravitational energy would correspond to 6 watts over the ridge width and would be almost insignificant.

The total heat flow then considering all these factors (Table II-1) would appear to be about 1975 joules/gram of new basaltic crust or 117 watts over the entire half-width of the mid-Atlantic ridge. As the total flow over the region in question is about 120 watts, which at a rate of 5.9×10^{-2} grams/cm/sec, would correspond to about 2000 joules/gram of new oceanic crust, the two estimates compare more favorably than could be expected from the large undertainty in the individual estimates used.

From the above calculations we conclude that the observed high heat flow at the ridge can be directly attributed to volcanic activity associated with sea floor spreading and is so small that for future calculations the excess flow may be neglected when considering the total flow over the western Atlantic Ocean.

TABLE II-1

MID-OCEAN RIDGE HEAT BALANCE

	Joules/gram	Watts
"Normal" conductive flow Q_{om}	950	56*
Latent heat	1375	81
Heat of fusion at surface	300	18
Heat of fusion below surface	-750	-44
Gravitational energy	100	6
	1975	117

*Average Atlantic ocean flow estimated by Langseth, et al. (1966).

All other values calculated on the basis of a "normal" observed oceanic heat flow of 5.6×10^{-6} watts/cm^2 and the formation of 5 km of basaltic crust at the rate of 1.25 cm/year.

3. Heat Liberated at Generation of New Crust and Upper Mantle

We now turn to the problem of heat liberated as a result of continental drift on the earth. To maintain isostatic equilibrium the westward movement of a continental mass of thickness h_{cl} at velocity v_c requires upwelling of an equal mass of mantle material to fill the void. If we accept the evidence from seismic measurements and viscosity interpretations, it seems appropriate to choose a value of h_{cl} of 125 km made up of 30 km of continental crust of mean density 2.77 grams and 90 km of upper mantle of density 3.36 grams/cc. Thus a total of 3.85×10^7 grams of lithosphere will overlie each square cm above a depth of 120 km. The mean density of this material will be 3.2 grams/cc. If the continent moves 1 cm, to maintain isostatic equilibrium and fill the void, 3.85×10^7 grams of mantle material will be required to replace it. This will correspond to 1.1×10^7 cm^3 at a density of 3.5 grams/cm^3.

We now turn to consideration of the heat liberated when this material moves up from the mantle toward the surface. On Figure II-3 we sketch an oceanic temperature distribution which would be compatible with a close approach to melting in the range 50 to 125 km. On the basis of this temperature profile and mantle densities taken from Anderson (1964) we estimate that there are 1.6×10^7 grams of material between 0 and 50 km and 2.2×10^7 grams between 50 and 125 km. Taking the mean temperature of the upper section to be 1000°K and of the section to be between 50 and 125 km to 1600°K would result in a total heat content at 1.1 joules/gram °C of 5.6×10^{10} joules/square cm.

If we assume that continental and oceanic temperature distributions between 125 and 300 km do not differ significantly and that mantle material moves up from this region to fill any void left by continental drift we are probably safe in taking the mean temperature of this material to be about 1900 °K $\pm$ 100°. At a specific heat of 1.1 joules/gram °C this corresponds to a total nominal heat content of 2.1×10^4 joules/gram.

Thus if 3.8×10^7 grams of material were to move upward from the lower mantle they would liberate 2.4×10^{10} joules/square cm/cm of continental movement if steady state conditions were to be maintained.

At a spreading rate of 1.0 cm per year this would correspond to a total heat liberated of 760 watts/sec/cm of ridge length. At a rate of 1.25 cm/year taken for our model this would correspond to 950 watts. It is interesting to compare this estimate with that of Langseth, et al. (1966), who get a value of about 800 watts over a width of 1000 km for a drift rate of 1 cm/year and 1100 for 2 cm/year, on a much more sophisticated model.

Since the total flow is about 2000 watts/cm of mid-Atlantic ridge length only about 1050 watts or 2.9×10^6 watts/ square cm would represent primary heat flow from the deep mantle Q_{om}.

E. IMPLICATIONS OF HEAT FLOW DATA FOR COMPOSITION

Although our original model was based on the apparent consistency between some calculations of MacDonald (1964) for an earth with "terrestrial ratios" of the elements and 1000° initial temperature, the above arguments point strongly toward a lower steady state heat flow from the deep mantle. Those in the following chapters seem to require a mantle composition which is somewhat like the "chondritic" composition used by MacDonald (1959), but with a higher rate of heat production than he used. It is also interesting to note that our heat flow requirements for a chondritic composition are satisfied by his Model 11 which has a photon mean free path of .1 cm at room temperature, an initial temperature of 0°C, and an insulated core. This model predicts a heat flow of 2.8×10^{-6} watts/square cm at the present time. MacDonald's Model 19, which assumed differentiation of a core 2.6×10^9 years ago in a uniform chondritic mantle, would have a similarly low heat flow. The present rate of heat production in the model we discuss in the following chapter would be about 30% higher than the one used by MacDonald due to the increased uranium content, and the heat production integrated over

all time would also be somewhat greater than the one he used. It may be that by removing the restrictions of an insulating core the revised chondritic model discussed in the next chapter would not be incompatible with an initially cold earth. While this point obviously needs further investigation and testing by computer simulation, this was not possible within the scope of this year's contract. It does seem clear however that by utilizing the thermal properties of our original model consistently we are being led toward a somewhat revised version which may be different for the moon and for the earth. The implications of this will be discussed in Chapter IV.

III. GEOCHEMICAL EVIDENCE FOR ORIGIN OF BASALT MAGMAS

A. INTRODUCTION

1. Observed Compositional Variations

Basalts vary to some degree in their composition in terms of both major and trace components. These variations and their genesis have been the subject of many papers.

Engel et al. (1965) have discussed the chemical characteristics of oceanic basalts. In Table III-1 (taken from their paper) are compared average compositions for three basalts characteristic of the basalts from the ocean bottom and from sea mounts and islands. These are remarkably similar but do show characteristic trends. One may note the trends in TiO_2 content, in Fe_2O_3/FeO and Na_2O/K_2O ratios. Engel et al. point out that oceanic tholeiites that form most of the deeply submerged volcanic features in the oceans are characterized by extremely low amounts of Ba, K, P, Pb, Sr, Th, U, and Zr as well as $Fe_2O_3/FeO < 0.2$ and $Na/K > 10$ in unaltered samples. In contrast, the alkali-rich basalts that cap submarine and island volcanoes are relatively enriched in Ba, K, La, Nb, P, Pb, Pb^{206}, Rb, Fe_2O_3, Sr, Sr^{87}, Ti, Th, U, and Zr. They tend to have Fe_2O_3/FeO and Na/K ratios more closely approaching 1. Tables III-2 and III-3 (also taken from Engel et al. 1965) present analytical data for numerous samples of oceanic tholeiitic basalts and alkali basalts. The wide fluctuations within these classifications are evident. Engel et al. on the basis of these analytical data coupled with field relationships indicate that alkali-rich basalts are derivative rocks, fractionated from the oceanic tholeiites by process of magmatic differentiation, and that the oceanic tholeiites are the principal or only primary magma generated in the upper mantle under the oceans. As is evident from Table III-1 the Hawaiian tholeiites are intermediate in many of their characteristics between the deep oceanic tholeiites and the alkali basalts.

TABLE III-1

COMPOSITIONS OF DREDGED OCEANIC THOLEIITIC BASALTS, HAWAIIAN BASALTS AND ALKALI BASALTS FROM SUBMARINE VOLCANOES AND ISLANDS

(Water-Free)

	1*	2†	3**
SiO_2	49.94	49.84	48.16
TiO_2	1.51	2.52	2.91
Al_2O_3	17.25	14.09	18.31
Fe_2O_3	2.01	3.06	4.24
FeO	6.90	8.61	5.89
MnO	.17	.16	.16
MgO	7.28	8.52	4.87
CaO	11.86	10.41	8.79
Na_2O	2.76	2.15	4.05
K_2O	.16	.38	1.69
P_2O_5	.16	.26	.93

*Column 1. Average of 10 samples of oceanic tholeiite dredge from the Atlantic and Pacific oceans (Table III-2)

†Column 2. Average of 181 tholeiites and olivine tholeiites from the Hawaiian Islands (MacDonald and Katsura, 1964, Table 9, col. 8, p. 124).

**Column 3. Average of 10 samples of alkali basalt from submarine volcanoes and islands of the eastern Pacific Ocean (Table III-3)

TABLE III-2

CHEMICAL COMPOSITIONS OF

OCEANIC THOLEIITIC BASALTS

	Atlantic Ocean					Pacific Ocean				
	AD 2	AD 3	AD 4	AD 5-5	AD 5-18	PV D-1	PV D-3	PV D4-C	PV 17	EM
					(parts per million)					
Ba	5	19	28	5	5	21	25	6	17	12
Co	32	34	33	26	28	28	35	34	38	35
Cr	220	320	260	280	300	350	160	420	200	460
Cu	66	86	75	73	81	64	80	87	76	83
Ga	20	17	16	11	16	14	20	18	20	16
Li	6	4	27	5	6	3	6	3	5	21
Nb	< 30	< 30	< 30	< 30	< 30	< 30	< 30	< 30	< 30	< 30
Ni	87	140	92	78	76	130	58	110	88	110
Rb	< 10	< 10	< 10	< 10	< 10	< 10	< 10	< 10	< 10	< 10
Sc	44	44	44	38	41	30	56	52	56	49
Sr	190	160	140	90	160	120	110	110	120	97
V	280	280	290	240	240	170	400	260	440	320
Y	60	44	36	30	32	21	62	42	60	38
Yb	6	4	4	3	3	2	7	5	7	4
Zr	160	88	84	62	65	44	150	78	150	67
					(weight per cent)					
SiO_2	49.20	49.48	48.54	49.02	50.13	48.53	49.80	49.64	49.94	49.13
TiO_2	2.03	1.39	1.50	1.46	.86	.76	2.02	1.37	2.27	1.23
Al_2O_3	16.09	16.72	16.70	18.04	19.65	22.30	14.88	16.19	14.85	14.97
Fe_2O_3	2.72	1.16	3.56	1.58	1.86	.69	1.55	1.35	2.17	3.28
FeO	7.77	7.58	4.95	6.22	4.77	4.82	10.24	7.85	8.07	5.72
MnO	.18	.19	.18	.13	.12	.16	.21	.18	.22	.16
MgO	6.44	8.20	7.12	7.85	5.95	7.14	6.74	8.37	6.42	7.68
CaO	10.46	11.14	11.31	11.51	12.57	12.86	10.72	12.01	11.92	12.68
Na_2O	3.01	2.66	2.98	2.92	2.77	2.18	2.91	2.75	2.70	2.37
K_2O	.14	.24	.14	.08	.21	.06	.24	.11	.26	.16
H_2O+	.70	.62	1.50	.64	.50	.38	.54	.30	.63	1.06
H_2O-	.95	.61	1.20	.57	.44	.01	.06	.01	.67	1.25
P_2O_5	.23	.12	.21	.12	.19	.07	.28	.09	.18	.15
Total	99.92	100.11	99.89	100.14	100.02	99.96	100.19	100.22	100.30	99.84
Fe_2O_3/FeO	.35	.15	.72	.25	.39	.14	.15	.17	.27	.57
Na/K	19.3	9.9	19.1	32.8	11.8	33.0	10.8	22.4	9.3	13.3

TABLE III-3

CHEMICAL COMPOSITIONS OF ALKALI BASALTS

FROM THE EAST PACIFIC RISE

Ag less than 3 ppm for all samples except PV 77 which contains 4 ppm. B less than 30 ppm for all samples except PV 77 which contain 48 ppm. Be less than 2 ppm for all samples except PV 50 which contains 2 ppm.

	PV 77	PV 316	PV 314	PV 50	Gu 22	Gu 15	Gu 77	Gu 52	PV 172	PV 305
					(parts per million)					
Ba	390	810	740	420	340	380	540	360	420	580
Co	41	27	22	33	25	26	21	23	18	17
Cr	300	180	120	170	30	14	7	22	84	15
Cu	42	48	34	56	58	15	10	38	37	20
Ga	18	20	19	22	20	23	22	24	24	28
La	< 80	< 80	120	< 80	< 80	< 80	100	100	< 80	120
Li	25	21	10	6	5	8	10	6	8	6
Mo	< 5	< 5	< 5	11	< 5	< 5	< 5	7	6	< 5
Nb	46	70	82	82	64	70	96	68	66	72
Ni	170	60	63	76	28	24	18	26	34	10
Rb	< 10	12	44	33	26	42	60	34	52	28
Sc	28	33	30	26	26	18	16	22	28	30
Sr	2400	440	740	1100	510	600	680	540	460	680
V	260	320	250	260	300	210	180	280	240	220
Y	42	52	52	48	46	52	53	52	56	83
Yb	3	5	4	4	4	4	4	4	5	6
Zr	200	260	340	350	300	380	420	360	360	360
					(weight per cent)					
SiO_2	41.04	42.95	44.90	45.33	48.00	50.08	50.48	51.26	50.32	49.71
TiO_2	2.83	2.81	2.85	3.53	3.20	2.90	2.25	2.82	2.45	3.05
Al_2O_3	18.71	19.10	22.80	15.50	17.42	18.77	18.31	16.29	18.99	14.34
$Fe_2O_3^*$	4.43	4.03	1.91	1.81	6.17	4.10	3.21	5.51	3.69	6.86
FeO	6.59	5.60	4.69	10.64	4.64	5.13	6.03	4.91	4.50	5.30
MnO	.21	.16	.12	.23	.13	.15	.21	.15	.11	.17
MgO	7.92	6.65	5.09	6.77	4.55	4.50	4.21	4.01	3.03	2.17
CaO	10.99	9.37	9.16	8.50	9.60	7.30	7.21	7.87	8.26	8.19
Na_2O	2.43	3.50	4.00	4.30	4.00	4.16	4.80	4.08	4.14	4.50
K_2O	.63	1.15	1.76	2.36	1.30	1.79	1.93	1.65	2.09	1.94
H_2O+	1.66	1.84	.54	.20	.42	.38	.46	.36	.50	1.55
H_2O-	1.51	1.46	.66	.01	.15	.01	.38	.40	.83	.69
P_2O_5	.98	.99	1.26	.73	.54	.79	.74	.77	1.03	1.38
Total	99.93	99.61	99.74	99.91	100.12	100.06	100.22	100.08	99.94	99.85
Fe_2O_3/FeO	.67	.72	.40	.17	1.33	.80	.53	1.12	.82	1.29
K/Rb	..	792	332	594	415	355	267	403	333	575
Sr/Rb	..	37	17	33	20	14	11	16	9	24
Na/K	3.4	2.7	2.0	1.6	2.8	2.1	2.2	2.2	1.8	2.1

Many other basalts can be found which are intermediate between the oceanic tholeiites and the alkali-rich varieties and Engel et al. point out that this is to be expected if the latter are derived from the former by a process of differentiation.

Engel et al. also compare oceanic tholeiites with continental basalts. They report that comparisons of the compositions of the largest eruptions of continental tholeiites that have volumes exceeding 10,000 km^3 with compositions of oceanic tholeiites indicate two significant differences. In most continental tholeiites the amounts of silica and potassium (with coherent trace elements) exceed the amounts in the oceanic tholeiites. To avoid an interpretation which would say that the mantle under the continents contains more K, U, Pb, etc. than that under the oceans Engel et al. infer that these differences represent contamination of the continental tholeiites by these elements and isotopes scavenged from the crust. They also point out that recent studies of very old Archean pillowed basalts (> 2.5 aeons) show compositions which are intermediate between those of oceanic tholeiites and the continental tholeiites (< 1.8 aeons). They point out that these data are consistent with the following interpretations: (1) the larger amounts of silica and alkalis in the younger continental tholeiites are the result of contamination from a progressively thickened and more differentiated sialic continental crust; and (2) within the limits of existing measurements, there is no evidence for a decrease with time, toward the present, in the amounts of alkalis and long-lived radioactive nucleides in continental tholeiites.

The work of Engel et al. discussed in the previous paragraphs presents a good review of the characteristics of submarine basalts, island and sea mount basalts, and continental basalts. However, Muir and Tilley (1966) have pointed out that there are exceptions to the generalizations of Engel et al. Muir and Tilley discuss basalts of the mid-Atlantic ridge. They point out that the basalts dredged by the Atlantic (1947) expedition at latitudes near 30° north may be

distinguished as a group from the Discovery II (1960) samples obtained from the ridge near 45° north (see Table III-4). The samples of the Atlantic expedition have very low potash values on the order of 0.17%. In contrast, the samples of the Discovery II collection average 0.47 potash and run as high as 0.77. Muir and Tilley point out that the emphasis placed by Engel et al. on the low potash content of deep ocean basalts is thus not strictly true; the Discovery II collection of basalt samples is a notable exception. The potash value in these samples are comparable to and overlap many Hawaiian basalt samples. In addition Muir and Tilley point out that basalts have been sampled on the Hawaiian Islands which are comparable to the major number of submarine basalts. They specifically refer to the lower-most group of basalts in the Pololu series of Kohala Mountain, Hawaii, which average 0.13% K_2O. Therefore, we must recognize that there is a range of tholeiitic compositions to be found both in submarine basalts and in the island and sea mount basalts.

As a further example of the variation in composition of basalts which have been noted and commented upon, we can mention the work of Kuno (1960). Kuno finds a trend in the basalt compositions from volcanoes as one moves from the oceanic to the continental side of the Japanese Islands. On the oceanic side one finds a tholeiitic with low alumina and alkalis. On the continental side one finds an alkali basalt with variable alumina and higher alkalis. In between these two zones is a region where one finds a basalt with higher alumina than either of the other two and with intermediate alkalis. Mineralogically in terms of a normative analysis the high alumina basalt is intermediate between the tholeiitic and alkalic basalt. Kuno proposes that these are not derivatives of a single tholeiitic basalt but represent partial melting of a primary mantle composition. Based on earthquake foci in the various basalt provinces, Kuno proposes that the tholeiitic basalt is formed by melting of the mantle at a depth of less than 200 km, that the high alumina basalt is formed by melting at approximately 200 km, and that the alkali basalt magmas are produced by melting of the mantle at depths greater than 200 km.

TABLE III-4

CHEMICAL ANALYSES OF BASALTS OF THE MID-ATLANTIC RIDGE

	1	2	3	4	5	6	7	8	9	10	11	12
SiO_2	48.68	49.59	49.76	49.80	50.34	48.98	50.48	48.40	48.65	49.91	49.79	49.86
Al_2O_3	15.68	14.54	14.85	14.76	14.35	15.35	14.79	16.12	15.99	15.55	15.96	16.00
Fe_2O_3	3.38	2.30	2.16	1.85	1.85	1.34	2.49	1.94	2.18	1.50	1.55	1.52
FeO	7.49	8.74	8.27	8.64	9.89	8.15	8.83	6.34	6.19	7.07	6.96	7.05
MnO	0.17	0.19	0.18	0.18	0.21	0.17	0.20	0.16	0.15	0.15	0.16	0.16
MgO	6.86	8.15	8.56	8.56	7.15	8.08	6.94	9.63	9.66	9.27	8.79	8.76
CaO	11.32	10.98	11.17	11.10	10.79	10.33	10.84	11.48	11.52	10.83	11.89	11.89
Na_2O	2.82	2.89	2.69	2.68	2.80	2.54	2.81	2.77	2.71	2.84	2.54	2.54
K_2O	0.25	0.17	0.15	0.15	0.11	0.10	0.26	0.53	0.57	0.42	0.27	0.26
H_2O+	0.78	0.68	0.61	0.47	0.52	2.79	0.42	0.86	0.75	0.93	0.62	0.46
H_2O-	0.75	0.11	0.16	0.16	0.06	0.60	0.13	0.28	0.30	0.10	0.06	0.12
TiO	1.77	1.66	1.49	1.51	1.74	1.47	1.73	1.43	1.44	1.38	1.24	1.24
P_2O_5	0.15	0.13	0.13	0.13	0.15	0.12	0.15	0.22	0.21	0.20	0.15	0.15
CO_2	-	-	-	-	-	0.38	-	-	-	-	-	-
	100.10	100.13	100.18	99.99	99.96	100.40	100.07	100.16	100.32	100.15	99.98	100.01

Olivine basalts from the Atlantis (1947) Collections:

1. 92544, Station 20, 4,144 metres (30° 04' N, 42° 16' W)
2. 92541, Station 21, 4,200 metres (30° 08' N, 43° 37' W)
3. 92542 } Station 8, 3,700 metres (31° 49' N, 42° 25' W)
4. 92545 }
5. 92543, Station 7, 4,200 metres (30° 01' N, 42° 04' W)
6. 92548 (dolerite) Station 20, 4,144 metres (30° 1' N, 42° 16' W)
7. 79487, Station 7, 4,280 metres (30° 01' N, 42° 04' W)

} (data from Table I Muir and Tilley 1966)

Basalts from Discovery II (1960) Collection:

8. 45/86931 olivine basalt, Station 4519
9. 67545 Station 4519-34, 3,370 metres } (45° 44' N, 27° 43' W)
10. 67546 Station 4519-46, 3,370 metres }
11. 1/86951, olivine basalt, Station 4520 } (45° 51' N, 27° 39' W) (3,370 metres)
12. 4/86953, olivine basalt, Station 4520 }

} (8, 11, 12 data from Table II Muir and Tilley 1966)

(9 and 10 data from Table I Muir & Tilley 1964)

Kushiro and Kuno (1963) considered a much wider composition range of basalt magmas and attempted to explain their origin again in terms of varying depths in the mantle. Basalts were separated into three groups based on their normative analysis. The basalts discussed by Kuno (1960) all fall within a single group. They conclude that this group of basalts are formed at shallowest depths.

2. A Variety of Interpretation

As noted above many people have noted and commented upon the compositional variations of basalts. Many attempts have been made to derive explanations for the observed compositional variations. The explanations have included fractional crystallization, contamination with crustal rocks, differing source compositions, and depth and temperature of origin factors. There has been no widespread acceptance of any one interpretation. A consistent and acceptable interpretation for the compositional variations is still needed.

3. Our Problem

In our development of a model of volcanism on the earth and application of it to volcanic behavior on the moon, we need to understand the origin of basalt magmas observed on earth for two reasons. First, we have derived the potassium and uranium content of the mantle for our model from the average potassium and uranium content of basalts observed on earth. However, recent work on submarine basalts has indicated that our original estimate or average may have been too high in uranium and too low in potassium. If this is true, then our value for the heat sources in our model planet will require modification. Secondly, we will want to predict the composition of magmas formed on a model planet and this will certainly be very difficult if we cannot understand the reasons for the variations observed on earth.

In order to answer these questions we have had to give some more thought to the origin of basalts. In an attempt to resolve the confusion which existed in our minds with respect to the wide variation in basalt compositions, we decided to re-examine the data interpretations in the light of two limitations. First, we examined the theoretical implications of our model with respect to the origin and variation of the composition of basalts. Second, we examined the geochemical data for the major basalt types. By major basalt types we mean those that exist in the world in the largest quantities. These include the submarine basalts, the sea mount and island basalts, and the continental basalts which occur in large flows. In general these are tholeiitic in nature.

B. THEORETICAL CONSIDERATIONS

1. Our Model

In our previous study (McConnell, et al., 1967) we adopted as the mantle composition for our model that of "pyrolite" as proposed by Green and Ringwood (1963) which consists of one part basalt to three parts dunite. For this composition we then derived the melting behavior as a function of pressure. A consideration of these data will indicate some of the variables possibly controlling the melt composition.

At shallow depths pyrolite is to a first approximation a three phase system, consisting of olivine, pyroxene, and plagioclase. The plagioclase phase is very acid and low melting. We anticipate that the composition of the melt will change with both pressure and fraction melted. However, the most important factor affecting the melt composition at very low pressures (i.e., near the surface) will be the melt fraction.

At pressures of 10-12 kb corresponding to depths of 30 to 40 km, the melting temperature of pyrolite is increasing rapidly with

pressure. In this region which we believe extends to depths no greater than 100 km (corresponding to pressures of 30 kb) the plagioclase phase is diappearing with a corresponding increase in the pyroxene phase. In this region we anticipate that the melt composition varies markedly with pressure as well as fraction melted. Within this pressure range albite is transformed to jadeite and quartz. Albite is a major mineral of the plagioclase phase while jadeite is a pyroxene mineral. In other words, aluminum which is found in the anion lattice of the plagioclase phase is increasingly found with increasing pressure in the cation lattice of the pyroxene phase. There is some evidence that for a mixture like pyrolite one can expect the Al_2O_3 content of liquids formed by partial fusion of the same parent material to increase as a function of depth up to pressure at which plagioclase disappears from the liquidus. Thus the melt composition can vary strongly with pressure and fraction melted, and one might expect some higher Al_2O_3 contents in the melt as one goes to higher pressures.

At a sufficient depth, which is probably no greater than 100 km (corresponding to about 30 kb) and maybe less, pyrolite is to a first approximation a two phase system consisting of olivine and pyroxene minerals. From this point on we would expect that the initial melt composition will not change in base to acid ratio significantly with increasing depth or fraction melted. To the extent that there are changes they would be towards greater base to acid ratio with increasing fraction melted and depth.

2. Variables Affecting Composition of Magmas

From our understanding of the melting of pyrolite as a function of pressure and from thermodynamic considerations we can list the following variables which might produce compositional variations in magmas.

a. Depth at Which Melting Occurs

There are two factors which can change with depth and significantly affect melt composition. The first of these is the fact that the solid phases present and thus the initial melt composition in equilibrium with these phases are a function of pressure. This has clearly been evident from a consideration of the melting behavior of pyrolite discussed in the previous section.

The second factor is that the distribution constants for ions between melt and solid are a function of pressure and temperature. Thus it is clearly possible that a specific ion such as aluminum may change its distribution between say a pyroxene phase and the melt with depth.

b. The Melt Fraction

The melt composition can change significantly with melt fraction. This is clearly evident from examination of the phase diagrams at a given pressure for two or three component systems.

One should also recognize that the relative concentrations of chemically similar ions with markedly different distribution constants and concentrations in the system can change with melt fraction.

c. Time Required for Equilibration

Since the concentrations of some ions in the melt may depend on distribution between the melt and a solid phase, the final melt composition can be dependent on whether equilibrium is achieved before the magma is ejected.

d. Fractional Crystallization Enroute to the Surface

If the melt stops enroute to the surface a new equilibrium situation characteristic of the pressure and temperature conditions where the melt is held up will tend to be established.

c. Any Possible Prior Differentiation Within the Mantle

If the mantle composition varies vertically with depth or horizontally with position due to prior differentiation processes, then magma obtained can certainly vary depending on the position of origin.

C. INSIGHTS FROM GEOCHEMISTRY

1. Classification of Basalts

We have pointed out in previous sections that a wide range of magma compositions has been observed, and that we can recognize many variables which could affect or cause these compositional variations. In actual fact many of the compositional variations of magma observed occur in very limited quantities on the face of the earth. In order to simplify our re-examination of the problem of the origin of basalt magmas we will restrict our examination to the basalts which represent the major volume of extrusive magmas found on the earth. The sheer volume of many of these flows implies a direct transit from the mantle to the surface.

Engel et al. (1965) have pointed out that tholeiitic basalts represent the main quantity of basalt errupted on the earth's crust during geologic time. The wide variety of alkalic basalts represent only a few percent of the total. The tholeiitic basalts can be broken down into three groups for our examination based on where they are found. The first group includes those basalts occurring on the ocean floor which we will call the submarine basalts. The second group includes the tholeiitic basalts which form the major portion of the sea mounts and islands, such as the Hawaiian chain, which we will refer to as oceanic basalts. On these islands the alkalic basalts represent only the "frosting on the cake" and are a very small portion of the total quantity of the basalts forming the ridge or island structure. The

third group of tholeiitic basalts which we will consider are those comprising the tholeiitic continental basalts which occur as huge surface flows and intrusive sills. By restricting ourselves to these major basalt types, in the sense of their being the ones found in greatest quantity, we eliminate the large variety of highly acid basalts which occur frequently but in rather limited quantities in numerous parts of the globe and the less numerous and still smaller quantity of highly basic magmas.

2. Trace Element Trends in Magmas

We have compiled in Table III-5 data for potassium, rubidium, cesium, thorium and uranium content of many tholeiitic magmas. These data are taken from the references cited in the Table. When these data are examined one observes two things. First, the potassium, rubidium, cesium, thorium, and uranium content in the basalts increases as one goes from the submarine to the continental basalts. Second, the alkali metal raios vary uniformly with increasing potassium content as one goes from submarine to continental basalts.

a. Alkali Metal Content

We have plotted in Figure III-1 the potassium content versus rubidium content taken from the data of Table III-5. One can note that the submarine basalts represent the lowest potassium and rubidium content. The continental basalts represent the highest, while the oceanic basalts, that is, those from sea mounts and islands are intermediate. One may also note that there is a tendency for these groupings to overlap. In other words, there is no clean cut break between our classifications.

While the actual content of potassium and rubidium increases in going from the submarine to the continental basalt, one may also note that the potassium to rubidium ratio is decreasing. The value for

TABLE III-5

TRACE ELEMENT CONTENTS OF BASALT AND METEORITE SAMPLES

(in ppm)

Sample Description	K	Rb	Cs	Th	U	K/Rb	K/Cs	Th/U	Reference
Karoo Dolerite (chilled contact, D/S 95)	6000	10.5	0.27	-	-	571	22,200	-	Table 2-Erlank & Hofmeyr (1966)
Red Hill, Tasmania (chilled contact, M172(a))	6600	32	1.3	-	-	206	5,080	-	Table 2-Erlank & Hofmeyr (1966)
Antartic Ferrar dolerites									
olivine tholeiite #26903	3200	12	-	-	-	267	-	-	
Hypersthene tholeiite 4012	6200	30	-	-	-	207	-	-	
4083	6400	32	-	-	-	200	-	-	Gunn (1965) Table 1
Pigeonite tholeiite 4174	10500	49	-	-	-	215	-	-	
4074	12000	55	-	-	-	218	-	-	
Submarine Tholeiites									
Atlantic									
Station 7I	1400	0.98	.04	-	.085	1430	35,000	-	
7II	875	0.75	-	-	-	1165	-	-	Gast (1965) Table 1
8	4500	9.5	-	-	-	475	-	-	
20	3040	5.61	-	-	-	540	-	-	
D2-1	1345	1.42	-	-	-	950	-	-	
Pacific									
D-3	1560	1.14	-	-	-	1370	-	-	
D-4	641	0.35	-	-	-	1830	-	-	
PV-17	2285	3.69	-	-	-	620	-	-	
Achondrites									
Pasamonte	425	0.23	0.011	-	0.05	1850	39,000		
Sioux County	335	0.24	0.012	-	0.06	1300	28,000	-	
Nuevo Laredo	367	0.37	0.018	-	0.126	990	20,000	-	
Moore County	187	0.16	0.005	-	-	1150	37,000	-	

TABLE III-5 (continued

Sample Description	K	Rb	Cs	Th	U	K/Rb	K/Cs	Th/U	Reference
Submarine Tholeiites									
Atlantic Ocean									
AD2-1	1160	1.14	-	0.15	0.16	1050	-	-	
	(1345)	(1.42)	-	-	-	(950)	-	0.9	
AD3-2	1990	2.63	-	0.29	0.10	760	-	2.9	Tatsumoto et al.(1965)
AD5-11	1100	0.66	-	0.13	0.09	1760	-	1.4	Table 1 and 2
Pacific Ocean									
PD-3	1990	1.06	-	0.21	0.09	1890	-	2.5	
	(1560)	(1.14)	-	-	-	(1370)	-	-	
PD4-G	920	0.45	-	0.13	0.07	2022	-	2.0	
	(641)	(0.35)	-	-	-	(1830)	-	-	
Tasmanian dolerite (Red Hill)									
chilled margin average	6900	-	-	3.35	0.87	-	-	3.9	Heir et al. (1965)
Skaergaard intrusion									Table 4
chilled margin	3200	-	-	-	0.2	-	-	-	
Tholeiitic Basalts									
Palisades sill									
828 pyr. diabase	13300	-	-	2.4	0.48	-	-	4.8	
817 qtz. pyr. diabase	5100	-	-	1.7	0.31	-	-	5.7	Heir & Rogers (1963)
804 pyr. diabase	7400	-	-	1.6	0.36	-	-	4.4	Table 4
918 pyr. diabase	3600	-	-	1.5	0.23	-	-	6.5	
826 pyr. diabase	7800	-	-	2.0	0.37	-	-	5.4	
Columbia River Basalts									
1064 pyr. basalts	5300	-	-	1.1	0.50	-	-	2.2	
1065 basalt	3400	-	-	0.94	0.22	-	-	4.3	
Hawaii									
1086 tholeiitic qtz. dolerite intr.	3600	-	-	0.41	0.06	-	-	6.8	

TABLE III-5 (continued)

Sample Description	K	Rb	Cs	Th	U	K/Rb	K/Cs	Th/U	Reference
Karoo									
1067 dolerite	6700	-	-	1.6	0.42	-	-	3.8	
1068 olivine dolerite	4000	-	-	0.60	0.17	-	-	3.5	
Bushveld									
1066 norite	2500	-	-	0.47	0.10	-	-	4.7	
Pigion Pt. Sill, Minn.									
824 diabase	8300	-	-	1.6	0.41	-	-	3.9	
Japan									
1080 tholeiite	600	-	-	0.05	0.03	-	-	1.7	
1081 tholeiite	3600	-	-	0.32	0.26	-	-	1.5	
1082 Li-Al basalt	6200	-	-	1.1	0.28	-	-	3.9	
1083 Li-Al basalt	3400	-	-	0.45	0.13	-	-	3.5	
1084 alk.ol.basalt	8100	-	-	4.2	0.48	-	-	8.8	
1085 alk.ol.basalt	10000	-	-	3.6	0.57	-	-	6.3	
Hawaiian Lavas									
Kauai									
Tholeiitic basalt of Napoli formation:	1200	-	-	0.73	0.19	-	-	3.8	
Tholeiitic basalt of Mahaweli formation	1500	-	-	0.53	0.15	-	-	-	
Oahu									
Tholeiitic basalt of the Koolau series	2600	-	-	0.53	0.10	-	-	5.3	
"	3100	-	-	0.63	0.23	-	-	2.8	
"	3600	-	-	0.83	0.17	-	-	5.0	Heir et al.(1964 Table 1
Tholeiitic basalt of lower member of Waianae series	3600	-	-	0.87	0.24	-	-	3.6	
Alk. basalt of lower member of Waianae series	10500	-	-	2.12	0.68	-	-	3.1	
Hawaiite, upper Waianae series	13400	-	-	3.20	0.74	-	-	4.3	

TABLE III-5 (Continued)

Sample Description	K	Rb	Cs	Th	U	K/Rb	K/Cs	Th/U	Reference
Hawaiian Lavas cont'd.									
Maui									
Ol. basalt of Wailuku series	9500	-	-	2.46	0.32	-	-	7.7	
Hawaiite of Kula volcanic series	13300	-	-	3.21	1.14	-	-	2.8	
Chondrites	840av	(3av)	-	.04-.06	.01-.015	-	-		Tables 24-1 and 24-2
Achondrites									
Angrite:									in
Angra dos Reis	-	-	-	0.97	0.20	-	-	-	Clark, Jr. (1966)
Aubrites:									
Bishopville	1100	-	-	0.04	.005	-	-	-	
Norton Co.	70-120	-	-	-	.01	-	-	-	
Diogenites:									
Johnstown	8	-	-	.030	.012	-	-	-	
Eucrites:									
Juvinas	240-480	-	-	.6	-	-	-	-	
Moore Co.	190	-	(.005)	.062	.020	-	-	-	
Nuevo Laredo	400-500	-	(.019)	.5-.7	.13-.17	-	-	-	
Pasamonte	400-600	-	(.011)	.52	.054	-	-	-	
Sioux County	250-350	-	(.012)	.35	.063	-	-	-	
Stannern	600-700	-	-	.50	-	-	-	-	
Howardites:									
Binda	-	-	-	.063	.023	-	-	-	
Nakhlite:									
Nahkla	1020	-	-	.19	.049	-	-	-	

TABLE III-5 (continued)

Sample Description	K	Rb	Cs	Th	U	K/Rb	K/Cs	Th/U	Reference
Hawaiian Basalts									
H-2-61,1955 Basalt flow, Puna	5700	10.6	-	-	-	-	538	-	Table 2 Lessing et al. (1963)
H-9-61b, 1801 Alkali Baslat flow Hualalai	5700	13.3	-	-	-	-	428	-	
H-11-61,1960 flow, Kapoho	4000	8.0	-	-	-	-	500	-	
H-12-61,1959 basalt flow, Kilauea Iki lava lake crust	3000	6.7	-	-	-	-	448	-	
H-16-61,1919 basalt flow, Kilauea caldera floor	3200	5.6	-	-	-	-	572	-	
11-59, 1955 olivine basalt Puna	4700	9.0	-	-	-	-	522	-	
3-5,Basalt flow, Halina Pali	2700	6.0	-	-	-	-	450	-	
Ultra-mafic inclusions									
Eclogite, Salt Lake Crater Hawaii(total rock minus spinel)	527	1.79	-	-	.043	-	-	-	Tilton & Reed (1963)
Hawaii, Hualalai, olivine nodule 1801 flow	-	-	-	-	.004	-	-	-	
(Hualalai basalt, 1801 flow)	-	-	-	-	.50	-	-	-	
Mohole basalt EM 7-5	-	-	-	0.229	0.195	-	-	-	Morgan & Lovering (1965)

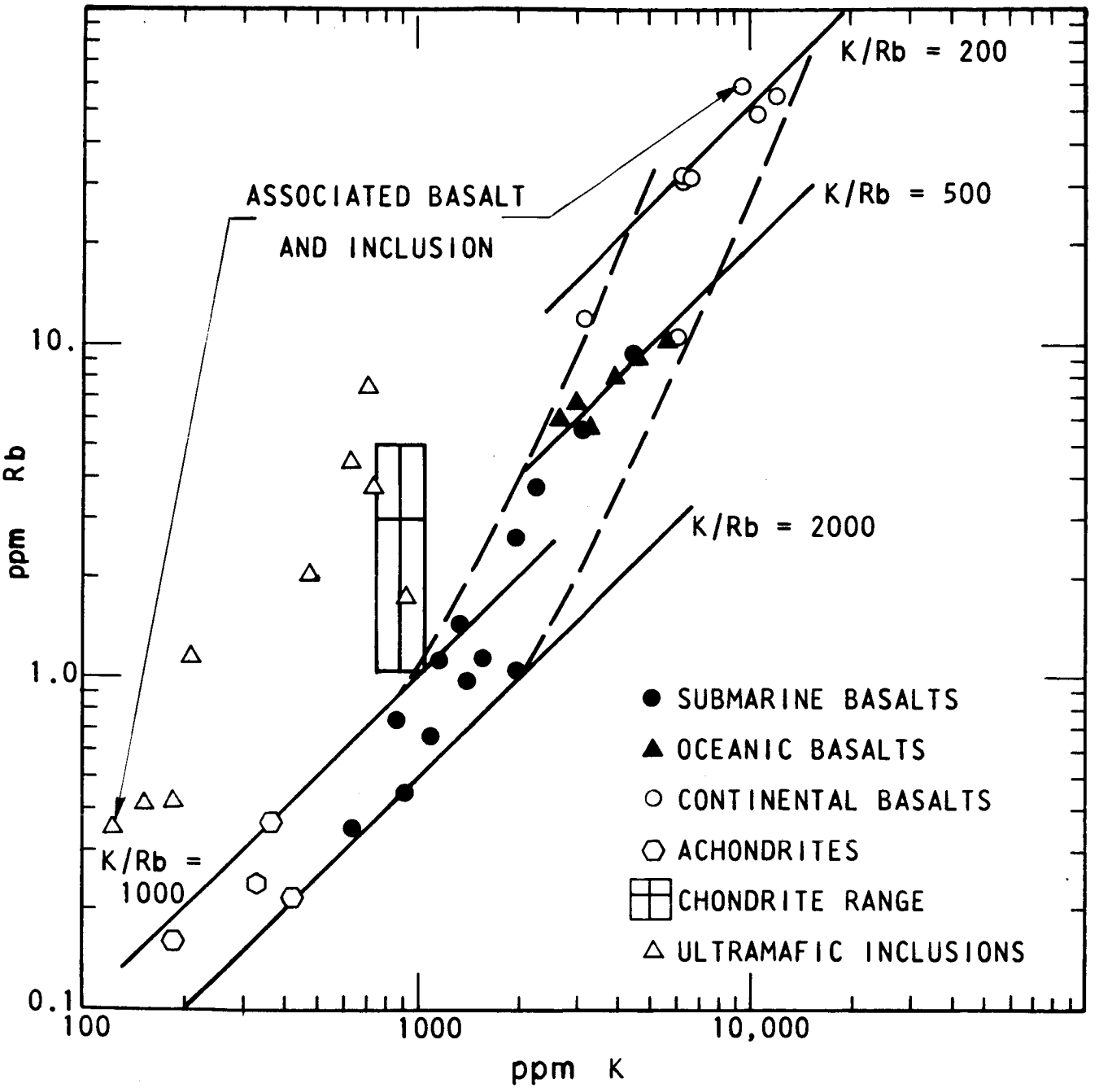

FIGURE III-1 K - Rb COMPOSITIONAL VARIATIONS IN THOLEIITIC BASALTS AND METEORITES

for the submarine basalt range between 1000 and 2000 while that for the continental basalts range between 200 and 500. Both the sodium to potassium and potassium to cesium ratios vary in the same way, that is, the ratios decrease as one goes from the submarine to the continental basalts. The data for cesium is somewhat limited but there does seem to be the same trend of increasing concentration in the basalt as one goes from submarine to continental basalts.

b. Thorium and Uranium Content

From the data of Table III-5 we have plotted on Figure III-2 the thorium content versus uranium content for the submarine, oceanic and continental basalts. The same trends are observable as mentioned for the alkali metals. The absolute content increases as one goes from submarine toward continental basalts. For thorium and uranium data there is much more overlapping that was observable in Figure III-1. There is not as much evidence for a change in the ratio of thorium to uranium with increasing concentration.

On Figure III-3 we have plotted the thorium concentration versus potassium concentration. Note again that thorium content increases with potassium content, and the concentrations increase as one goes from submarine to continental tholeiitic basalts. On this plot we have presented a few data for alkalic basalts. These lie at concentrations equal to or greater than those reported for the continental basalts.

c. Data for Chondrites and Achondrites

We have included in Table III-5 existing data for the chondrites and achondrites. We should examine the relationship of the chondrites and achondrites to the tholeiitic basalts, because it has been requently claimed that the chondrites and achondrites are related to each other and represent differentiates from a small planet.

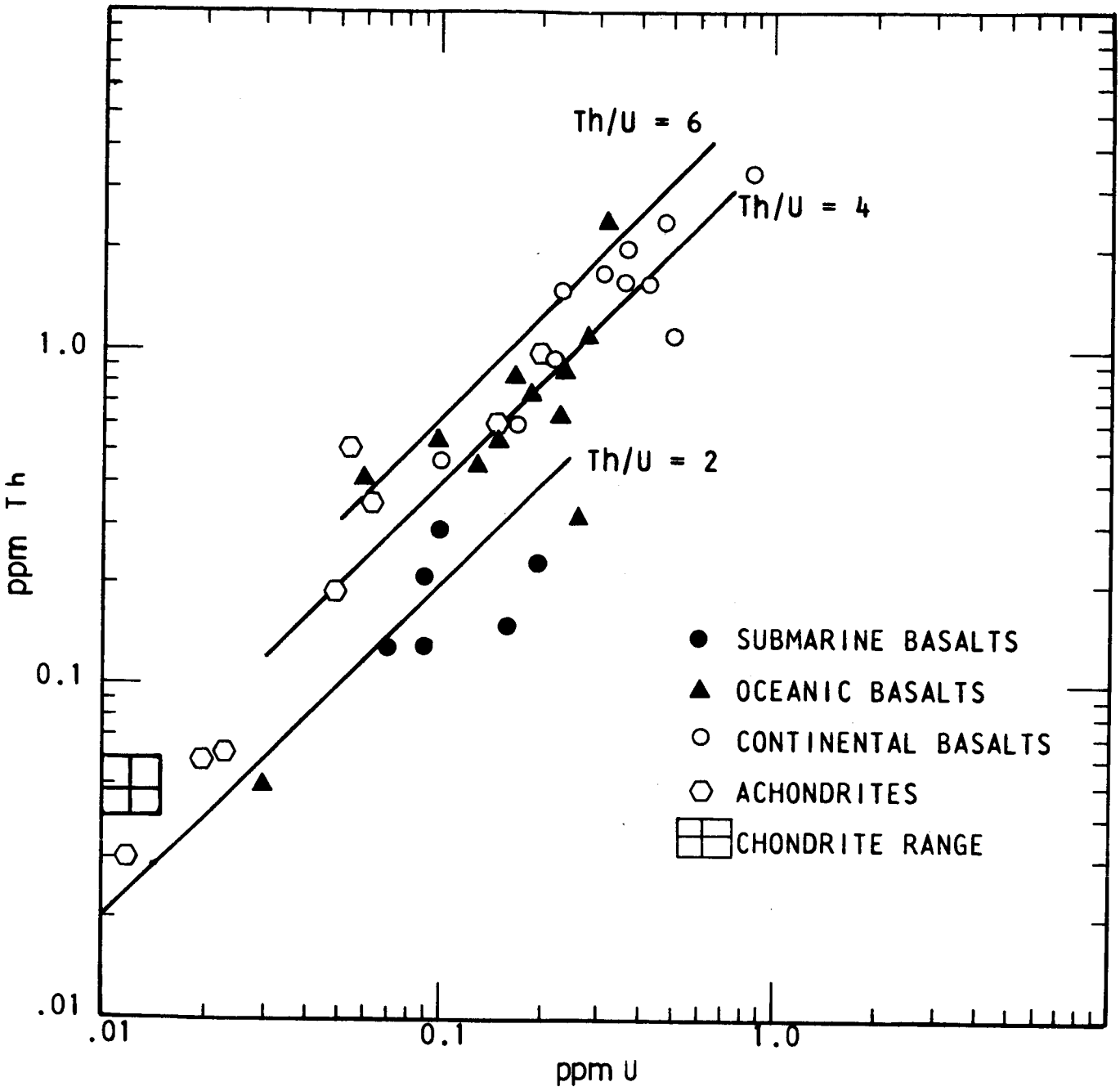

FIGURE III-2 Th-U COMPOSITIONAL VARIATIONS IN THOLEIITIC BASALTS AND METEORITES

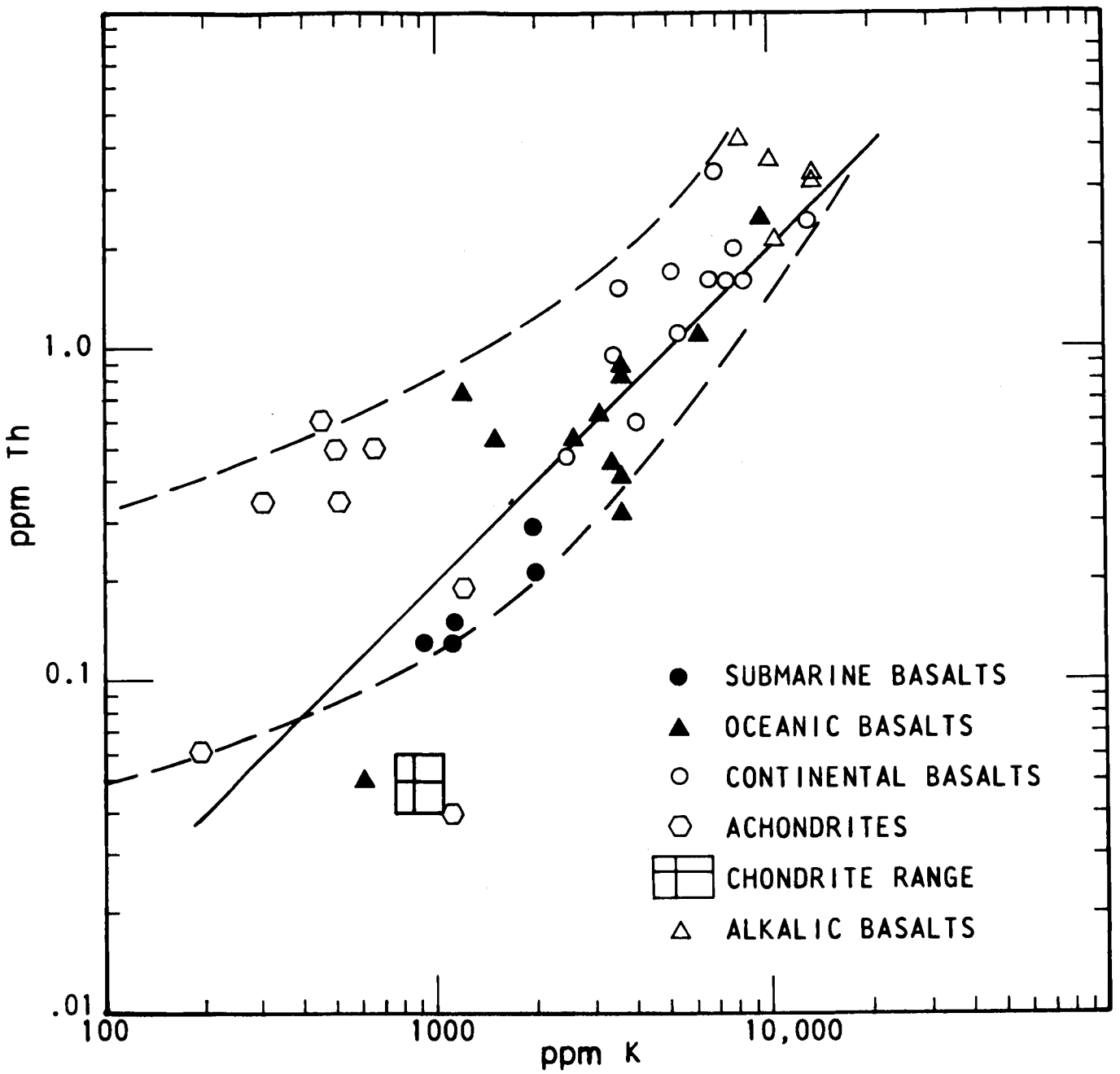

FIGURE III-3 K - Th COMPOSITIONAL VARIATIONS IN BASALTS AND METEORITES

If the achondrites represent the partial melt fraction of a primary mantle composition, then the chondrites may represent the unmelted residue. Thus if the tholeiitic basalts represent the partial melt fraction from a similar primary mantle composition then the achondrites should be similar to the tholeiitic basalts and the chondrite composition should be roughly representative of the source material.

In Figure III-1 it will be noted that the achondrites fall at lower concentrations and somewhat in line with the submarine basalts. In Figure III-3 the achondrites fall at lower potassium concentrations but thorium concentrations are roughly equivalent to those of the oceanic basalts. In Figure III-2 the achondrite points scatter widely ranging from below the submarine into the oceanic basalt points. In each case we have indicated the chondrite range on the graphs.

d. Rare Earth Data

Frey and Maskin (1964) examined the rare earth abundance distribution patterns in three basalts from the mid-Atlantic ridge and one from the experimental moho project. They found that the absolute rare earth concentrations are 10 to 16 times those of chondritic meteorites and are comparable to those of calcium rich achondrites. They pointed out that the relative distribution patterns are barely altered from that characteristic of chondritic meteorites. These and other rate earth data are compiled in Table III-6.

Earlier work of Haskin and Gehl (1962) on sediments has indicated a fractionation of the lighter rare earth elements relative to the chondritic abundance; the lighter rare earth elements have the larger atomic radii and are more concentrated in the sediments than the heavy rare earth elements relative to the chondritic abundances. Schilling and Winchester (1966) have examined four tholeiites from the Hawaiian Islands and have again found a fractionation of increasing abundance of the lighter rare earth relative to the chondritic abundance.

Again (see Table III-6) there seems to be a changing trend in the behavior of the rare earths as one goes from the submarine basalts towards the continental basalts. The rare earth concentrations in the submarine basalts are comparable to those in the achondrites. Both the achondrites and the submarine basalts show the same relative abundance as the chondrites. However, the tholeiites from the Hawaiian Islands show a fractionation behavior with a greater abundance of the lighter rare earths corresponding to those with the greater ionic radii. A similar behavior has been observed in sediments. Note also that the Y/La ratio behaves in the same manner as that observed for the alkali elements.

e. Ultramafic Inclusions

In Figures III-1, 2, and 3 we have included data for the chondrites which in many peoples thinking represents the residual source from which the achondrites were derived. Similarly, many people believe that the ultramafic inclusions found in basalts represent samples of the source mantle which have been carried along in the magma.

Steuber and Murthy (1966) have studied the potassium to rubidium ratio in ultramafic rocks. The rocks studied included ultramafic inclusions from basalts and kimberlites. These data are plotted on Figure III-1. It may be noted that these data trend from the vicinity of the chondrite data towards lower rubidium and potassium compositions. This is the direction one would expect if they truly represent samples of the source rock from which the tholeiitic basalts were derived and if the original mantle composition was approximately chondritic. The compilation of Steuber and Murthy included one sample of a basalt from which a corresponding inclusion had been derived. These coupled samples are indicated on the graph. The basalt sample lies at the upper limit of our band of potassium-rubidium concentrations in the tholeiitic magmas while the ultramafic inclusion lies towards the lower concentration limit of these inclusions.

TABLE III-6

COMPILATION OF RARE EARTH ANALYSES

(reported in ppm)

	1	2	3	4	5	6	7	8	9	10	11	12	13	14	15
Y	1.80	-	33.7	47.3	33.7	29.9	16.4	15.2	18.75	22.4	22.1	19.31	.319	1.87	53
La	0.30	3.21	4.51	3.0	4.98	1.87	5.30	7.22	6.24	8.41	8.78	13.3	.115	.995	25.3
Ce	0.84	8.08	17.8	17.9	-	13.9	-	15.8	-	-	-	-	-	-	-
Pr	0.12	1.26	2.12	2.45	2.41	1.92	2.56	3.48	2.86	3.86	4.32	4.88	-	.277	7.90
Nd	0.58	5.66	13.2	13.5	14.0	8.63	12.8	20.1	14.59	19.31	20.9	21.52	.294	1.36	36.6
Sm	0.21	1.90	4.38	4.76	4.41	2.83	3.74	4.94	4.09	5.26	5.06	4.78	.051	.336	10.0
Eu	0.074	0.68	1.80	2.07	1.89	1.35	1.28	1.77	1.31	2.03	1.77	1.55	.014	.103	-
Gd	0.32	2.69	6.54	8.35	7.25	4.58	-	-	-	-	-	-	-	-	10.2
Tb	0.049	-	1.25	1.27	1.65	0.83	.66	.85	.73	1.00	.868	.69	-	.060	1.66
Dy	0.31	3.06	-	-	-	-	3.72	3.14	4.20	4.80	4.99	3.80	-	.318	9.6
Ho	0.073	0.69	1.66	2.10	1.40	1.06	.57	.85	.67	.75	.787	.68	.008	.048	1.94
Er	0.21	1.63	4.67	5.79	-	3.34	-	-	-	-	-	-	-	-	-
Tm	0.031	0.03	0.79	0.83	1.18	0.41	.20	.32	.22	.26	.267	-	-	.0215	0.75
Yb	0.17	1.67	4.00	4.00	4.20	2.80	1.26	1.85	1.45	-	2.06	1.70	.025	.112	-
Lu	0.031	0.50	-	0.92	0.79	0.57	.19	.30	.20	-	.288	.28	.004	.020	0.64

1. Average of 20 chondrites (from compilation of Schilling, 1966)
2. Pasamonte achondrite (Schmitt et al., 1963)
3. Atlantic ridge basalt GE-159 (Frey & Haskin, 1964)
4. Atlantic ridge basalt GE-160 (Frey & Haskin, 1964)
5. Atlantic ridge basalt GE-260 (Frey & Haskin, 1964)
6. Experimental mohole basalt (Frey & Haskin, 1964)
7. #9948, Olivine Tholeiite, Koolau series, Oahu (Schilling, 1966)
8. JP-12, Tholeiite, Koolau series, Oahu (Schilling, 1966)
9. 10398, Diabase Koolau series, Oahu (Schilling, 1966)
10. 10396, Tholeiite, Koolau Series, Oahu (Schilling, 1966)
11. 10403, Tholeiite, Koolau Series, Oahu (Schilling, 1966)
12. 1801 flow, Alhali olivine basalt, Hualalai, Hawaii (Schilling, 1966)
13. Olivine rich nodule - 1801 flow, Haulalai, Hawaii (Schilling, 1966)
14. Peridotite nodule, Salt Lake Crater, Oahu (Schilling, 1966)
15. Columbia plateau tholeiitic basalt (Schmitt et al., (1964))

FOLDOUT FRAME 1

FOLDOUT FRAME 2

D. DISCUSSION

1. Variations in Tholeiite Composition

a. Observations to Interpret

We have observed consistent trends in compositions of some of the trace elements as we proceed from submarine towards continental tholeiites. These trends consist of variations both of absolute and relative concentrations. We would like to develop in this section an interpretation of these trends and of the relationships between the tholeiitic basalts, the ultramafic inclusions, and the chondrite-achondrite data.

b. Some Basic Assumptions

We assume that the tholeiitic basalts are obtained directly from the mantle. This is supported to some extent by the seismic studies described by Eaton and Murata (1960) which indicate a source region at about 45 to 60 km for the Hawaiian volcanos. We also assume that the tholeiitic basalts reach the surface without contamination or extensive fractional crystallization enroute. Continental basalts are the one most likely to have been contaminated because of their passage through the continental crust. However, these flows are of extreme size and many workers have indiated that there is no real evidence for contamination by surrounding rocks.

If we consider that these basalts come to the surface directly from the mantle then we must consider whether they come from a mantle of constant composition or from a mantle of varying composition. We have considered the possible consequences of a mantle of variable composition either in a vertical or horizontal direction and have found no real evidence to support such variations. It is conceivable from thermodynamic considerations that there could be a

vertical differentiation of the mantle as a result of variation in molecular weight and partial molar volumes of the ions. We have made some order of magnitude estimates which indicate that this factor could become significant in terms of concentration ratios over distances on the order of 100 km. Our estimates for the alkali elements indicate that such a differentiation would favor concentrating light elements near the surface and heavy elements at depth. In other words, in a basalt from a depth where sodium and potassium are high, rubidium and cesium would be extremely low and vice versa. This behavior is contrary to the experimental evidence. The experimental results for the tholeiites indicate that all the alkali metals we have examined (potassium, rubidium, and cesium) are increasing as one goes from the submarine towards the continental basalts. It is also very questionable in our opinion that the diffusion coefficients are sufficiently great to have permitted this differentiation to occur.

Alternatively, one might consider that the mantle composition varies significantly horizontally from place to place due possibly to previous extrusion of basalts. However, the data indicate similar compositions of submarine basalts in both the Atlantic and Pacific and we see no basis yet for accepting a marked horizontal variation in mantle composition.

Thus, the simplest concept and the one which appears most reasonable at this time is to interpret the formation of the tholeiitic basalts by a partial melting of a mantle of essentially uniform composition; the magma proceeds to the surface without extensive fractional crystallization or contamination by the rocks through which it passes.

c. Some Factors Which Can Cause Compositionsal Variations During Partial Melting

The variations in tholeiite compositions which we observe are probably the result of several factors. The pressure and temperature

conditions at the point of origin of the tholeiite certainly determines the solid phases present and the fraction melted and thus affects the compositions of the melt which we observe at the surface. The effect of pressure and temperature can be more readily pictured by looking at a plot such as that for the forsterite-nepheline-silica system which has been presented by Kushiro (1965) as shown in Figure III-4. This three component plane is certainly not the one in which the basalts melt or can be correctly represented since it does not include many components of the basalts or of the mantle source. However, it does help to picture the changes in melt composition caused by pressure and temperature. Note that with increasing pressure the binary eutectic between the forsterite and enstatite phases is moving on the compositional diagram. Also with increasing pressure the third phase changes from albite to jadeite to nepheline. We have placed an X on this diagram indicating the composition corresponding approximately to pyrolite 3:1 which we adopted in our earlier work as a model for the mantle composition. We have also indicated points on the 1 bar, 10, 20, and 30 kb binary eutectic lines which show the melt composition at approximately 25% melting of the pyrolite. It is easily seen that the melt composition will change with pressure and likewise would change at a given pressure with the fraction melting. Thus it is not surprising if we consider both pressure and melt fraction to change that we find no consistent trend in the major components as we move from submarine towards continental basalts. It is easily seen that considerable changes in fraction melted combined with changes in pressure on the order of 10-15 kb would tend to smear out the compositional data for the melt over a range which is not inconsistent with variations observed in major component composition.

While we observe only relatively small compositional changes for the major components of the tholeiites this is not true for the minor elements. As we have seen in an earlier section of this report there are changes of an order of magnitude or more for many of those elements which are present in quantities of less than 1% such as

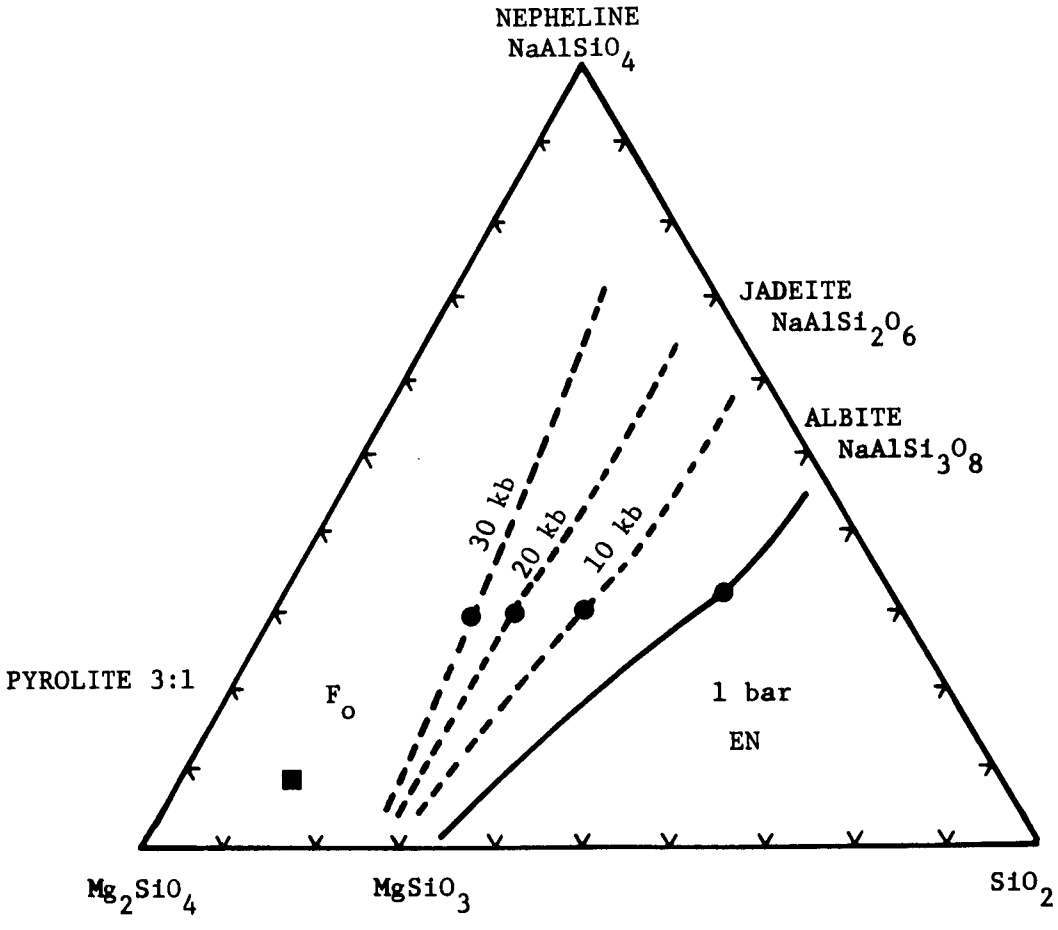

FIGURE III-4 THE FORSTERITE-NEPHELINE-SILICA SYSTEM
(after Kushiro, 1965)

potassium, rubidium, cesium, thorium, and uranium. If the mantle composition is to be considered relatively constant, then we can conceive of two mechanisms in the process of formation of these tholeiitic basalts by which one might obtain the vary trace elements concentrations observed. These are the consistent variation with depth of the melt fraction and/or the distribution constants.

1) Variation in Melt Fraction. Let us consider first the changes to be expected for trace element distribution between a melt and a solid phase as melt fraction is varied. From thermodynamics we can express the chamical potential or escaping tendency of a component i of a single phase by the expression

$$\mu_i = \mu_i^o (P,T) + RT \ln c_i$$

where c_i represents the concentration of component i and μ_i^o is a constant which is a function of pressure and temperature. At equilibrium between the melt and a solid phase the chemical potentials are equal.

$$\mu_i^s = \mu_i^\ell$$

$$\mu_i^{os} + RT \ln c_i^s = \mu_i^{ol} + RT \ln c_i^\ell$$

$$\ln \frac{c_i^\ell}{c_i^s} = (\mu_i^{os} - \mu_i^{o\ell})/RT$$

$$\frac{c_i^\ell}{c_i^s} = e^{\frac{\mu_i^{os}(P,T) - \mu_i^{o\ell}(P,T)}{RT}} = K_i (P,T)$$

Thus the concentration ratio equals a constant which represents the distribution between the two phases at constant pressure and temperature.

Now to examine the effect at constant pressure and temperature of varying melt fractions, one other relationship is required. This is the mass balance equation for the component c_i. If the total concentration of component i is c_i^o and F is the melt fraction, then

$$c_i^\ell \; F + c_i^s \; (1 - F) \; = \; c_i^o$$

Taken together one derives from the two relationships

$$c_i^\ell \; = \; \frac{K_i \; c_i^o}{1-F + K_i F}$$

Examination of this expression will show that for K_i greater than one, the smaller the melt fraction the larger the concentration of component i anticipated in the melt. For two chemically similar components with K_1 not equal to K_2 the ratio of concentrations is given by the expression

$$\frac{c_1^\ell}{c_2^\ell} \; = \; \frac{K_1 \; C_1^o \; (\frac{1}{F} - 1 + K_2)}{K_2 \; C_2^o \; (\frac{1}{F} - 1 + K_1)}$$

Again examination of this expression will show that the smaller the melt fraction the greater the difference in the liquid ratio as compared to the original composition ratio.

If we are to assume that the observed changes in absolute concentration of our basalts are due to changes in the fraction of the mantle melted then we can anticipate that when we have the maximum absolute concentrations we will have the maximum relative change in concentrations from that existing in the mantle. Likewise, a high melt fraction will give low absolute concentrations and relative concentration ratios more comparable to those in the original mantle. These trends are contrary to those we observe if we assume that the relative concentrations in the mantle composition are comparable to those observed in chondrites.

2) Variation in Distribution Constants. In the previous paragraphs we observed that the two trends in trace element composition, that is, the absolute change and relative change in concentrations, are not mutually consistent with the variation expected due to variations in the fraction melted of the mantle. Earlier we argued that these were not consistent with a prior differentiation of the mantle. We will now explore whether these data can be consistent with a variation in distribution constants with depth.

We believe that this possibility is strongly indicated by the rare earth data. We know from studies of magmas which have been subjected to fractional crystallization near the earth surface and from laboratory studies that large ions tend to be concentrated in the residual liquid indicating larger distribution constants for the large ions. Experimental studies have indicated that the rare earths in the Hawaiian basalts may be differentiated with respect to ion size. The lower atomic number or larger rare earth ions are concentrated in Hawaiian basalts with respect to their relative concentrations in the chondrites. On the other hand experimental data show that in the mid-Atlantic ridge or submarine basalts the relative concentrations of the rare earth elements are the same as those in the chondrites. In other words under some conditions of formation of the tholeiitic basalts the rare earth elements are distributed in a manner contrary to that we would expect in a surface laboratory and contrary to that we observe in other tholeiitic basalts. In our opinion the most likely factor affecting this change in distribution is the pressure.

In order to consider the effect of pressure on distribution constants let us look for factors which might influence the distribution and that change with pressure. We should consider at least three: number of sites, the size of sites, and the size of ions. The number of sites and the size of the sites both in the liquid and in the solid reflect differences between the solid and liquid. The size of ions has long been considered a factor controlling the incorporation of trace elements in crystallizing compounds.

Based on a consideration of these factors we can make the following qualitative statements with regard to the trend of a distribution constant with pressure.

1. With increasing pressure the volume of the liquid becomes more like that of the solid. In other words, the liquid and the solid become more alike in terms of the size and nature of the sites and thus we might expect on this basis that the distribution constant should approach 1 with increasing pressure.

2. As one goes from low pressures to high pressures we recognize that the solid phases present at the liquidus change; the plagioclase tends to disappear and we tend towards an olivine-pyroxene system with the solubility of aluminum in the pyroxenes becoming greater with pressure. This factor might be expected to increase the number of sites for alkali ions in the pyroxene mineral and thus to decrease K with increasing pressure.

3. The size of ions certainly will decrease with increasing pressure. In addition the larger ions tend to be more compressible than the smaller ones. Thus with increasing pressure a chemically similar series like the alkali metals becomes more alike in size and thus we might expect more similarity in distribution constants with increasing pressure. The major changes in distribution constants would occur for the more highly compressible ions.

If we assume that the mantle composition is chondritic, then according to statement (1) the tholeiites which most closely approach the chondrites in trace element composition must be derived from partial melting at greatest depth corresponding to melting under the highest pressure conditions. We do observe as shown on Figures III-1, III-2, and III-3 that the alkali ions, thorium, and uranium content of the submarine basalts approach closest to the chondrite composition. The continental tholeiitic basalts are furthest removed in concentrations of these trace elements from that of the chondrites.

Now assuming that the submarine basalts are derived from partial melting at greatest depths, then as the depth of melting is decreased the most compressible ions should change the most in size and thus favor their concentration in the more voluminous liquid. As indicated on Figure III-1 rubidium does increase more rapidly than potassium and we find decreasing ratios of potassium to rubidium as we move from submarine to continental basalts. The same relationship holds true for the sodium to potassium ratio, the potassium to cesium ratio and the yttrium to lanthanum ratios. In addition the rare earth data show a relatively greater concentration of the larger ions as we move away from the submarine basalts towards the continental basalts. In every case there is a relatively greater increase in the concentration of the more compressible ions in the melt.

In our opinion the existence of marked changes in distribution constant with pressure is a likely explanation for the observed data. This is not to say that it is the only factor. Melt fraction may also change and there may exist some degree of differentiation of the mantle. But these are apparently not the major factors causing the observed changes although they must contribute to some degree to the scatter of the observed data.

d. Compressibility Data

Our argument that pressure effects on distribution constants are the critical factor in determining the compositional variations of the minor elements requires a more detailed discussion of compressibility data. We recognize from fractional crystallization data that for a chemically similar series such as the alkali metals the distribution of these ions between two phases such as a solid compound and a melt can be dependent on the size. The size increases with atomic weight and thus we observe larger distribution constants for cesium than for potassium. However, we must also recognize that in general the compressibility increases as one goes down a column of the periodic table. In other words with increasing pressure the chemically similar ions become more alike in size and thus on this basis we would expect the distribution constants to also become more alike with increasing

pressure. This compressibility effect is recognized in compounds as well as in metals and can be illustrated by some data from Drickamer et al. (1966) who have recently summarized X-ray diffraction studies of lattice parameters of solids under very high pressure. For example $\frac{V}{V_0} = 0.9$ at approximately 225 kb for MgO while this degree of compression is achieved at 130 kb for CaO. For carbides the compressibility change is greater for ZrC than for TiC and for TaC than for NbC.

We present in Table III-7 data on the relative ionic radii of the ions of interest and in Table III-8 compressibility data for several metals. Assuming that the relative compressibility of the ions is the same as the metals one can see that the relative difference in size decreases markedly with increasing pressure.

e. Rare Earth Data

The rare earths are of course very much alike chemically and differ only slightly in atomic weight. There is, however, a decrease in ionic radius as electrons are added due to an electrostrictive effect. One might therefore expect that the larger ions would be more compressible than the small ones which have already been partially compressed due to the electrostrictive effect. Thus with increasing pressure the rare earths should be expected to become more alike in size. They are already chemically similar, thus with increasing pressure or at high pressures one would expect less fractionation than at low pressures. Thus, assuming that the submarine tholeiites are formed at greatest depth, it is to be expected that they show the least fractionation relative to the chondrites.

f. Chrondrite-Achondrite Data

As shown in Figures III-1, III-2, and III-3 the achondrite data in general falls within or is an extension of the tholeiitic basalt data. Assuming that the achondrites represent the melt fraction of a "chondritic" mantle and that the chondrite data represent the

TABLE III-7

RELATIVE IONIC RADII

	1 atm*	50 atm**
Na^{+}	0.95	(.85)
K^{+}	1.33	(1.12)
Rb^{+}	1.48	(1.23)
Ca^{+}	1.69	(1.28)
Mg^{++}	0.65	(0.63)
Fe^{++}	0.77	
Ca^{++}	0.99	(0.93)
Al^{+++}	0.50	
Th^{+4}	0.99	
U^{+4}	0.93	

* Taken from Wells (1962)

** Estimated from compressibility data of Table III-8.

TABLE III-8

COMPRESSIBILITY DATA FOR SOME METALS

P	$(Vo - V)/Vo$							
(kg/cm^2)	Mg	Ca	Na	K	Rb	Cs	Th	U
10	.02634	.058	.1115	.1862	.1982	.2392	.01733	.095
20	.0499	.103	.1836	.2772	.2920	.3442	.03188	.0181
30	.07056	.139	.2350	.3360	.3530	.4261	.04555	.0255
40	.081	.168	.2740 / .263	.3774	.3954 / .388	.4816	.063	.0324
50	.096	.195	.292	.405	.422	.569	.076	.040

Data from Table 7-2, S. P. Clark, Jr. (1966).

residual mantle we can calculate the distribution constants for the alkali metals between the melt (achondrite) and solid (chondrite). We find a distribution constant for sodium of approximately 1, potassium approximately 0.5, rubidium and cesium approximately 0.1. If all of the alkali metals are competing for sites in the chondrites, then the distribution constants observed are in agreement with the relative stability observed for the alkali chlorides, bromides and iodides. In the chloride, bromide and iodide series one finds the cesium halide to be the most stable compound. This is consistent with general behavior across the periodic chart of the elements, and the fact that the fluoride and oxide compounds of the alkali elements do not show this general stability behavior is attributed to an ion size effect; the usual explanation is that the fluoride and oxide ions are not large enough with respect to the alkali ions. However, it should be noted that with increasing pressure the oxygen ion size would decrease less with pressure than the high atomic weight alkali ions and thus we would expect that pressure should tend to restore the natural stability order to the alkali oxides and fluorides which is that order observed in the chondrite-achondrite data.

In general the achondrite data for the trace elements appears to indicate that they were melted at pressures equal to or slightly greater than the submarine basalts. In addition we can say that the relative distribution constants between the chondrites and achondrites are at least consistent with our picture of variation in distributions constants with pressure due primarily to the effect of pressure on the size of the higher atomic weight elements.

g. Ultramafic Inclusions

We have plotted on Figure III-1 data for the ultramafic inclusions from basalts and kimberlites reported by Steuber and Murthy (1966). In our opinion these data are also consistent with changes in distribution constants with pressure if the mantle composition is

originally close to "chondritic" in nature, thus as we remove a larger proportion of the potassium and rubidium due to melting at different depths the residual mantle composition would become lower and lower in these elements. The one pair of data points consisting of the basalt and associated inclusion represent extreme limits of the distribution.

2. Composition of the Mantle

When order of magnitude differences exist between the concentrations in the melt and in the residual solid then the element ratios in the melt might be expected to approximate those in the original mantle. If we examine Figure III-1 we find that the ratios in the most alkali rich basalts are relatively consistent with those for both the chondrite composition and the ultramafic inclusion compositions. In Figure III-2 we find that the thorium to uranium ratios in the continental basalts are essentally consistent with the ratio found in chondrites. However, in Figure III-3 when we attempt to relate the data at high concentrations to those in the chondrites we find that they are not equal. Chondrites must be low in thorium relative to the original mantle composition. This is easily understandable since one sees from Figure III-3 that there is a very high distribution constant for thorium as compared to potassium assuming that the achondrites and chondrites represent melt and residual solid. It appears from Figure III-3 that the original chondrite-achondrite source material or "chondritic" mantle composition must have been approximately 750 ppm potassium and 0.15 ppm thorium. Consequently from Figure III-2 the corresponding uranium composition must have been approximately 0.035 to 0.04 ppm. It is interesting to observe that MacDonald (1964) in his studies of the "Dependence of the Surface Heat Flow on the Radioactivity of the Earth" found it necessary to invoke higher amounts of heat producing elements in the mantle than those found in chondrites in order to produce the observed heat flows at the surface of the earth.

It appears to us that these levels of uranium and thorium compositions in the mantle are also consistent with the derivation of the mantle from Type I carbonaceous chondritic material by loss of volatiles and metallic iron and nickel. In Table III-9 we show the range of uranium and thorium content of Type I carbonaceous chondrites reported by Morgan and Lovering (1967) and the SiO_2 content as reported in Mason (1962). Assuming that the U and Th remain with the SiO_2 to form a mantle composition we estimate the content of these elements in pyrolite based on its SiO_2 content. The values estimated by this procedure agree well with the values predicted for the mantle composition in the previous paragraph from the trace element distributions. For comparison we also list an average composition for chondrites from Mason (1962).

E. CONCLUSIONS

Thus we conclude that the depth of origin primarily accounts for the compositional variations observed in the tholeiitic basalts. The variation in fraction melted may contribute in some degree to the scatter observed.

We have at no point discussed the effects of fractional crystallization on the composition of these magmas. We have assumed that the tholeiitic magmas for the most part rise directly to the surface from their point of origin in the mantle and thus the compositional data variations give a measure of the relative depth of origin. Fractional crystallization, however, is very likely the important mode for compositional changes in basalts which stop for extended periods enroute to the surface. We believe that for the most part the alkalic basalts which occur in very small quantity relative to the tholeiitic are differentiates of tholeiitic basalts which have spent considerable time in secondary magma chambers near the surface..

There are two other pieces of evidence which we believe offer some support to the picture which we have developed regarding the relative depth of origin of the tholeiitic basalts. The first is seismic studies

TABLE III-9

PREDICTION OF POTASSIUM, URANIUM AND THORIUM CONTENT OF PYROLITE

BASED ON CARBONACEOUS CHONDRITE COMPOSITIONS

MATERIAL	COMPOSITION			
	U	Th	K	SiO_2
Carbonaceous Chondrite (Type I)	.008 - .024 ppm[1]	.028 - .071 ppm[1]	320 - 600 ppm[2]	22.5%[2]
Pyrolite	(.016 - .048)[3]	(.056 - .142)[3]	(640 -1200)[3]	43 [4]
Mantle[5]	.035 - .040	~0.15	750	--
Chondrites[2]	0.014	0.04	750 -1050	36

(1) Morgan and Lovering (1967)

(2) Mason (1962)

(3) Prediction based on silica content and carbonaceous chondrite composition

(4) Pyrolite composition as used in previous study, see McConnell et al. (1967)

(5) Potassium, uranium and thorium content as derived from Figures III-3 and III-2.

in the region of the Japanese Islands by K. Aki (1967). Kuno has very well documented the variation in basalts as one goes from the ocean towards the continental side of the Japanese Islands. The basalts vary from a tholeiitic to a high alumina to an alkalic basalt. Based on our present understanding, we would claim that the tholeiitic basalt was derived from the greatest depth, the alkalic basalt from a secondary magma chamber close to the surface, and the high alumina basalt from an intermediate region. K. Aki found it necessary in order to interpret his seismic data to develop a model which placed melt closer to the surface as one moved inland away from the ocean.

The second argument which we believe offers some support to the relative depth of origin of tholeiitic basalts is based on the idea that the mid-Atlantic ridge is indicative of an upward convective current in the mantle. The basalts from the mid-Atlantic ridge are of extremely deep origin in terms of our interpretation based on trace element concentrations. These basalts have been flowing out and moving away from the mid-Atlantic ridge for millions of years. Under such steady state flow conditions they must be derived at greater depths in the mantle than basalts arising from non-flow situations such as those we presume to exist in the Hawaiian Islands.

IV. IMPLICATIONS OF HEAT FLOW AND COMPOSITIONAL DATA FOR LUNAR THERMAL HISTORY

A. INTRODUCTION

At the end of the previous contract we reported: "After examining the available evidence we have found no compelling reasons to assume that the moon's composition differs significantly from that postulated by Ringwood and others for the earth's mantle. We have approximated the composition by a mixture of basalt and dunite and have used published data on silicate minerals to predict the thermal properties and melting relationships as functions of pressure and temperature. The more important aspects of these predicted functions have been selected and used to extend the normal thermal history calculations of the moon to include the effects of differentiation through igneous activity. The calculations indicate that a brief period of intense volcanic activity is likely to have occurred; the time at which this activity took place will be primarily a function of the moon's temperature at the time of its formation and the concentration of radioactive heat sources."

We have seen in the previous chapters how more detailed examination of the implications of the original model have led us to the conclusion that to be consistent with present day observations of the earth's upper mantle some minor changes are necessary. Recent work by Shoemaker (1966, and private communication) on crater statistics, and observations by several groups of apparent color changes can be interpreted to mean that volcanic activity is now occurring or has occurred in the relatively recent geological past. While these data and the conclusions derived from them are are not yet conclusive, it does appear that the possiblity of recent volcanism must also be considered. We will therefore first of all examine the implications of a revised terrestrial mantle composition for the moon and then briefly discuss some further changes in the model that might be necessary if volcanic activity is demonstrated.

B. IMPLICATIONS OF A "MANTLE FOR THE MOON"

We have not yet had the opportunity to carry out a detailed computer simulation of the lunar or terrestrial thermal history to examine all the implications of the revised model. Nevertheless, from the discussion in the previous chapters and by comparisons with the results developed in our first report, it is possible to make some estimates about the way in which the revision will influence our predictions of the time at which lunar volcanic activity begins, the duration of the activity, and the composition of resulting melts.

1. Beginning of Volcanic Activity

If we take the specific heat of the moon's interior to be 1.1 joules/gram °K, the heat required to raise its temperature from 273°K to 1500°K, approximately the pyrolite solidus at 15 kb, will be about 1350 joules/gram. To raise it to 1650°K, and melt 25% at 500 joules/gram will require another 300 joules per gram. Figure IV-1 compares these values with the total amount of heat generated per gram of material for the revised mantle model (mean values from Table III-9), pyrolite-1:4 with "terrestrial" isotope ratios, and the chondrite model used by MacDonald (1959). We see that for the revised mantle model, after about 1×10^9 years from the time of formation enough heat will have been generated to begin melting. For the terrestrial and chondritic models the same amount of heat would be generated after about 1.5×10^9 and 2.0×10^9 years from the time of formation, respectively. Thus we expect that a more rigorous computer simulation would predict a volcanic history of the moon which began considerably earlier for the mantle model than it did for the pyrolite one. If direct observation of the lunar surface indicates recent volcanic activity, it seems clear that its composition cannot be the same as that predicted for the earth's mantle in the previous chapter. Although a lower temperature at the time of formation might make some small change in the time of onset of volcanism, it is difficult to see how this could have any major effect.

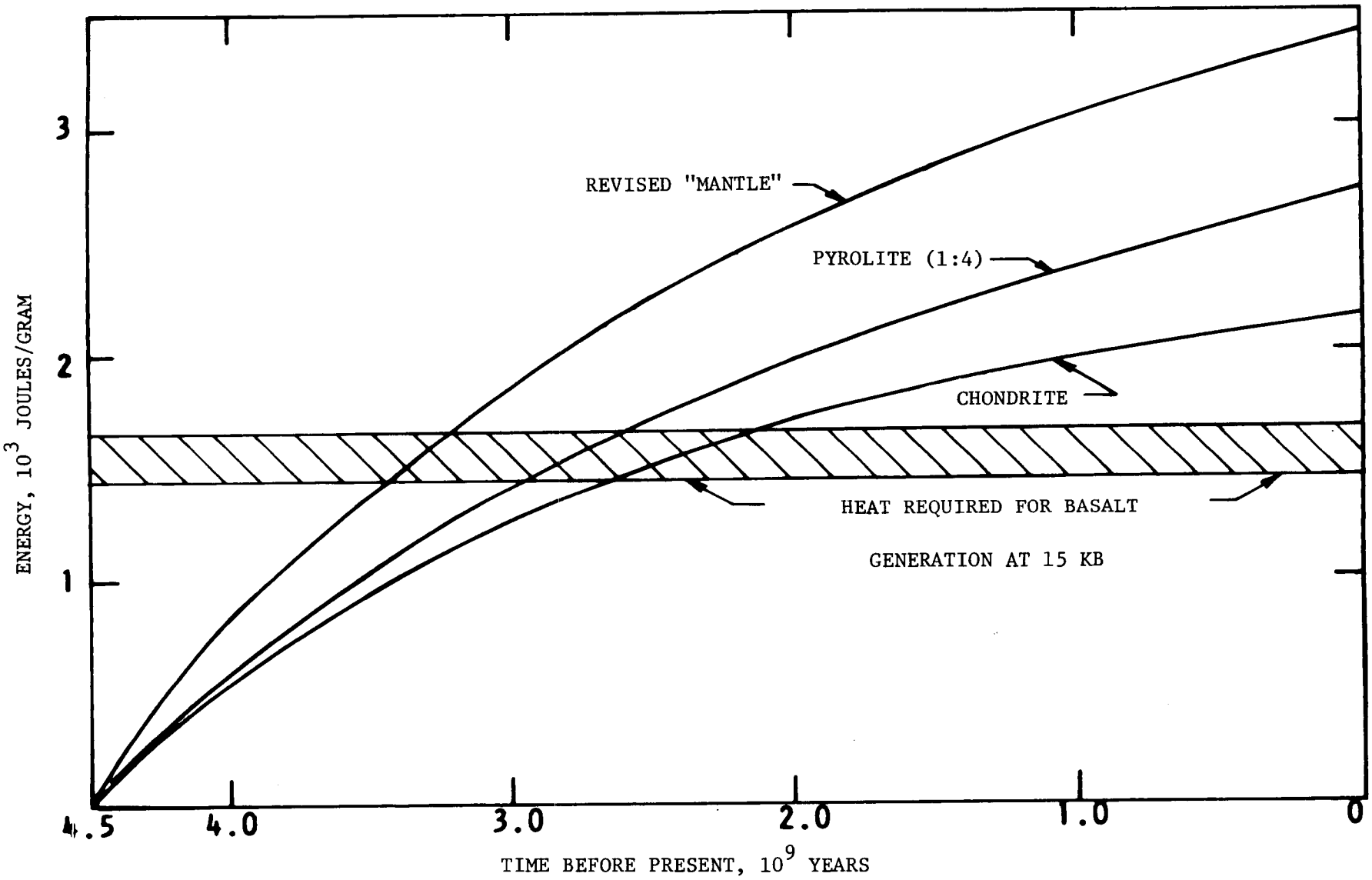

FIGURE IV-1 ACCUMULATED HEAT PRODUCTION FOR VARIOUS COMPOSITIONS AS A FUNCTION OF TIME COMPARED WITH AMOUNT REQUIRED FOR FORMATION OF 25% BASALT MELT AT 15 KB

2. Duration of Volcanism

In McConnell, et al. (1965, 1967) we showed that the duration of volcanism predicted by the computer model should be roughly proportional to the rate of heat generation at the time that volcanic activity begins. The rate of heat production as a function of time for the models of Figure IV-1 is shown in Figure IV-2. We estimated the half life of volcanic activity for the pyrolite-1:4 with terrestrial ratios to be about 3×10^8 years. An examination of Figure IV-2 suggests that the duration of volcanic activity would not be very much different from this either for the revised mantle model or for MacDonald's chondrite model. For the mantle model we would estimate the half-life to be about 2×10^8 years and for the chondrite about 4×10^8 years on the basis of the rate of heat production at the time melting began. These estimates are based on the assumption that all the radioactive isotopes are equally distributed in the basalt fraction. Calculations of the implications of a more realistic partitioning of the trace elements as derived in Chapter III would require modification of our computer programs and will have to be left for future work.

3. Composition of Melts

In our discussion of compositional variations of basaltic magmas we concluded that differences in the depth of origin primarily account for the variations observed in the tholeiitic basalts. We pointed out that we believe the "oceanic" tholeiites such as those found on the Hawaiian Islands have been derived from shallower depths than "submarine" basalts.

Eaton and Murata (1960) have interpreted the seismic evidence to mean that the Hawaiian magmas are derived from depths of 45-60 km where the pressure is around 13-18 kb. We expect that melts derived under similar pressure and composition conditions on other planetary bodies would have a similar composition. The work of Toksoz, Chinnery, and Anderson (1967) has indicated a region of very low shear velocity under the oceans which is centered around 100 km where the pressures are about 30 kb. Recalling that our interpretation of the chemical evidence was that the "submarine" basalts

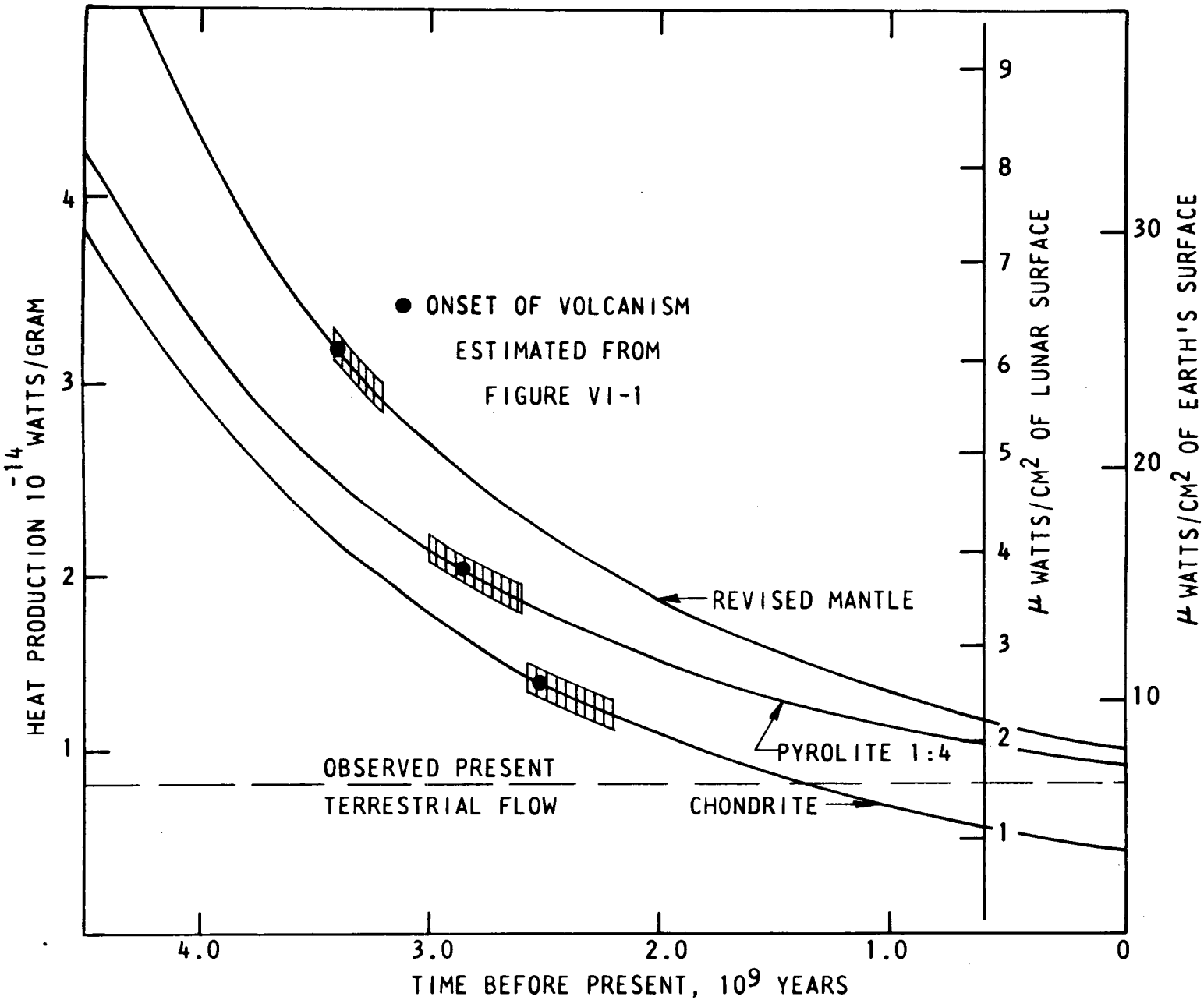

FIGURE IV-2 RATE OF HEAT PRODUCTION FOR MODEL COMPOSITIONS AS A FUNCTION OF TIME IN (a) WATTS/GRAM, (b) MICROWATTS/CM^2 TERRESTRIAL SURFACE WITH ALL HEAT SOURCES IN MANTLE, (c) MICROWATTS/CM^2 OF LUNAR SURFACE AREA

are formed under higher pressure conditions than the "oceanic" basalts it seems logical to postulate that the source of the deeper melts is in this region (Figure IV-3).

Having established the probable pressures under which terrestrial basaltic melts of the different compositions are derived, we may proceed to estimate what compositions would be most compatible with melting under lunar conditions. Most reasonable thermal models for the moon, including those described by McConnell, et al. (1965, 1967) indicate that the minimum depth of melting probably lies between 350 and 800 km on the moon. As these depths correspond to pressures of 18-30 kb even the shallowest lunar primary melts are likely to have been formed at pressures equal to or greater than those for "oceanic" basalts. Thus, we conclude that if the composition of the moon does not differ significantly from the earth's upper mantle, its primary magmas are likely to be more like "submarine" tholeiites than the "oceanic" ones.

Below 1000 km on the moon, pressures are even greater than those we infer for the source region of the submarine basalts. Recalling that we interpreted the trace element data for basaltic achondrites to indicate that they were melted at pressures equal to or greater than submarine basalts, it would seem that these might represent melts very similar to those from the lunar interior, if it has a "mantle" in its composition.

C. IMPLICATIONS OF POSSIBLE RECENT LUNAR VOLCANISM

So far we have neglected the implications of the possibility that the moon's primary period of igneous differentiation has taken place recently. Such recent activity also implies a late beginning of volcanism which in turn requires much lower initial concentrations of radioactive elements than those in the revised mantle model.

Among the natural materials which would seem to have low enough radioactivities are the Type I carbonaceous chondrites. These have a lower density, lower content of radioactive elements and larger volatile fraction than other types of chondrites and Ringwood (1966) has pointed out that

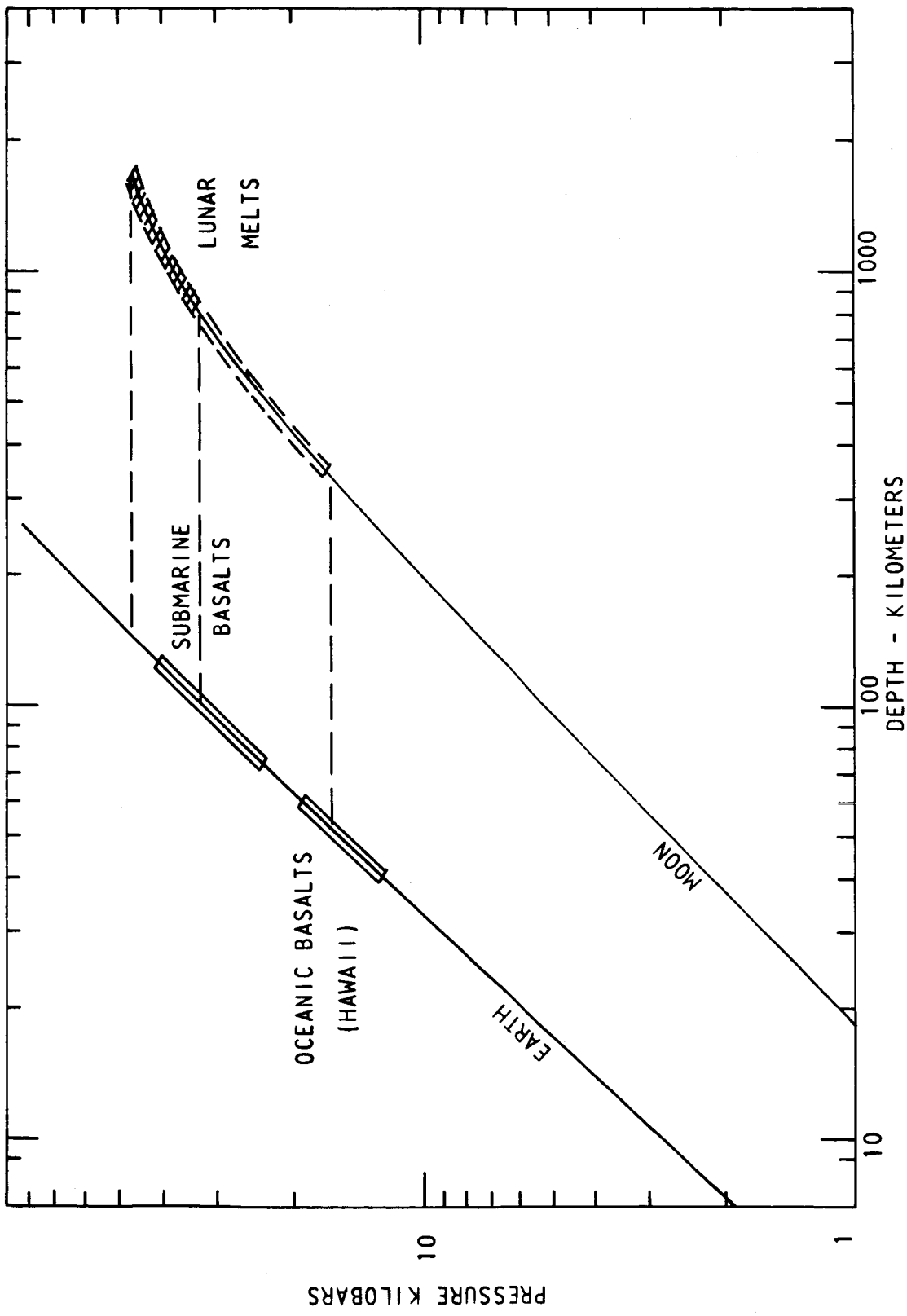

FIGURE IV-3 COMPARISON OF PRESSURES AND DEPTHS OF INFERRED MAGMA ORIGIN ON EARTH AND MOON

these may well be samples of very primitive material. While it is clear from Table III-9 and Figure IV-4 that their radioactive element concentrations are low enough to produce volcanic activity at almost any stage in the history of the moon, depending on the sample picked, their low densities (2.2) make it difficult to match that now observed for the moon. Nevertheless, it is interesting to note in Table III-9 that the revised mantle composition could be derived from a carbonaceous chondrite by removing enough volatile materials to bring the silica content up to that for pyrolite. Whether an intermediate stage in this transition can be found which will also be compatible with the density requirement of the moon has not been established.

It is possible to draw some qualitative conclusions about the implications of a lunar composition closer to that of carbonaceous chondrites:

1. Melting will result in more volatiles in the primary melt;

2. The presence of these volatiles will result in a lower melting temperature; and

3. Extrusive behavior of the melt will differ from that on earth to the degree that it is controlled by the volatile content. On earth, high enough volatile concentrations for highly explosive activity are apparently obtained only through concentration in residual melts by fractional crystallization in secondary magma chambers. On the moon, even a primary "basalt" might have enough volatiles to behave in the same way that andesitic or more acid melts do on the earth.

In view of the above considerations, it now appears appropriate to consider the consequences of a moon of carbonaceous chondritic composition.

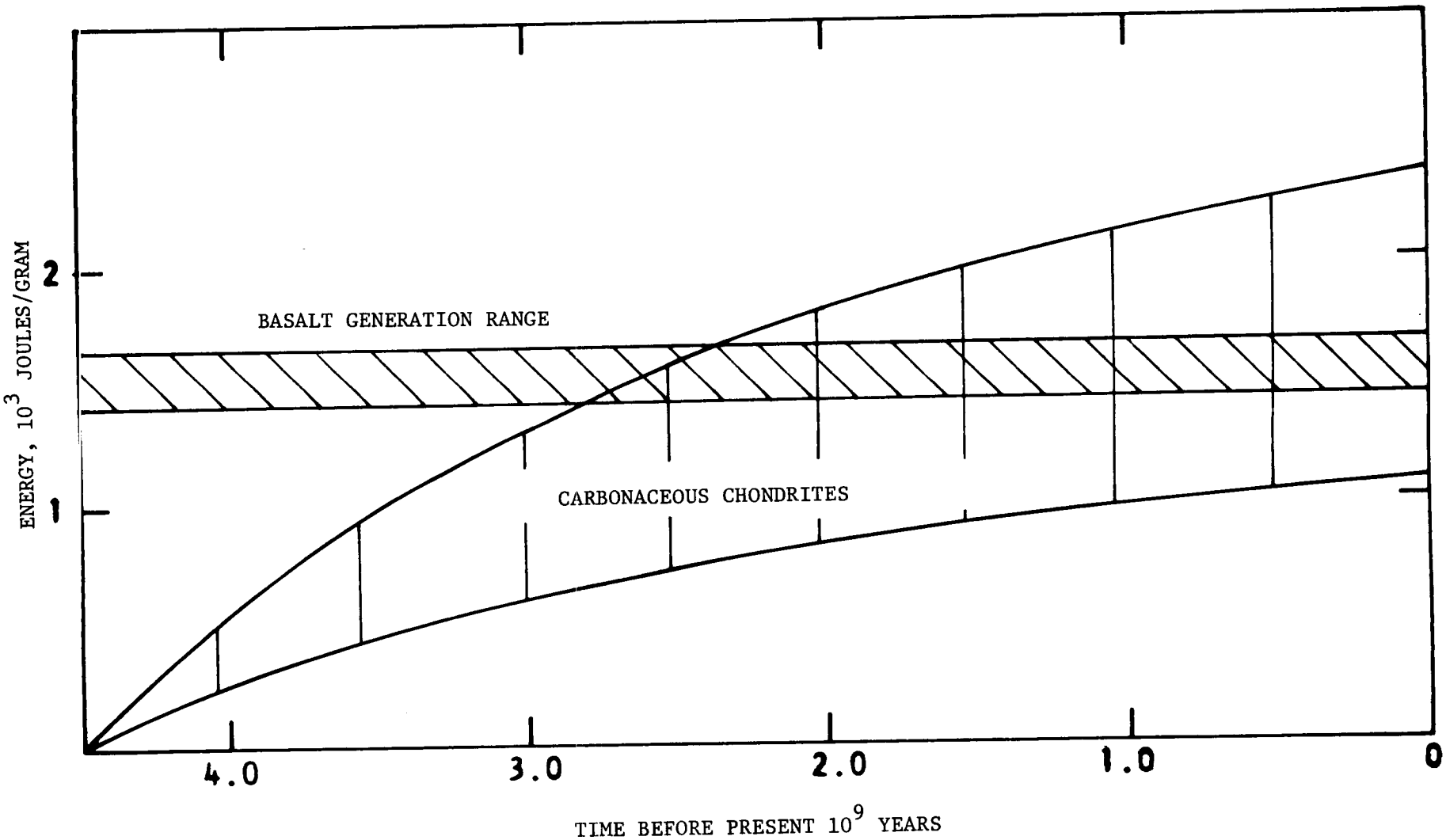

FIGURE IV-4 ACCUMULATED HEAT PRODUCTION FOR RANGE OF CARBONACEOUS CHONDRITE COMPOSITIONS

V. VAPORIZATION PHENOMENA

A. INTRODUCTION

When magma reaches the surface through volcanic action we often observe a violent release of gases. Dense smoke clouds are sometimes formed over the volcano and surface magma flows occur from which vapors are evolved. These phenomena are related to the dissolved gas content of the magma and the vaporization behavior of the oxide components of the magma.

In order to predict how volcanism on the moon might differ from that on earth we are in the process of developing a quantitative model of the dynamics of magma extrusion. In this portion of the report we present information assembled during the year from literature and experimental studies on the dissolved gases in magmas, on the effect of dissolved gases on the extrusion process, and on the vaporization behavior of oxide components of the magma. These data are discussed under the headings of Dissolved Gases, Oxide Volatility, and Volcanic Smoke Clouds.

B. DISSOLVED GASES

1. Experimental Evidence

a. Composition of Volcanic Gases

With a little thought one can readily imagine the problems of obtaining representative gas samples from highly active volcanos. Thus it is not surprising that in spite of many reported samplings we are still uncertain as to the detailed composition of the gases and to the variation of the composition of the gases from volcano to volcano. White and Waring (1963) have tabulated and discussed most of the reported analyses for a chapter on "Volcanic Emanations" in "Data of Geochemistry." Because of the extreme fluctuations and the obvious contamination of most of the studies by air it is difficult to draw firm conclusions from these data. We will discuss results obtained for the Hawaiian volcanos and current work on the Surtsey group of volcanos.

The Hawaiian volcanos have been studied rather intensively over the years. Eaton and Murata (1960) in a review of volcanism have presented a typical volcanic gas composition based on their review of the work of several other people on the Hawaiian volcanos. This typical composition cited for the gases from the Hawaiian volcanos is given in Table V-1. Also tabulated in Table V-1 are two separate samplings of the gases from the Surtsey volcano, as reported by Sigvaldason and Elisson (1966). In their opinion these represented the only successful samplings from many attempts. They claim that the samples of October 19, 1964 were collected under relatively ideal conditions which are probably not often found during volcanic eruptions. These samples were collected from narrow cracks in the consolidated roof of a lava tube associated with a large discharge of lava. The lava tube was essentially closed except for the small crack in the roof where the gases were escaping under pressure. The samples of February 21, 1965 were collected from active chimneys on a consolidated lava surface. The openings were on the order of 10 cm in diameter and the gases were being released under atmospheric pressure. Other samples collected from chimneys with openings on the order of a meter in width were heavily contaminated with air. In the discussion of their results these authors, based on their field observations, believe that "the process of degassing from the lava stream at 1400°K is essentially restricted to a relatively short time after the lava has appeared at the surface. During this short period of time, the lava loses up to 80-90% of its volatile constituents in essentially the same proportions as initially present in the magma."

Ellis (1957) has calculated by means of thermodynamics the equilibrium compositions as a function of pressure and temperature for certain selected molecular ratios of gases commonly gound in volcanic emissions. We show in Table V-1 the compositions at 1400°K and one atmosphere calculated by Ellis for a molecular ratio of $H_2O:CO_2:H_2:S_2$ = 100:10:2:1. This molecular ratio was chosen by Ellis based on reported samplings of Hawaiian volcanos. It also provides very good order of magnitude agreement with the Surtsey compositions reported in Table V-1.

TABLE V-1

COMPOSITIONS OF VOLCANIC GASES

	Surtsey[1] 10-15-64		Surtsey[1] 2-21-65			Theoretical[2]	Hawaii[3]
H_2O	79.20	79.20	86.16	86.16	86.13	86.0	79.31
HCl	0.80	0.80	0.40	0.40	0.43	--	--
SO_2	5.40	4.02	3.28	1.84	2.86	1.49	6.48
CO_2	9.18	9.64	4.97	6.47	5.54	8.05	11.61
H_2	4.56	4.88	4.74	4.70	4.58	3.58	0.58
CO	0.68	0.70	0.38	0.36	0.39	0.82	0.37
N_2	0.18	0.76	0.07	0.07	0.07	--	1.29
Cl_2	--	--	--	--	--	--	0.05
CH_4	0.00	0.00	0.00	0.00	0.00	--	--
S_2	--	--	--	--	--	--	0.24
T(°K)	1400			1400		1400	1400

(1) Sigvaldason and Elisson (1966). 10-15-64 sample from narrow crack in consolidated roof of a lava tube with gases escaping under pressure. 2-21-65 sample from active chimney on consolidated lava surface with gases escaping under atmospheric pressure.

(2) Ellis (1957). Thermodynamic calculation assuming composition with molecular ratios of H_2O: CO_2: H_2: S_2 = 100: 10: 2: 1.

(3) Eaton and Murata (1960). Typical composition reported by authors based on work of others.

His calculations indicate that increasing the pressure will decrease SO_2,H_2, CO and S_2 while H_2O, H_2S, CO_2 and COS will increase. Chlorine in the form of HCl would be expected in these gases. The presence of chlorine and sulfur in elemental state in volcanic gases collected from molten magma would be evidence for oxidation by atmospheric air. A system such as Ellis has used in his calculations accounts for the general differences between high and low temperature magmatic gases without any further assumptions than his initial one of the chemical equilibrium between constituents. The effect of pressure on these systems is to favor water, carbon dioxide and hydrogen sulfide which are the most likely constituents in the magma in which the gases originate. The hydrogen sulfide and carbon dioxide would exist in equilibrium with sulfides, carbonates, and high temperature water fluid, all dissolved in the hot magma.

In summary we believe that the results presented in Table V-1 for the Surtsey and Hawaiian regions represent relatively careful and intensive studies compared to most other data available. They are in quite reasonable agreement. The behavior with temperature of gases associated with volcanos does appear to be in accord with theoretical predictions of Ellis. However, there have been many other samplings reported which differ markedly from those of Table V-1 and whether the extreme differences are representative of different magma histories or are the result of sampling difficulties is not clear. It seems reasonable to expect that primary magmas would have very little difference in their gas compositions. One might expect, however, that magmas derived from near surface magma chambers where the magma may have spent a long period of time and been subjected to fractional differentiation and the possible selective loss of some of the components could give quite different gas compositions. When necessary in subsequent work we will base the molecular ratios of gases to be expected from primary magmas on the results tablulated in Table V-1.

b. Solubility of Gases in Magmas

Hamilton, Burnham and Osborn (1964) determined the solubility of water in basaltic and andesitic melts. The basaltic melt represented a

sample of the Columbia River tholeiitic flows. The study was carried out over a range of 1 to 6 kilobar pressures at 1100°C. Their results for the Columbia River basalt gave a straight line when plotted on a mole percent versus square root of pressure plot. The straight line for the Columbia River basalt passed through the origin. The data for the andesitic basalt was also a straight line somewhat displaced towards higher mole percent solubilities and does not pass through the origin. In their discussion they point out that the square root relationship has been previously observed in alkali silicates below one atmosphere. They compare their data to the work of other investigators on various silica and silicate systems. Other work on silica and pegmatite melts lie both below and above their curves in percent solubility. However, even with the variations in melts the results do not differ by more than $\pm$ 50%. Thus for our purposes the curve given by Hamilton, Burnham and Osborn for basalt is very good. It provides an order of magnitude solubility of water in tholeiitic basalts at 1100°C. The authors discuss the effect of temperature on solubility and conclude that no good data exist. They find for basalt at 1100°C a solubility of 3.1 weight percent (10.2 mole percent) at 1000 bars and 9.4 weight percent (25.5 mole percent) at 6000 bars.

No comparable data exist for the solubility of CO_2 or H_2 in basaltic magmas. According to a recent review of Wyllie (see Bradley, 1963) on the "Applications of High Pressure Studies to the Earth Sciences," no quantitative data at high pressures on the solubility of CO_2 in silicate melts is available. He does mention that some of his qualitative results with liquid feldspar and granite suggest that CO_2 is practically insoluble in these melts.

Some studies on pure silicate melts have been carried out. Weyl (1931) studied the reaction of CO_2 with silicates under high pressure. At 1100°C he reported 2.7% CO_2 in Na_2SiO_3 solution at 100 atm, 4.9% at 400, and 6.7% at 800. He found that the temperature effect on solubility was small compared to the pressure effect. Sodium disilicate absorbed much less CO_2 than the metasilicate and calcium metasilicate did not absorb any CO_2. The mixtures of sodium and calcium metasilicate absorbed CO_2 approximately in proportion to the sodium metasilicate content.

Some data on the solubility of gases in glass compositions are available. We have found one study by Naughton (1953) on the solubility of hydrogen in pyrex glass. He found that at 1170°C and under 10 mm hydrogen pressure pyrex glass dissolved 0.060 mm at standard temperature and pressure in one gram. This corresponds to a solubility of 5.4×10^{-6} grams of hydrogen per gram of pyrex glass at 1170°C and 10 mm hydrogen and assuming that solubility is proportional to the square root of pressure 0.0047 weight percent at one atmosphere of hydrogen. The comparable value for water in basalt is approximately 0.1 weight percent at 1100°C and one atmosphere of water pressure.

Faile and Roy (1966) have reported studies at 800°C and to pressures of 10 kilobars on the solubilities of Ar, H_2O, and CO_2 in a silicate glass of the composition $K_2O \cdot 4SiO_2$. The argon solubility appears to saturate very rapidly. It is comparable to that of H_2O at very low pressures and equals that of CO_2 at 1 kb; at higher pressures it is very much less than CO_2. The CO_2 solubility data vary in proportion to the pressure over the pressure range studied and, with allowances for the differences in temperature and composition, appear to conform in magnitude to the solubilities reported by Weyl (1931) for sodium silicates. At one-third kilobar pressure the water solubility in mole percent is 16 times greater than that for CO_2.

In summary, solubility of gases is dependent on composition of the melt. The data for H_2O solubility appears reasonably good. Other gases appear to be less soluble and the solubility in basalt melts is not well defined. Some estimates of behavior can be obtained from reported studies on glasses. However, it must be recognized that the solubility of mixed volatiles can be different due to the chemical nature of the solution phenomena. Wyllie (see Bradley, 1963) reports on qualitative evidence that $CO_2 + H_2O$ is less soluble than H_2O alone in feldspar and granite melts, whereas mixtures of H_2O + HF are more soluble than H_2O alone.

c. Gas Contents of Primary Magmas

We concluded in our previous report that basalt contained less than 1% of water on the basis of the reported lack of vesiculation of the submarine basalt flows and the average water content generally reported for basalts. Recent work continues to support this view. Bjornsson (1966)

has reported on efforts under way to determine the water content of Surtsey magma by calculating the radon content of the magma before eruption from its radium content and measurements on the radon to water ratio in the liberated magmatic gas. At the time of his report the radon to water ratio in the magmatic gas had been determined. The radium content in the basalt had not yet been determined. However, if the radium content for an average alkali olivine basalt was assumed as characteristic of that in the Surtsey lava then the method yielded an estimate for the water content of 0.9 weight percent. In our opinion this value may be somewhat high based on the use of a radium content for an alkali olivine basalt. Radium content in a tholeiitic basalt will probably be somewhat lower. This work is continuing in Iceland and we anticipate that this project will contribute much more reliable data than has previously been available.

Moore (1965) has collected some 20 dredge samples from the submarine part of the east rift zone of the Kilauea volcano near the island of Hawaii. These basalt samples are very similar chemically to the tholeiitic lavas extruded on the island. Apparently the only obvious difference in chemical content is the higher combined water content. Samples were collected at depths ranging from about 500 to 5000 meters. The water content of the submarine lavas is quite constant and did not show any definite relationship with depth. The average weight percent of combined water is $0.45 \pm 0.15\%$. Moore believes that this water content represents that characteristic of the magma at its point of origin under the Hawaiian ridge.

Another very interesting aspect of this study is that vesicles were recognized in all of the samples, even those at the 5 kilometer depth level. Moore reports that the vesicularity and bulk density of the basalts shows a systematic change with depth. Samples collected from progressively deeper water have a higher specific gravity and contain fewer and smaller vesicles. The very interesting data curves of Moore are reproduced in Figure V-1. The sharp break in specific gravity and in volume percent vesicles appears to occur at an ocean depth of approximately 1 kilometer. This corresponds to approximately 100 atmospheres pressure.

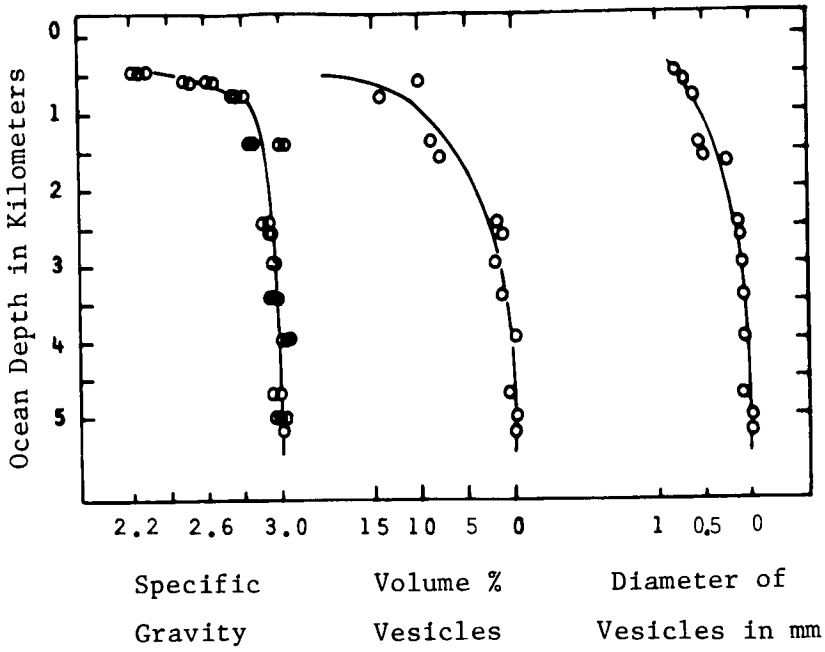

FIGURE V-1 CHANGE IN BULK SPECIFIC GRAVITY, VOLUME PERCENT VESICLES, AND AVERAGE DIAMETER OF VESICLES WITH DEPTH FOR BASALTS OF THE EAST RIFT ZONE OF KILAUEA (from paper of Moore, 1965)

It is of interest to determine what we can say about the nature of the gases present below 1 km and those causing the sudden increase in gas volume. We have indicated above that the solubility of water at one atmosphere is approximately 0.1 weight percent. From the square root of pressure dependence we calculate that the pressure corresponding to complete solution of the approximately 0.5% H_2O reported in the basalts in 26 atm. On this basis one might believe that ex-solution of water is not cause of the sudden increase in gas volume observed by Moore near 1 km (100 atm). For water to be responsible it would require either a water content of approximately 1 weight percent or a two-fold decrease in water solubility in the basalt due to the presence of the CO_2 or to other gases.

It is also instructive to estimate the relative gas contents of basalt based on the compositional analyses on gases evolved from magma. From the data of Table V-1 we adopt for our calculations relative volumes of H_2O:CO_2: H_2 of 80: 8: 4. Assuming that 0.5 weight percent H_2O is lost from basalt (based on a solubility at 1 atm H_2O of 0.1 weight percent this

corresponds to a total water content of slightly less than 0.6 weight percent) we can then calculate from the volume ratio of H_2O: CO_2: H_2 = 20: 2: 1 that 0.12 weight percent CO_2 is evolved and 0.0027 weight percent H_2. Note that the quantity of hydrogen indicated is comparable in magnitude to the solubility under 1 atm hydrogen reported in pyrex glass (0.0047 weight percent H_2). Thus it is not likely that ex-solution of hydrogen accounts for the sharp volume increase in vesicles observed by Moore. However, if we assume that the sharp increase is due to ex-solution of CO_2 and that CO_2 solubility is proportional to the CO_2 pressure, then we estimate a CO_2 solubility at 1 atm of 0.0012 weight percent. The magnitude of this value appears reasonable in terms of the CO_2 solubility data discussed earlier.

As discussed in the previous paragraph we can estimate from the relative volumes of H_2O, CO_2 and H_2 evolved from magma and an assumption as to the total H_2O content of basalt that the weight percent of H_2O, CO_2 and H_2 evolved are 0.5, 0.12, and 0.0027. These correspond at one atm and 1100°C to gas volumes per gram of basalt of 3100 cc H_2O, 307 cc CO_2, and 152 cc H_2. Now note that the vesicle volume at about 1 km where the sharp break occurs in Moore's curve corresponds to about 10%. Per gram of basalt this is equivalent to about 0.35 ml of gas at 100 atm pressure and the melting point of basalt which corresponds to a volume at 1 atm of only 3.5 ml; this is 1/1000 of the volume of H_2O evolved. Thus the gas present in the vesicles at depths below 1 km (100 atm) must represent trace quantities in terms of the compositional analyses obtained to data of gases evolved from magmas. We ssume it probably represents the noble gases such as He and Ar.

The studies of Moore tend to support the conclusion that the water content of basaltic magmas is less than 1%. Combined with data on gas solubility in silicates and compositions of gases evolved from magmas we have been able to speculate on the gas compositions of primary magmas.

2. Volcanic Behavior Related to Dissolved Gases

a. Viscosity Effects

In our previous report we indicated that the evolution of gases as a magma rose through a conduit might have a marked effect on its viscosity and thus its flow behavior. It is well known that the relative viscosity of a liquid will increase as the volume percent of solid spheres is increased. The question then is whether or to what extent the gas bubbles will behave in their effect on viscosity like solid spheres. To answer this question we have searched the literature for information on the viscous behavior of gas-liquid systems.

Foams represent one type of gas-liquid system which has a very high gas to liquid ratio. Bikerman (1953) mentioned several studies of foams which indicate that the viscosity increases as the volume percent of gas increases. The most pertinent study with respect to our interests to which he refers is that of Grove et al.(1951). These workers investigated the the effects of pressure, rate of shear, and air to water ratio on the apparent viscosity in order to provide data which could be used for predicting pressure drops on transporting foam in pipes. They found that an increased pressure on the foam decreased the viscosity for the reason that the accompanying reduction in air volume gave the effect of a foam of decreased expansion.

Further search of the literature produced another reference which is even more pertinent to our question. Hayward (1962) studied the viscosity of bubbly oil containing up to 25% of air. Bubbly oil is defined as oil in which discrete bubbles of air are entrained and are separated from each other by relatively thick films of oil. Thus it is distinguished from foam in which the air bubbles are separated by only thin films of oil. Hayward carried out his study primarily with a mineral oil of 38 centistokes of viscosity at 25°C and with bubbles ranging preponderantly from 0.125 to 0.5 mm. He found over a range of bubble contents up to 25% that the relations between bubble content and relative viscosity is linear and follows the law $\left(\frac{\eta}{\eta_o}\right) = 1 + 0.015\ \beta$ in which $\left(\frac{\eta}{\eta_o}\right)$ is a relative viscosity and β is the percent volume of the air. He could not control the bubble size in his system and thus was not able to study the effect of bubble size in an

adequate manner. He attempted to explore the effect of the viscosity by using an oil with a six-fold greater viscosity. A change in viscosity of this magnitude did not produce marked changes in the behavior of the bubbly oil. This relationship found experimentally by Hayward may be compared with the theoretical equation developed by Einstein for the viscosity of a suspension of rigid spheres: $\frac{\eta}{\eta_o} = 1 + 0.025\ \beta$.

Thus experimental evidence does exist for an increase of viscosity with gas content. We are interested in the behavior of a system at much higher viscosity, pressure, and surface tension. These factors should favor more rigid gas spheres and thus a still closer approach to the Einstein relationship. Certainly one can expect the small bubbles to move with the liquid and to show very little tendency for separation from it. An examination of glass technology literature indicates that the removal of small gas inclusions from the highly viscous glass is a very difficult task. Cable (1966) has studied the kinetics in mechanisms of fining glasses. He reports that the primary process for removing small bubbles is their rate of dissolving in the liquid and he stresses in his paper the very slow movement of these bubbles through the viscous glass.

b. Oxide Transport

As the magma rises a gas phase appears. There is an opportunity for an interaction between the gas and the metallic oxides of the magma to form gaseous hydroxides, hydrates, halides or sulfides. If the magma should stop enroute to the surface the formation of these volatile compounds provides a means for differentiation and the formation of ore bodies through the various possible transport reactions. Many of these reactions occur at considerable depths below the surface and thus the high gas pressures associated with these depths favor the formation of many volatile compounds which we would not recognize as existing at the surface. As the magma and gas system continues towards the surface we can expect a reversal of some of these reactions, as gas pressure decreases, leading to the formation of a smoke or fume. This can be the basis for the formation of much of the smoke associated with volcanic action. The details of these oxide transport reactions will be discussed in much greater detail later under our discussion of smoke formation.

C. OXIDE VOLATILITY

1. Laboratory Observations

a. Knudsen Cell Studies

One way of studying vaporization phenomena is by the Knudsen technique. In this technique the sample is heated in a cell which is closed except for a small hole into the vapor chamber. The hole is very small so that little gas can escape and thus, in principle, the vapor is at equilibrium with the solid or liquid sample. The rate of loss through the orifice is a function of the pressure of the gas inside the cell and of the molecular weight of the gas. Thus from data on weight loss as a function of time one can calculate vapor pressure. The apparatus used in this study is provided with a collector plate which is suspended from a microbalance so that it is held over the orifice and thus provides a surface on which the effusing vapor can be condensed and weighed as a function of time of heating. In our experiment, the collector plate enabled us to obtain a sample of the condensate for analysis.

We have studied a sample of basalt obtained from Gordon A. MacDonald of the University of Hawaii. The sample is a specimen of the 1881 lava of Mauna Loa, Hawaii which was collected at a place called Kaumana on the northeast slope of Mauna Loa. The basalt composition is presented in Table V-2.

We started our experiments using a finely powdered portion of this basalt sample and immediately ran into experimental difficulty. As the sample began to melt a foam was formed which tended to overflow the container, run down the sides, and drip into the interior of the vacuum system. We attributed this foaming to dissolved gases and eventually found that by premelting the sample and by using very small samples this difficulty could be avoided and the sample retained within the sample cell.

Once we were able to retain the sample within the cell, we obtained a "successful" run with approximately a 2% weight loss over a total of four hours heating at 1365°C. We had observed in some of the previous work that the collector plates seemed to gain weight once the system was

open to the air. It was not clear whether this was due to reaction with oxygen in the air or with moisture in the air, therefore, at the completion of this run we introduced dry oxygen but observed no weight gain of the collector plate. However, once the system was open to air the weight gain was observed. Thus we conclude that the reaction is with moisture in the air. The deposit on the collector plate surface was analyzed by the microprobe laser emission spectroscopy technique, and it was found that sodium was present in quantities on the order of 1 to 10%. This represented a greater than 10^5 increase over the blank. No other elements showed increases of this magnitude although silicon, aluminum, and barium did show increases of from 1 to 3 orders of magnitude over that of the blank. Thus we conclude that the vapor condensate is primarily sodium oxide.

TABLE V-2

BASALT AND GLASS COMPOSITIONS

	Basalt (%)	Container Glass (%)	E-3 Glass (%)
SiO_2	51.85	71.50	70.16
TiO_2	1.93	-	0.018
Al_2O_3	14.04	1.28	2.56
Fe_2O_3	1.56	0.044	0.022
FeO	9.16	-	0.0034
MnO	0.17	-	-
MgO	7.85	2.50	-
CaO	10.45	10.24	12.26
Na_2O	2.07	13.50	14.99
K_2O	0.37	0.26	-
H_2O^+	0.27	-	-
H_2O^-	0.24	-	-
P_2O_5	0.22	-	-
BaO	-	0.35	-
SO_3	-	0.21	-
F_2	-	0.21	-

In a subsequent experiment we attempted to study the concentration and temperature effect on the vapor pressure by examining weight changes of the collector as a function of time and temperature of heating. We found no gain beyond the first 15 minutes of heating. Thus, we conclude that the weight losses observed in this and the previous experiment represent material lost in a period less than 15 minutes, and we have calculated vapor pressures based on the assumption that the weight loss occurred over a time on the order of 10 minutes. Based on the results of mass spectrometry studies to be discussed in the next section we have also assumed that the vaporization process is by way of sodium atoms and oxygen gas. The results of these calculations and the experimental data are summarized in Table V-3.

We have found from these studies weight losses on the order of 2% at 1365°C. It must be recognized that these samples have been premelted and that considerable material might have been lost before the experiment was started by this action. The results do indicate that sodium oxide is the major oxide component of the basalt vaporized. Assuming that the vaporization occurred over a 10 minute period average vapor pressures of 1 to 2 x 10^{-5} atmospheres have been calculated as shown in Table V-3.

b. Mass Spectrometry

Mass spectrometry studies on two glass samples have recently been completed in our laboratories. The results obtained from these studies are pertinent to our interests and will be described here. One study was on a container glass whose composition is given in Table V-2. The principal vapor species observed over this glass were atomic sodium and sulfur dioxide. It was also observed that residual water was liberated in the form of sodium hydroxide dimer. By a silver calibration of the mass spectrometer the sodium vapor pressure was found to range from 10^{-5} torr at 500°C to 10^{-2} torr at 1333°C. The pressure was observed at the very first to decrease very rapidly with time. The behavior appeared to

TABLE V-3

VAPORIZATION OF BASALT

A. KNUDSEN EXPERIMENT #XIV

52.86 mg = sample weight

1.031 mg = weight loss through 51 mil orifice over 4 hour heating period at 1365°C

Calculate average pressure assuming loss over time on order of 10 minutes and that vaporization process is

$$Na_2O = 2\ Na(g) + 1/2\ O_2(g)$$

$$P = 17.14\ G\sqrt{\frac{T}{M}}$$

where P = pressure in torr

G = loss rate in $gm/cm^2/sec$

T = temperature in °K

M = molecular weight

$$P = 17.14 \times 1.25 \times 10^{-4}\sqrt{\frac{1638}{25}}$$

$$= 1.7 \times 10^{-2}\ torr$$

$$= 2.2 \times 10^{-5}\ atm \qquad Log\ P = -4.66$$

B. KNUDSEN EXPERIMENT #XV

54.23 mg = sample weight

.913 mg = weight loss through 52 mil orifice over initial 15 minute heating period at 1365°C

Calculate average pressure and that vaporization process is

$$Na_2O = 2\ Na(g) + 1/2\ O_2(g)$$

$$P = 17.14 \times 8.8 \times 10^{-5}\sqrt{\frac{1638}{25}}$$

$$= 1.2 \times 10^{-2}\ torr$$

$$= 1.6 \times 10^{-5}\ atm \qquad Log\ P = -4.8$$

indicate a surface depletion of the sodium species. The second glass composition studied is that referred to as E-3 glass in Table V-2. No SO_2 was observed over this material. Atomic sodium was observed and above 1250°C a release of oxygen was observed. Thus the vaporization reaction appears to be that of $Na_2O = 2Na + 1/2\ O_2$. The conclusions from this work were that the major mechanism of loss under vacuum conditions is in the form of atomic sodium which reaches the surface by diffusion and then volatilizes. Any residual water is lost in the form of sodium hydroxide dimer.

c. Thermogravimetric Studies

To obtain further information on the vaporization behavior of the basalt sample we carried out several thermogravimetric studies. Three were carried out in a commercial apparatus which has a useful limit of about 1150°C. These runs showed an initial weight loss up to about 400°C corresponding to 0.1 to 0.2% of the total weight of the sample. This was followed by the appearance of a weight gain at still higher temperatures, with eventually a further weight loss becoming evident at 1100 to 1150°C. The upper limit of this apparatus was right at the point where the oxide components of the basalt system appeared to become volatile. The exact behavior varies with the rate of heating. We attribute the weight gain to pickup of moisture from the nitrogen atmosphere being passed over the sample. While the initial weight loss which we attribute to water was on the order of 0.1 to 0.2% the analyses reported by MacDonald indicates approximately 0.5% by weight of water in the basalt sample.

To obtain data in the temperature region of interest to us we carried out two experiments in an apparatus designed originally for the study of refractory nitrides as a function of temperature and composition. This system enabled us to heat inductively a platinum crucible containing the sample to a specific temperature, to hold the system at temperature for a given period of time, and to determine the weight loss following each heating period. The crucible and sample were suspended from a quartz spiral balance within a sample chamber which could be maintained closed

or which could be pumped continuously. In the first experiment the sample was weighed initially, the system was then evacuated, closed, and the sample temperature raised intermittently until the sample had fused and a considerable portion of the volatiles had been evolved. The sample of 109 milligrams was in an open crucible within a sample chamber containing a dry ice trap. We started with an initial pressure of less than 10^{-5} torr and the sample was heated gradually over a 50 minute period to approximately 1400°C. When the sample first started to heat, the pressure gauge went off scale and then came back to about 3 to 4 x 10^{-2} torr. At approximately 1100°C the sample was noted to be molten and bubbling. At this point the pressure began to decrease and continued to decrease until reaching a value of approximately 8 x 10^{-4} at 1400°C. At this point the heating was stopped. On removing the dry ice trap the pressure inside the closed system increased to approximately 5 x 10^{-3} torr. This corresponds to about .007 mg of water, representing less than 0.01% by weight of the original sample. Apparently the water which was initially driven out of the sample on heating at low temperatures and which was trapped by the dry ice trap has back reacted either with the sample or with the products evolved from the sample at higher temperatures. On weighing the sample after heating we found a total weight loss of 5 mg corresponding to a total weight loss of the sample of close to 5%. Our original objective was to obtain some idea of the total amount of permanent gases and of water evolved from the sample. The indications are that the permanent gas content evolved is essentially negligible in terms of our measuring capability, and that the experiment cannot determine the total water evolved because of its back reaction with other products volatilized from the sample.

In the second experiment on this apparatus we attempted to determine the weight loss between each heating interval at successively higher temperatures in order to permit plotting a more conventional curve for weight loss as a function of temperature. In this experiment a sample of 82 mg was contained in a platinum crucible which had a lid containing three holes. The purpose was to provide better temperature data by using

the hole into the crucible as a blackbody upon which to make temperature measurements using an optical pyrometer. The data are presented in Table V-4 and Figure V-2. The radio frequency power was increased in steps and held at this power reading for the number of minutes indicated. During this period at constant power level temperature and pressure readings were obtained. Following almost every period at a given power level the sample was cooled and the weight change of the sample and crucible were measured. This enabled us to calculate the weight losses which were obtained during each heating interval. The data are plotted on Figure V-2 and show an initial weight loss which we interpret as a loss due to water volatilization. In this experiment we were pumping continuously on the system; however, because of the slow rate at which the system is pumped out pressure changes within the system were apparent and were noted. The pressure changes are also plotted on Figure V-2. On initial heating we had a very high pressure reading which fell off in time during the heating period. After the initial spike corresponding to the initial weight loss which we attribute to water, the pressure during the heating period remained fairly constant until the power reading reached 1100. Above this power reading the sample began to lose weight again and at the same time the pressure reading averaged over the heating period began to fall. Eventually at power readings above 1500 both the weight loss and the pressure began to rise very sharply. By 1900 the pressure had dropped and the weight loss had become very great. During this experiment at approximately 1100°C or slightly above the sample apparently foamed and small portions of liquid came out through the holes in the crucible lid. Thus accurate temperature readings were not available above 1100° and we have indicated this in Table V-4. By the time the power reading of the system was at 1900 volts the crucible holes were again clear and a firm temperature reading could be obtained. As we lowered temperature we took a series of temperature readings as listed in Table V-4. Note that there is a considerable difference in the readings taken on the final cooling period where the blackbody holes were clear and those approximated in the earlier part of the experiment. Thus the temperature history of the sample is subject to some uncertainty. The results do, however, clearly indicate an

TABLE V-4

SUMMARY OF THERMOGRAVIMETRIC EXPERIMENT

(As shown in Figure V-2)

RF Power Rdg	RF Power Min	Temp. Rdgs. (°C)	Δ Rdg. (cm)	Wt. Loss (mg)
600	5	~ 800	.0081	.78
700	5	~ 850	.0070	.67
800	5	980	--	--
900	6	1050	.0081	.78
1000	6	1080	--	--
1050	4 1/2	--	--	--
1100	4 1/2	1100	.088	.85
1150	7	~ 1125	.0121	1.16
1200	7	~ 1140	.0151	1.45
1250	9	~ 1150	.0145	1.4
1300	7	~ 1160	.0137	1.3
1350	7	~ 1185	.0161	1.5
1400	8	~ 1205	.0150	1.4
1450	5	--	--	--
1500	5	~ 1200	--	--
1600	5	~ 1240	.0222	2.25
1700	7	--	.0258	2.5
1800	7	--	.0441	4.2
1900	7	1500	.0754	7.2
1800		1445		
1700		1400		
1600		1350		
1500		1300		
1400		1255		
1300		1190		
1200		1130		
1100		1065		
1000		1005		
900		940		

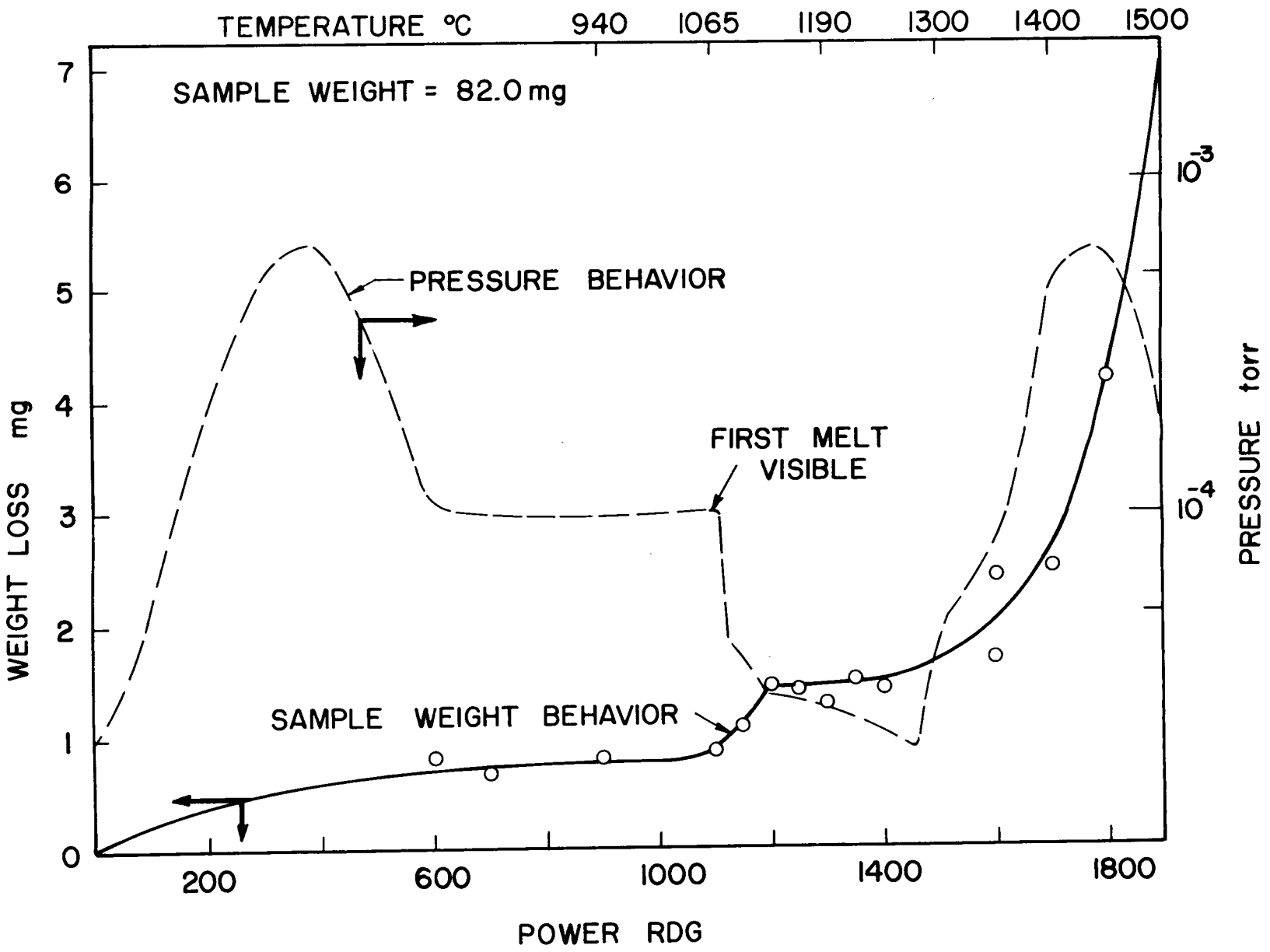

FIGURE V-2 THERMOGRAVIMETRIC EXPERIMENT ON BASALT

initial loss of weight corresponding to approximately 1% of sample weight which we attribute to loss of H_2O. No further weight loss occurred until approximately 1100°C when again we had a very sharp weight loss of about 1% within approximately a 100° range. At about 1250°C we again began to get a very sharp weight loss and this loss continued to increase with temperature up to 1500°C, the highest temperature to which the experiment was carried.

The sample residues from the high temperature thermogravimetric experiments were analyzed for Na, Ca, and K. These results are compared in Table V-5 with a comparable analysis of the original basalt. The samples were reacted with HF to remove silica and dissolved in 3N HCl and analyzed by flame photometry. The K level was too low for the procedure, the changes in calcium content do not appear meaningful. However, marked changes are noted for Na. The #2 sample corresponding to the experiment summarized in Figure V-2 and Table V-4, was heated to 1500°C whereas the temperature limit was about 1400°C for the #1 sample.

2. Conclusions

The work described above has greatly increased our understanding of the vaporization process from basalt magma and will be valuable in considering the behavior to be expected on the lunar surface.

We are primarily concerned with behavior in the 1000-1300°C range. The thermogravimetric experiment summarized in Table V-4 and Figure V-2 indicates a weight loss of about 1% on melting at about 1100°C with essentially no further loss until temperatures of 1350°C and above are reached. The Knudsen experiments showed that heating basalt at 1365°C produced a weight loss within the first 15 minutes with no additional loss on further heating. Analyses of the condensate from the Knudsen experiments and the residue from the thermogravimetric experiments indicate that sodium oxide is the major basalt component being lost in this temperature interval.

The mass spectrometry studies on glass indicate that in the absence of H_2O the vaporization process is $Na_2O = 2Na + 1/2\ O_2$. In the presence of water the sodium hydroxide dimer is the principal vaporizing

TABLE V-5

ANALYTICAL DATA FOR HIGH TEMPERATURE THERMOGRAVIMETRIC STUDIES

Sample		Analytical Results		
Code	Concentration in Solution (mg/ml)	Element	Concentration in Solution (mg/ml)	Concentration in Original Solution (%)
Basalt	5.19	Na	0.99	1.9
		K	< 0.01	-
		Ca	0.22	4.3
#1	4.06	Na	0.035	0.86
		K	< 0.01	-
		Ca	0.20	4.9
#2	2.23	Na	0.011	0.49
		K	< 0.01	-
		Ca	0.13	5.8

species. The behavior of the condensate from the Knudsen experiment in oxygen and moist air indicates that it was Na_2O or NaOH rather than Na. In both the thermogravimetric experiments we observed a pressure decrease as the sample melted and the vapors were evolved; this must represent the interaction of gaseous water with the vaporizing species.

We have plotted on Figure V-3 the vapor pressure as a function of reciprocal temperature for pure Na_2O vaporizing as $2Na + 1/2\ O_2$. We also show as a dotted line the behavior to be expected for Na_2O in basalt assuming ideal behavior. For comparison with the predicted curve we indicate the data obtained from our Knudsen experiments and the mass spectrometry study of glass as well as some data for a tektite glass. The mass spectrometry study showed initially a rapid decrease in vapor pressure with time. The heating history of the sample and its behavior are represented on Figure V-3. This study indicates that the vaporization process is rate limited by diffusion within the glass. The vapor pressures calculated from our Knudsen experiments also fall almost 3 orders of magnitude below that anticipated if the solution was ideal (the dashed curve) and the vaporization process was not rate limited in some manner. Centolanzi and Chapman (1966) have studied the vapor pressure of tektite glass by several dynamic techniques involving a rate of weight loss. All data from these dynamic measurements are again very low in terms of the Na_2O content of tektite glasses (about 1.5%). Their data are from measurements at higher temperatures than ours and their results agree quite well with vapor pressures obtainable by the same technique from pure SiO_2. They mention in their article the work of Walter using a bubble pressure technique. This technique which observes the first formation of bubbles approaches much more closely to an equilibrium situation than the rate of mass loss techniques and this may account for the much higher results observed. Thus the tektite results provide further evidence for a non-equilibrium situation in the vaporization of Na_2O.

Thus one can conclude that near the melting point of basalt magmas Na_2O is the primary component being vaporized. In view of the relatively larger water content of basalt we might expect sodium hydroxide

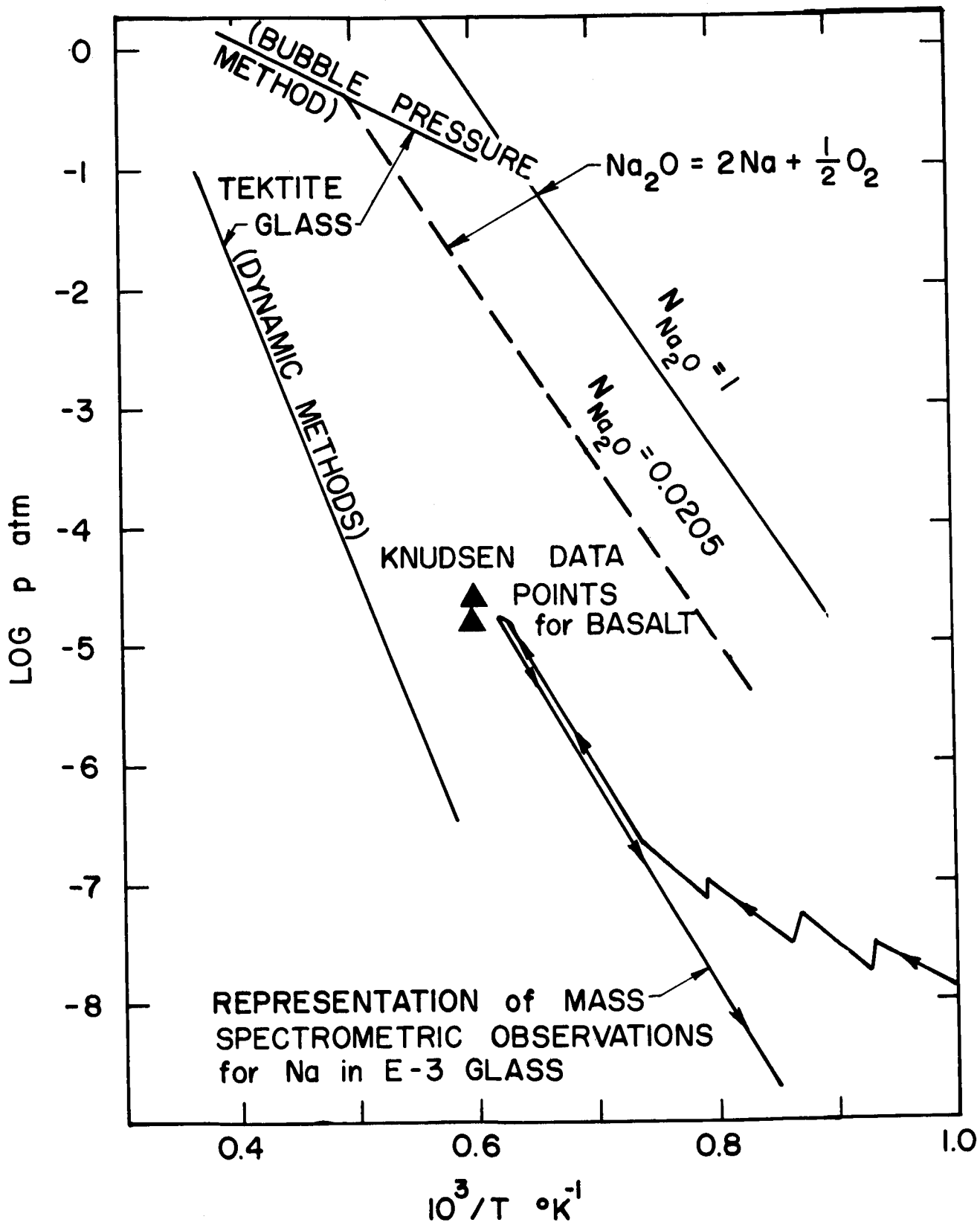

FIGURE V-3 VAPOR PRESSURE FOR Na_2O AND VARIOUS GLASSES

dimers to be the primary vapor species. The vapor pressure is apparently several orders of magnitude below that to be expected based on the Na_2O content of the basalt; this may well be due to a rate limiting diffusion step within the melt. Without question the data show an extreme difficulty in vaporizing the Na_2O component and indicate that the Na_2O component is the primary one being lost near the melting point of basalt.

D. VOLCANIC SMOKE CLOUDS

1. Background

Vonnegut et al. (1966) discussed the possible mechanism of formation of the dense clouds of dark smoke associated with the eruptions on the volcanic island of Surtsey. They note that these clouds are similar in location and appearance to the clouds of white steam observed from erupting geysers and from heated pools in geothermal areas. The resemblance is so strong that these authors proposed that the black volcanic clouds are formed by a similar mechanism. They postulated that the vapor pressures of magma components were high enough for appreciable quantities of these components to evaporate, then on mixing with the cooler atmosphere the vapor condenses to form visible aerosol particles.

In conjunction with our study of lunar volcanic activity we have attempted to further define the nature of the smokes in order to increase our understanding of their mode of formation and thus our ability to predict the nature of volcanic activity on the moon. To this end we have sampled the eruptive cloud of the volcano Surtlinger off the south coast of Iceland. The particulate samples were examined by use of a probescope which permitted examination of the morphology and chemical content of individual particles of the smoke.

2. Experimental Details

a. Samples

Samples were obtained both on the island Surtsey and from the eruptive cloud of the volcano Syrtlingur, just east of Surtsey. Both are off the south coast of Iceland. These samples were collected over the period of June 24-29, 1965.

Several samples (8-14 and 21-23) were obtained by flying light aircraft through the volcanic cloud downwind of the volcano. Two different airplanes were used for this purpose, a Navion and a Cessna 172. Samples were collected on aerosol monitor type millipore filters, one and one-half inches in diameter and mounted in plastic holders with full surface exposure. The filters for samples 21-23 were hand held out the open window of the plane at speeds during sampling which approximated 100 miles per hour which corresponds to an estimated flow through the millipore filter of about 3 liters/min. Samples 8-14 were obtained with the millipore filters affixed to a sampling probe and with a flow of 12.5 liters/min. maintained through the filter by use of a portable 6 volt Gast pump. Samples 4-7 and 20 were collected on the island Surtsey. Sample 20 was collected over a steaming vent. Samples 1-3 and 15-19 were collected from a boat using the Gast pump. Nos. 15-19 were in the fallout area of the eruption. Control samples were taken in the airplane at a point about 15 km north and somewhat upwind of the volcano.

Figure V-4 is a detailed map showing the flight paths through the eruptive cloud for the samples examined here. These locations must be considered approximate due to the difficulties of exactly determining position at the time of sampling. There was a strong odor of sulfur compounds whenever the smoke clouds were entered. This was especially noticeable in the boat at the time when we were as close as 200 yards from the eruption.

After collection the samples were sealed and returned to the laboratory. There selected samples were prepared for the probescope. This preparation included the following steps:

1. Carbon coating the sample,
2. Inverting the sample and dissolving the millipore filter in acetone, and
3. Floating the carbon raft with sample particles on to an electron microscope grid.

b. Technique

The samples were analyzed by M.A.Shippert at Advanced Metals Research Corporation, Burlington, Massachusetts using a probescope developed by them. This instrument consists of an electron optical column combining

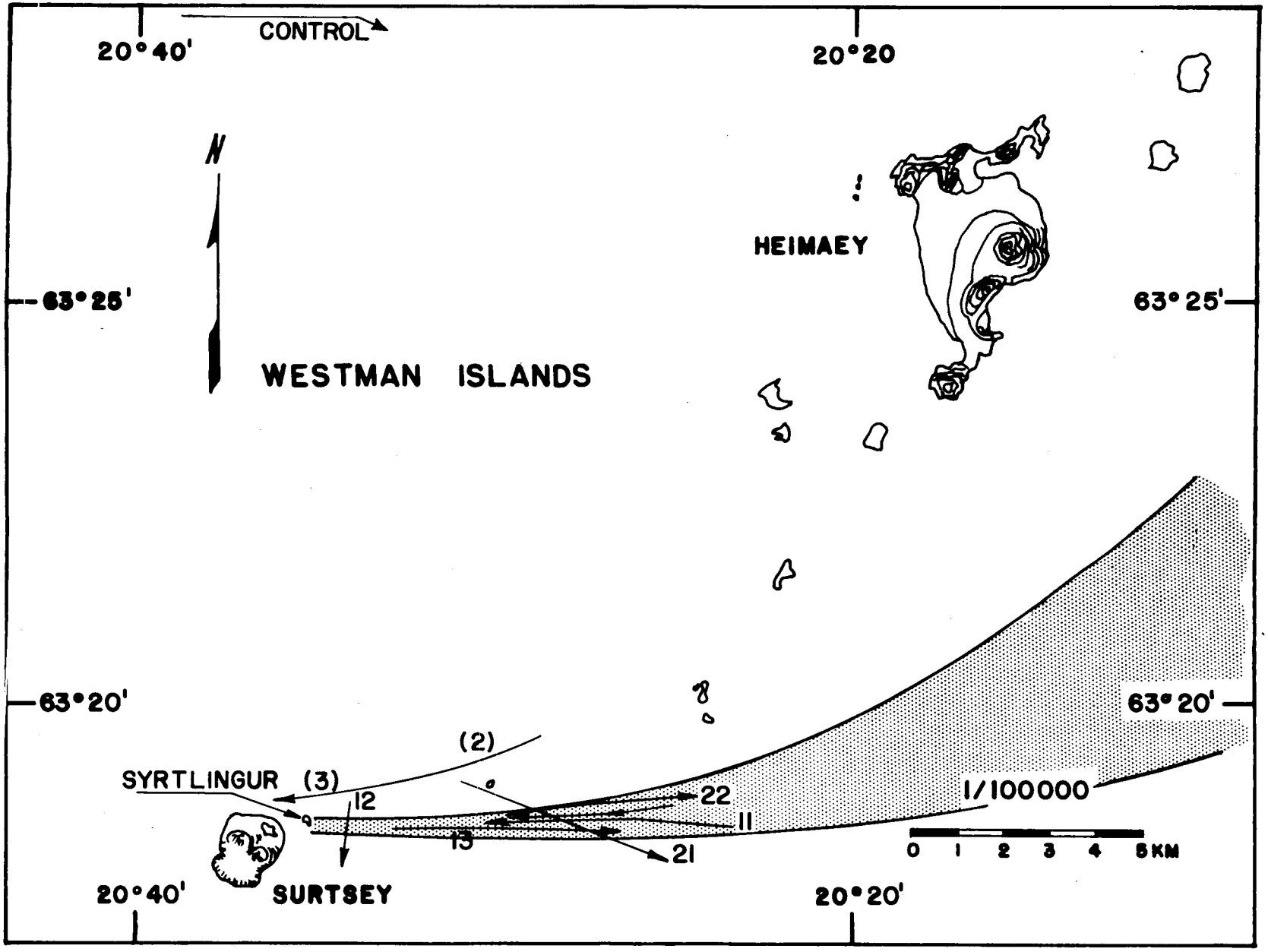

FIGURE V-4 PATHS AND APPROXIMATE LOCATION AT WHICH SAMPLES WERE OBTAINED

the resolution and magnification capability of an electron microscope with an electron beam intensity and small probe spot size of a high quality electron microprobe. A dispersive and non-dispersive X-ray detection system serves as high resolution and high sensitivity data retrieval facilities, respectively.

In contrast to the conventional electron microprobe analyzer, in which the specimen can be viewed directly with medium power light optics only, the probescope is especially suited for sub-micron area or particle investigation, where the specimen is electron transparent as in electron microscopy or where the particles are mounted on a nitro-cellulose or carbon film. Such a specimen may be investigated in order to determine simutaneously, its morphology, its crystal structure by electron diffraction, and its chemical composition by X-ray analysis.

The non-dispersive X-ray detection system consists of a high resolution flow proportional counter which is coupled with a four hundred channel pulse height analyzer. The accumulated spectrum may be stored within the analyzer, displayed on a cathode ray tube, or recorded on an X-Y recorder. In this work, when the display on the cathode ray tube indicated the accumulation of sufficient information it was recorded on the X-Y recorder. The identity of specific energy peaks could then be checked by use of the vacuum X-ray spectrometer. In addition, standard samples such as sodium silicate, iron and nickel chloride were run to obtain information on the relative sensitivity of the instrument to these elements in known atomic ratios. The non-dispersive X-ray system could accumulate information when the intensities were too low for use of the vacuum X-ray spectrometer.

3. Results

The results obtained from the probescope examination of selected aerosol samples obtained from the island Surtsey and the vicinity of the Syrtlingur volcano are summarized in Table V-6. Samples 2 and 3 represent those collected during a boat trip to the island Surtsey. These were collected in the vicinity of the Syrtlingur volcano. Samples 11, 12, and 13 were collected by flying through the smoke cloud from the volcano.

TABLE V-6

SUMMARY OF PROBESCOPE EXAMINATION OF AEROSOL SAMPLES

Sample	Date	Chart	Photo	Description	Elements Indicated: Non-dispersive Analysis	Elements Indicated: Dispersive Analysis
BOAT SAMPLES						
2(A)	11-16-66	3	4	1μ	Si,Ca	--
		4	5	1.2μ	Cu,Fe,Ca,Si/P/S	Si,Ca,Fe
2(B)	12-2-66	17	18	2	Fe,Si,Ca	Fe,Si,Ca,Cr
		18	19	1.2	Si,Ca,Ti	Si,Ca,Ti
		19	20	5	Ca,Mg/Al,Si/P	Mg,Ca,Si,Al
3(A)	11-16-66	6	7	1	Cu,Ca,P	(No Cl,S,Al,K,Ca,Si)
		5	6	0.7	Si	Si (No Al,Cl)
		7	8	3.5	Si	Si
FLIGHT SAMPLES						
11(A)	10-28-66	17	8	4	Si,K	Si,K (No Ca)
		18	9	2.5 x 0.6	Cr,S/Cl	Cr (No Si,Cl,P,S)
		19	10	area	Cl,Cr,Al/Si/P/S	Cr,S (No Si,Ca)Al
		20	11	general area	Cr,Cl	
		20	11	specific areas 1,2 & 3	Cr	
		21		area similar to 20	Cr,Cl	Cr,S
				after burn	Cr,S	

TABLE V-6 (Cont.)

Sample	Date	Chart	Photo	Description	Elements Indicated: Non-dispersive Analysis	Elements Indicated: Dispersive Analysis
FLIGHT SAMPLES (Cont.)						
12(A)	11-16-66	8	9	typical area pattern	Cr,Cl/S,Si	Cr,Cl,S
12(B)	11-16-66	9	10	2	Si,Cu,Ca	Si
		10	11	1.3	Ca	Ca
		11	12	1.0	Ni,Cl,Ca,Si	Cl (No Si,S,P)
		12	13	1.4	Si	Si
		13			Ni/Cu,Ca,Si	Ni,Cu
13(A)	11-16-66	14	14	area	Cl,Cu,S,Ca	S,Cl
		15	15	0.8	Ni/Cu,Cl	Cl
		16	16	7μ agglomerate	Cu,Si/S,Ca	None detectable except Cu
		17	-	2	Al/Si,Ca	
		18	17	0.5 x 1	Ni,Si/P/S,Ca	Ni
13(B)	12-2-66	4	4	10	Si,Ca	Ca (No Mg,Al,P) Si
		5	5&6	6	Si,Al	Si,Al
		6	7	1.2	Cu,Ca,Si/P/S	Cl,P,Ca,K,Si (No S)
		7	8	1.5 x 2	Si,Ca	Si, Ca
		8	9	1 x 4	Si,Al,Ca	Si,Al,Ca
		9	10	1 x 2	Cu,Cr,Si/S/Cl,Ca	Cu,Cr,Ca,Si,S

TABLE V-6 (Cont.)

Sample	Date	Chart	Photo	Description	Element Indicated: Non-dispersive Analysis	Element Indicated: Dispersive Analysis
ON SURTSEY ISLAND						
20(A)	11-16-66	19	18	5μ	Cr,Cl/S	Cr,S (No Si,Mn,Fe)
		20	19	1.6	Si	Si
			20	6	Si	
		22	21	1μ	Cl,Ni	Ni,Cl (No S,Ca)
		23	22	1μ	Cl,Cr,Si/S,Cu	Cr (No S,Cl,Si,K,P,Mn,Fe)
		24	23	1.6 x 3	Ni,S/Cl/Ca	Ni,Cl
20(B)	12-2-66	10	11	1.1 x 0.5	Ni,Si/P/S/Cl,Ca	Ni,Si,S,Cl,P
		11	12	1	Ni,Si/P/S,Ca	Ni,S (No P,Ca,Si)
		12	13	1	Ni,Si/P/S,Ca	Ni
		13	14	2 x .6	Ni,Si/P/S,Ca	Ni,Si
FLIGHT SAMPLES						
21(A)	10-28-66	22		1 x 2	Si,Ca	Si,Ca,Fe
		23	13	2 x 3	Si	Si
		24	14	2.5	Si, Ca	Si
22	10-25-66	x	-	?	Si, Ca	Si,Ca (No Mg)
		y	-	?	Cl,Cr	S,Cr
		z	-	0.8	Cr,Si/P/S,Cu	
		9	-	2.5	Si/P,Ca	
		10	1	1 x 3	Si,Ca	Si,Ca

TABLE V-6 (Cont.)

Sample	Date	Chart	Photo	Description	Elements Indicated: Non-dispersive Analysis	Elements Indicated: Dispersive Analysis
FLIGHT SAMPLES (Cont.)						
22 (cont.)	10-25-66					
		11	2	1	Cl,Ni	
				after 10 min.	Ni,Si,Ca	
		12	3	2	Fe,Si,Ca,Ni	Fe,Ni,Al,Si,Ca
		13	4	2.1	Si,Ca,Ni,Fe	Si,Ca,Fe,Ni,P,S
		14	5	1 x 1.5	Si	Si
		15	6	1	Ca,Si	Ca,Si
		16	7	1.1	Cl,Ni,Ca,Si/P/S	Ni,Cl

Sample 11 was taken over a period of one and one-half minutes while flying upwind through the cloud at approximately 1500 feet. Sample 12 represents a five-second sampling while flying across the cloud at approximately 1 mile from the volcano. Sample 13 was collected over a period of one and one-half minutes while flying downwind through the cloud at approximately 1800 feet. Sample 20 was collected on the island Surtsey over a period of approximately 30 minutes by placing the filter along side a fuming fissure in a magma flow near the rim of the crater. Samples 21 and 22 again were flight samples collected in a very dense cloud. Sample 21 represents a one-minute sampling during a traverse of the cloud while Sample 22 represents a five-minute sampling flying up and then downwind through the cloud.

The results of both the non-dispersive analysis and the dispersive analysis are represented on Table V-6. The elements identified are listed in the order of their relative peak intensities and the major elements indicated are underlined. Many times in the non-dispersive spectra it was impossible to uniquely resolve a given peak. In such a case the elements which might be contributing to the peak are indicated. Generally, a subsequent dispersive analysis was able to resolve which element or elements were actually represented by the peak on the non-dispersive spectra. In the summary of the dispersive analyses the elements strongly detected by the spectrometer are underlined. A copper grid was used to support the microprobe samples and thus copper could always be found. Thus, it is not generally listed in the dispersive analyses. When it is listed in the non-dispersive analysis it is because the copper peak was strongly evident in the spectra. Generally this indicated a very long counting period and thus a very high background pickup. Copper was not strongly evident in the non-dispersive spectra when high concentrations of other elements were present.

The non-dispersive spectra for some standard samples are given in Figure V-5. It is evident that the spectra are quite distinctive for different compounds and compositions. Oxygen, of course, is not detectable. Such spectra of known compounds could be used to develop a quantitative analysis procedure for the aerosol particles. We have not attempted to do

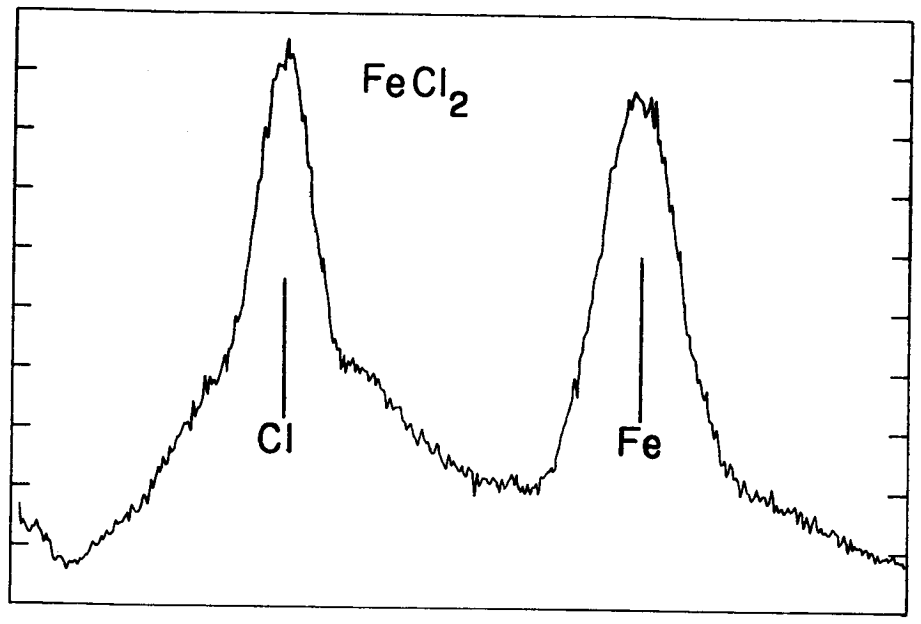

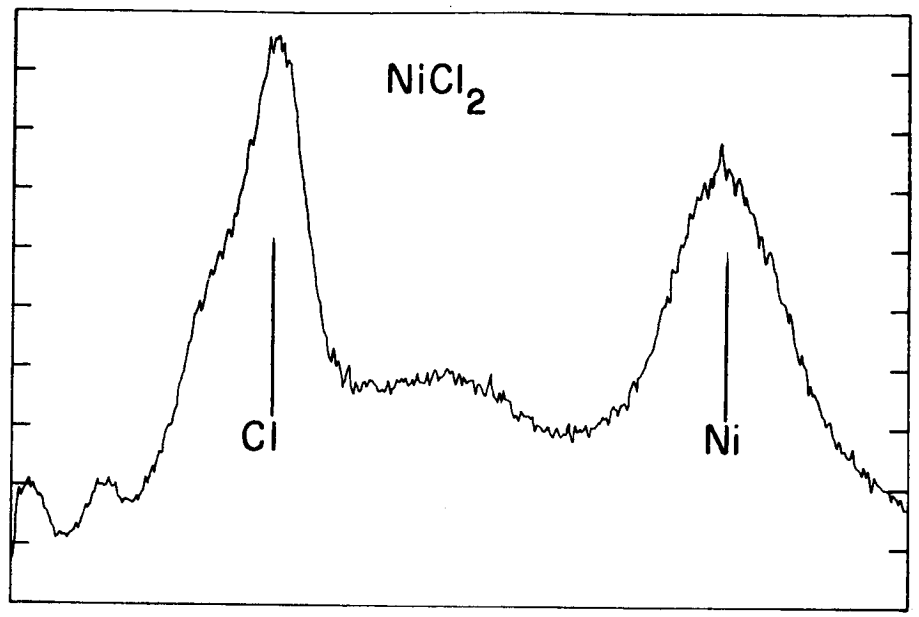

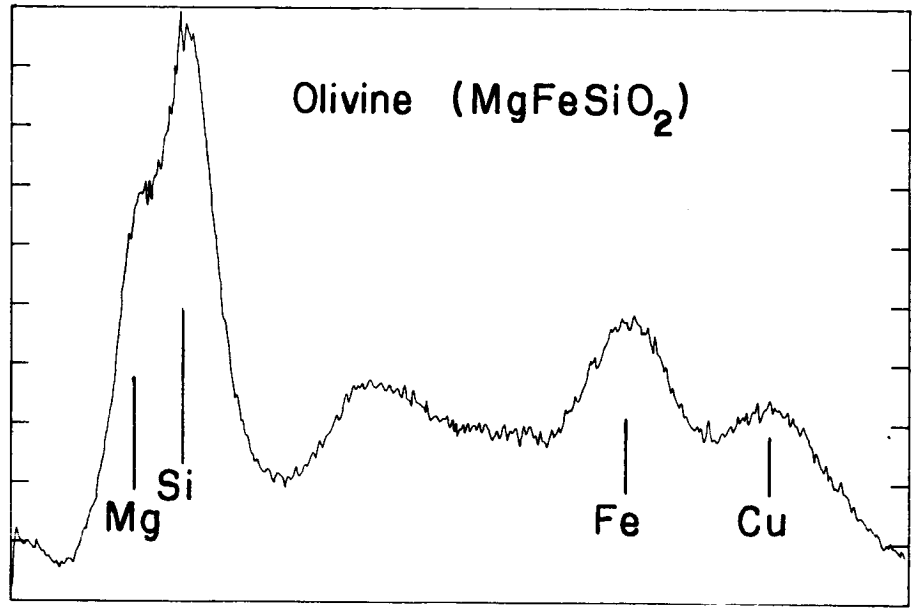

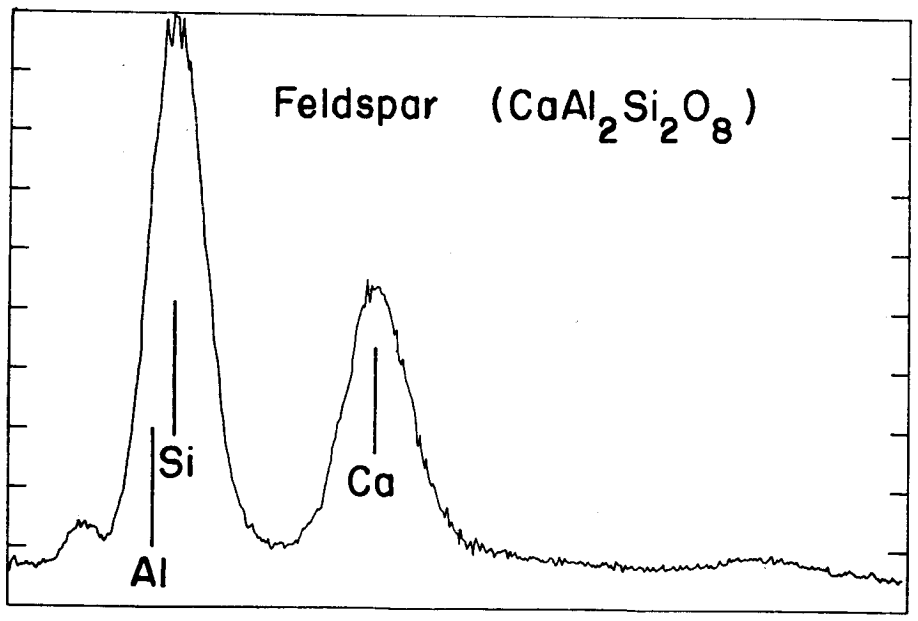

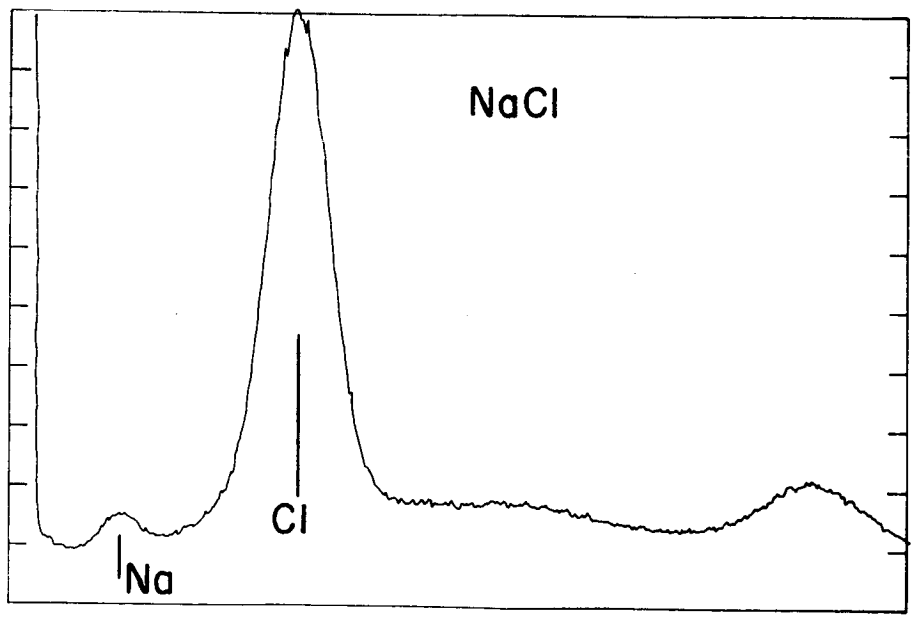

FIGURE V-5 A SPECTRA FOR STANDARD SAMPLES

Fig. V-5 B

110-A

110 B

this in this report. It can readily be seen in the spectra for the feldspar and sodium chloride standards that the copper peak which represents the radiation coming from the copper grid supporting the sample is very low relative to the other peaks in these spectra. The probescope is relatively insensitive to sodium and, in general, we were not able to reliably determine sodium by this technique.

The non-dispersive spectra for two areas of a control sample are given in Figure V-6. This sample was collected about 15 miles north and slightly upwind of the Syrtlingur volcano. No large particles were evident on the filter samples. In obtaining the spectra for the two areas of the control sample a very high background count of copper was obtained, indicating the relatively low concentrations of materials on the filter. The upper spectra of Figure V-6 shows a strong peak which we would attribute to chlorine. This may be due to the presence of sodium chloride. The quantities of material were too low to obtain any identification by use of the X-ray spectrometer.

The variety of spectra obtained from the aerosol particles are indicated in Figures V-7, 8, and 9. In Figure V-7 we present three spectra obtained from flight Sample 11. The upper spectra of Figure V-7 represents a unique combination of silicon and potassium. This is the only particle which we observed with this particular combination. The second spectra taken from Chart #19 shows a very characteristic spectrum for this particular sample indicative of chromium combined with chlorine and/or sulfur. We have identified, by use of the spectrometer, the presence of both chlorine and sulfur with chromium in some particles or areas. However, many times we have not been able to identify chlorine even though the non-dispersive spectra indicates its probable presence. One possible reason for this is evident from the lower spectra of Figure V-7. Curve A represents the initial spectra observed for this particular area. However, after a few moments of observation when the spectral data accumulation was repeated we obtained spectra B. This is characteristic of the apparent volatilization of what appears to be the chlorine component of the aerosol particles. Use of the spectrometer to determine the presence of chlorine

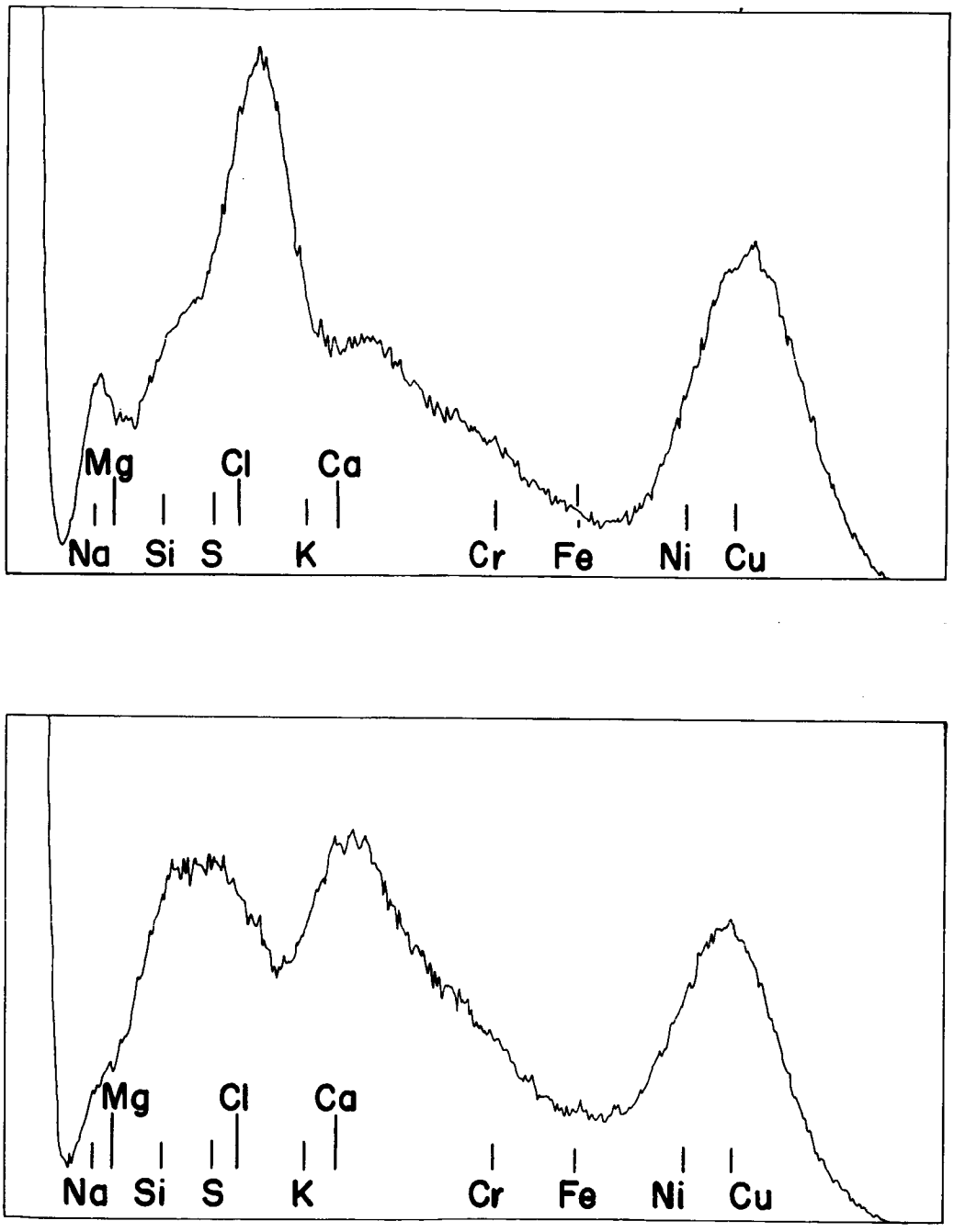

FIGURE V-6 SPECTRA FOR TWO AREAS OF CONTROL SAMPLE. NO LARGE PARTICLES WERE EVIDENT

is a much more time consuming operation than collection of the non-dispersive data. Thus we believe that in the process of measurement we frequently volatilize most of the chlorine so that it is not identifiable on the spectrometer.

In Figure V-8 we present several spectra from Sample #20 which was obtained on Surtsey Island alongside of a steaming vent. Examination of the spectra and the data summarized in Table V-6 show that nickel, chlorine and chromium are strongly evident in these aerosol particles. There appears to be much less silicon and calcium than was obtained in the flight samples.

Figure V-9 presents some selected spectra indicating the compositional variety observed in Flight Samples 21 and 22. In these samples the pure silicon and silicon-calcium particles were highly evident. However, nickel-iron-chromium-chlorine-sulfur containing particles were also found. In Figure V-10 we present several electron microscope photographs taken in our laboratories on the Hitachi electron microscope. These are of better quality than those obtained from the probescope and are presented for that reason. They are representative of the nature of the aerosol particles observed on the filters. Photograph A illustrates a general area view showing a relatively dense collection of submicron material. Spectra of such areas were presented in Figure V-7, Charts 19 and 21. Photograph B clearly shows some particles with a pronounced angular nature. This was characteristic of a large portion of the discrete particles observed. Photograph C shows a large particle which has just begun to melt on the righthand side due to the heating effect of the electron beam. Some reaction with the carbon substrate is indicated. Photograph D shows the final result of completely melting the particle. Such melting will apparently occur for all particles if precautions are not taken to prevent it. Such heating undoubtedly accounts for the apparent chlorine volatilization mentioned above.

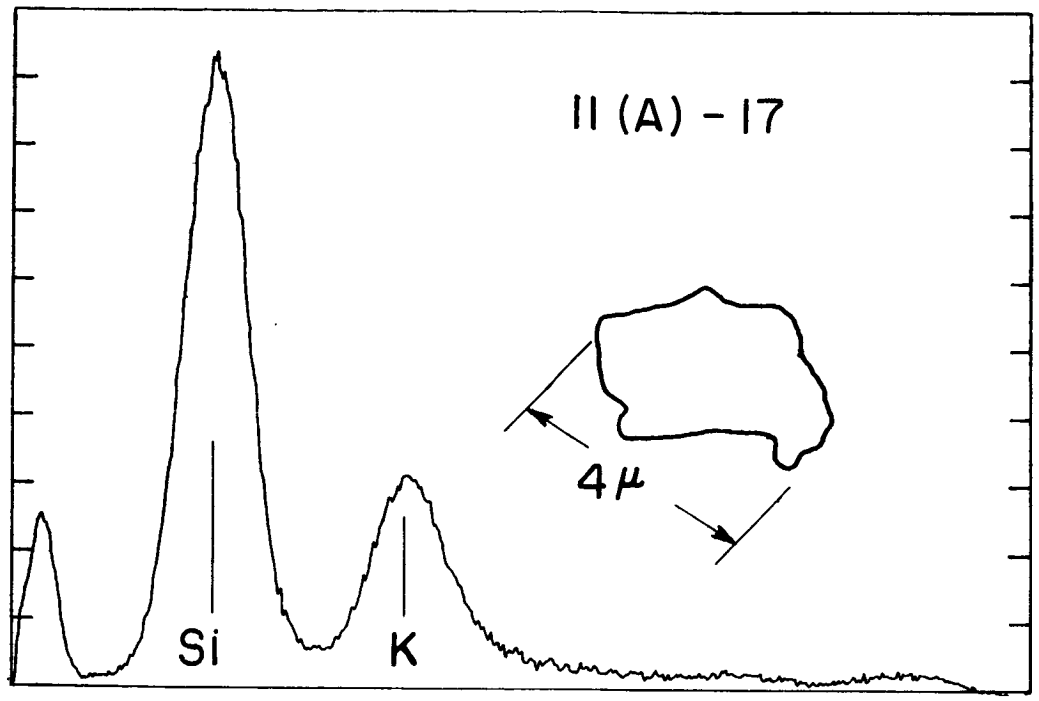

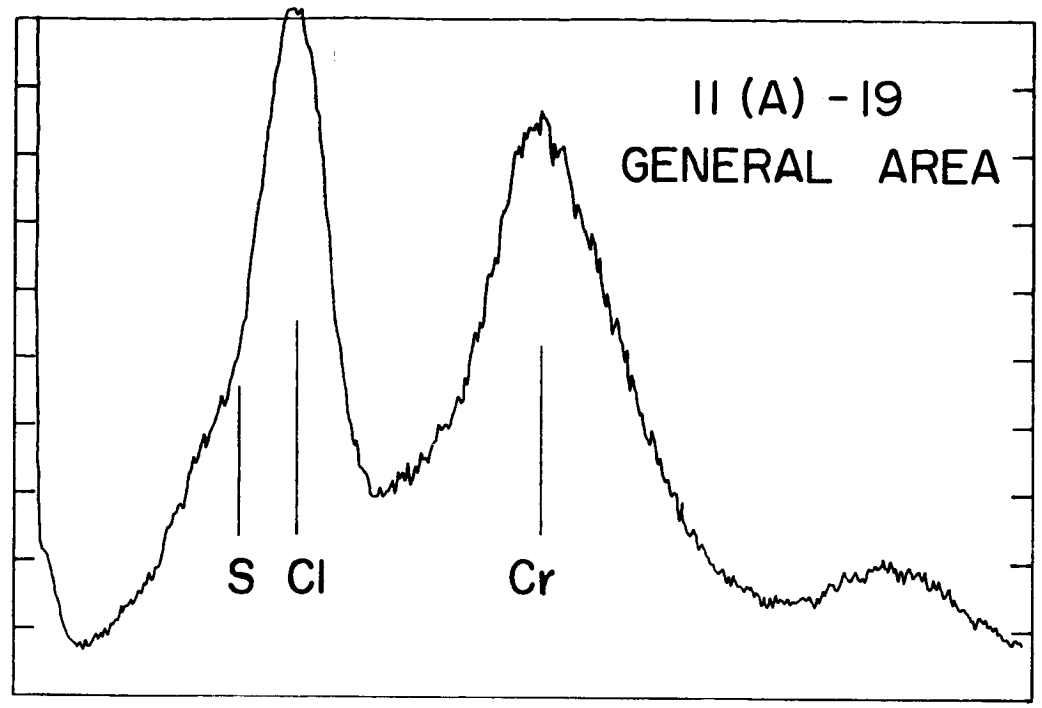

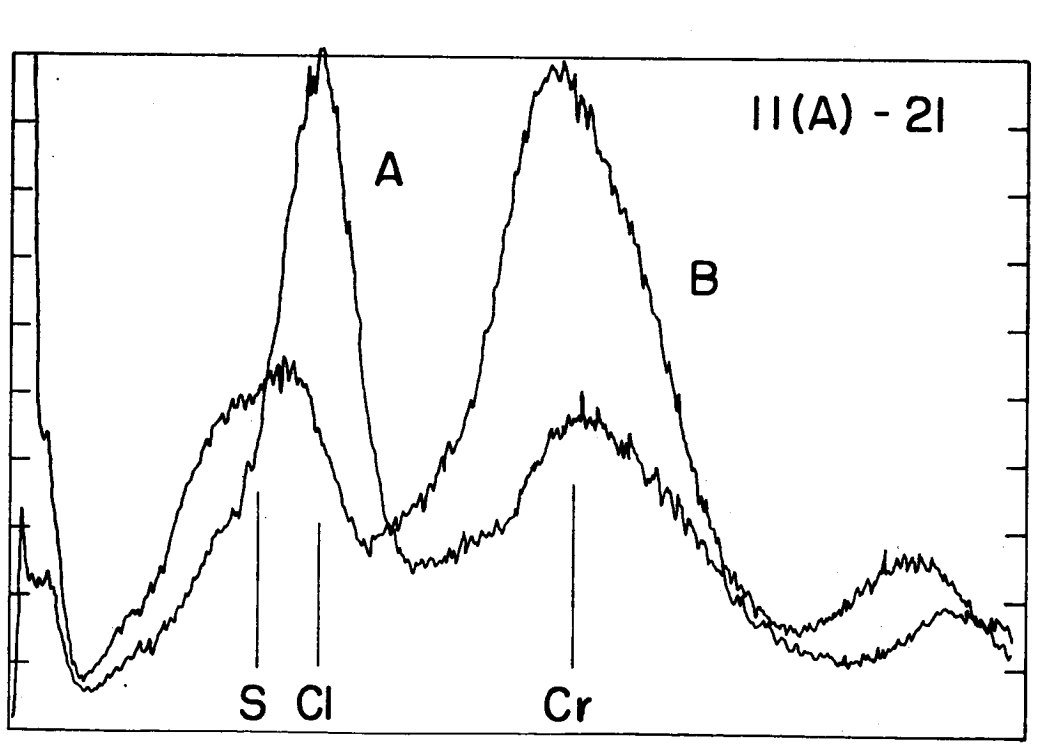

FIGURE V-7 SPECTRA FROM FLIGHT SAMPLE #11

FOLDOUT FRAME 1

FOLDOUT FRAME 2

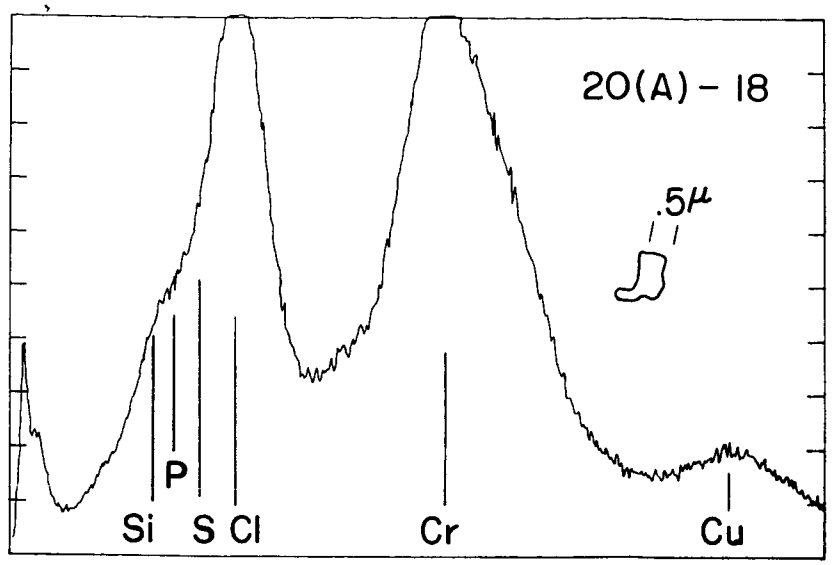

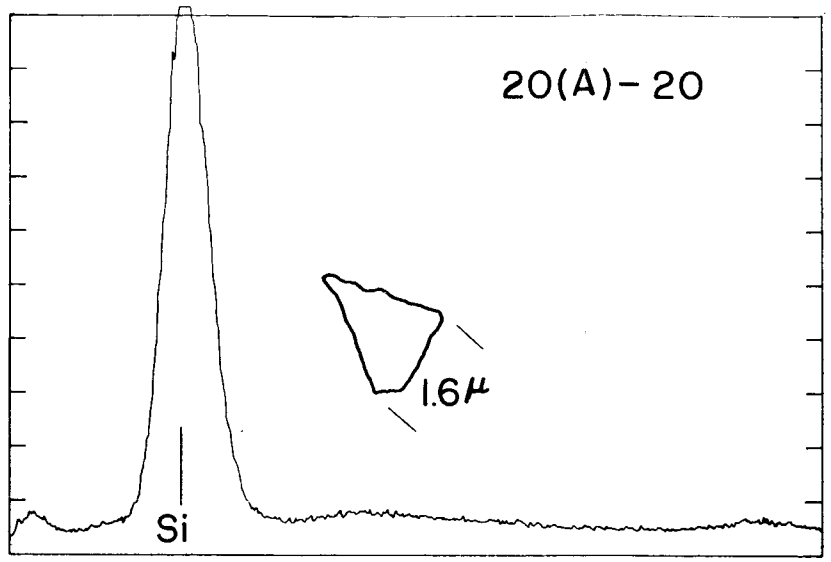

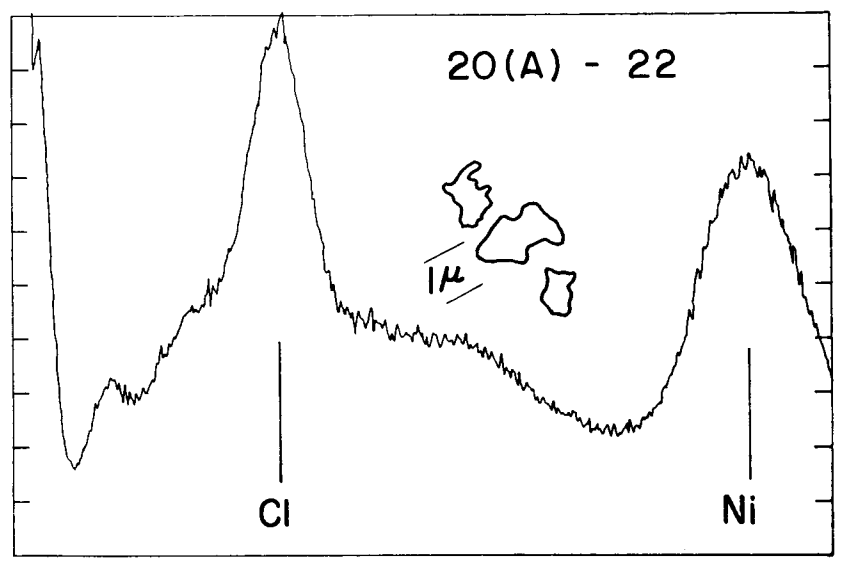

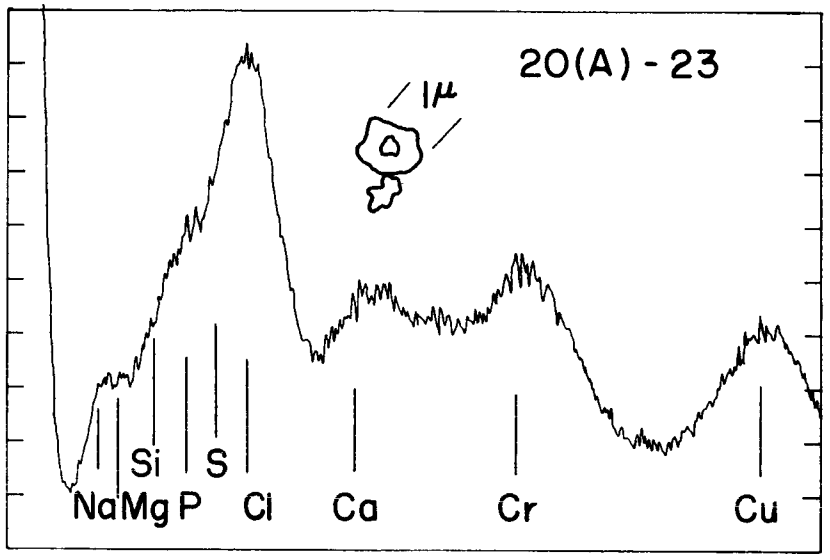

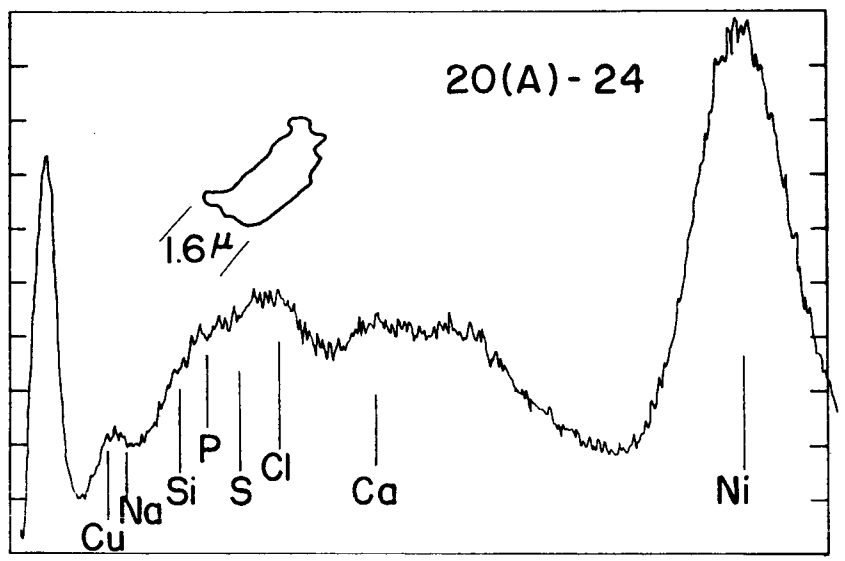

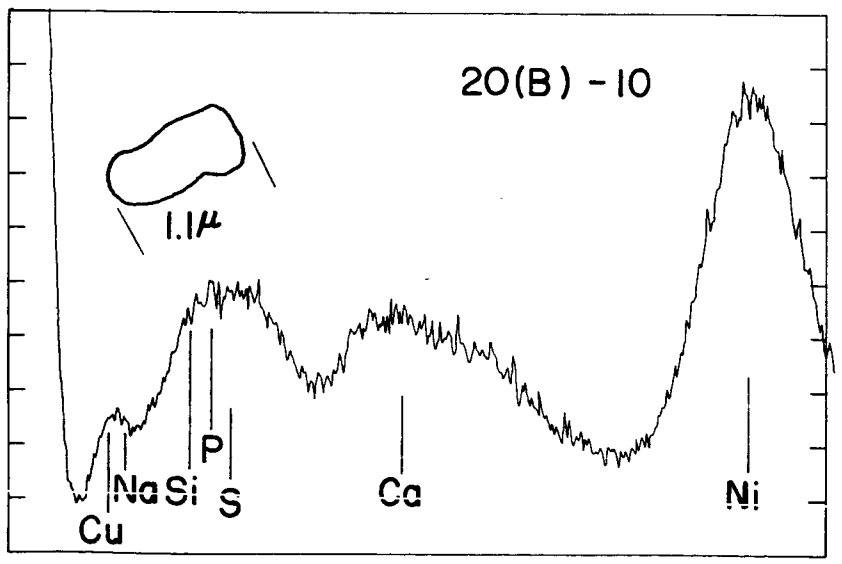

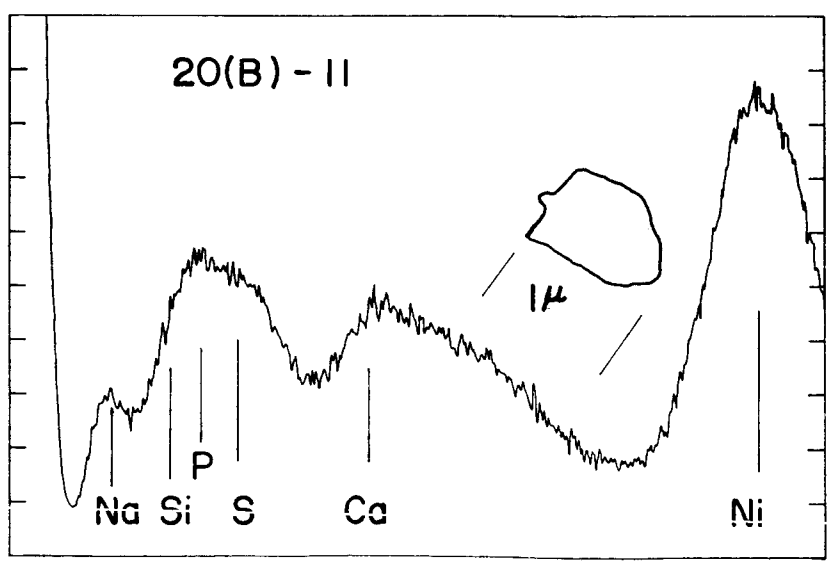

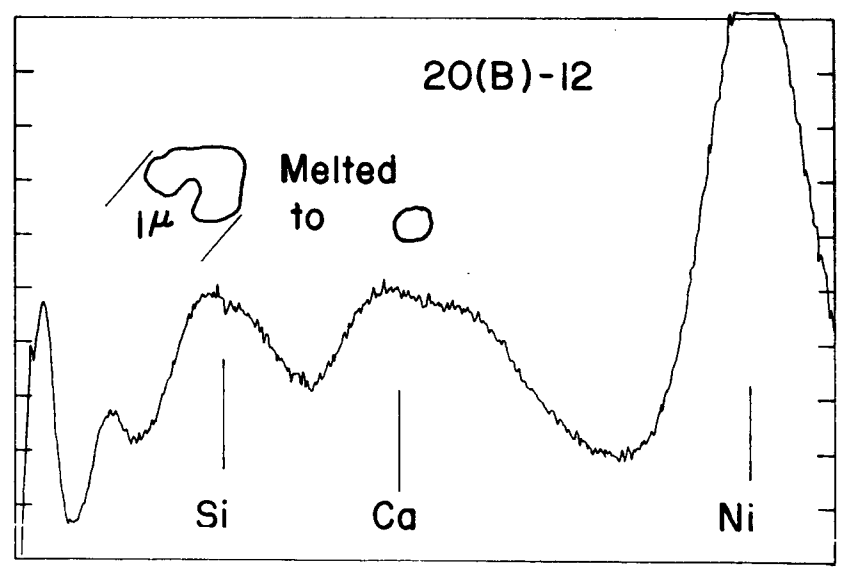

FIGURE V-8 SPECTRA FROM SAMPLE #20 OBTAINED ON SURTSEY ISLAND

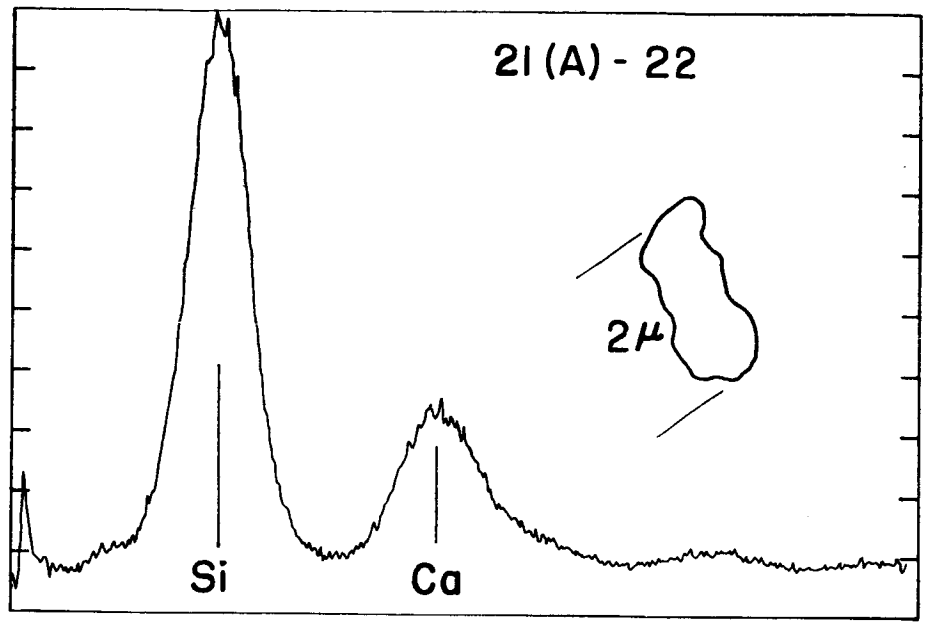

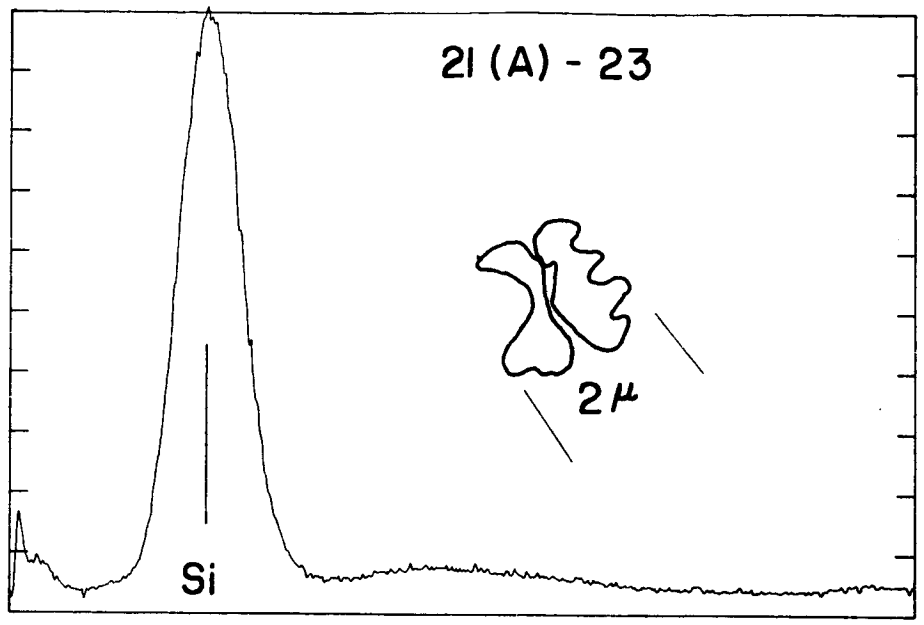

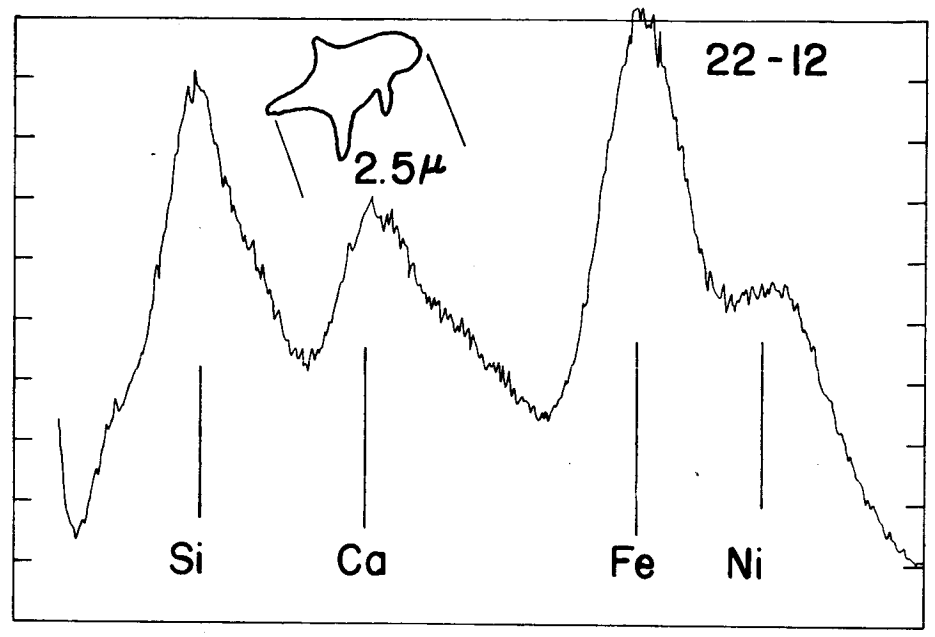

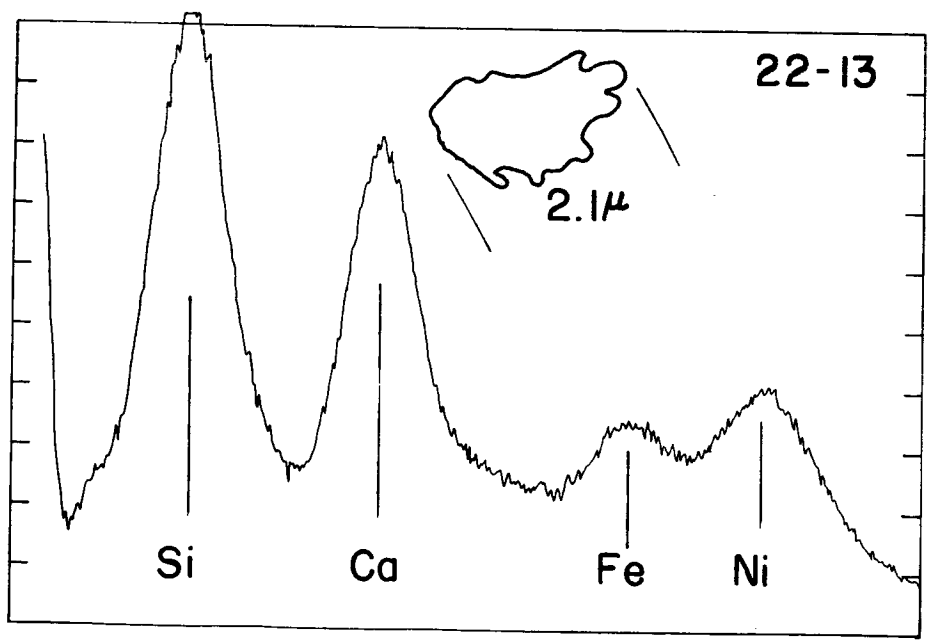

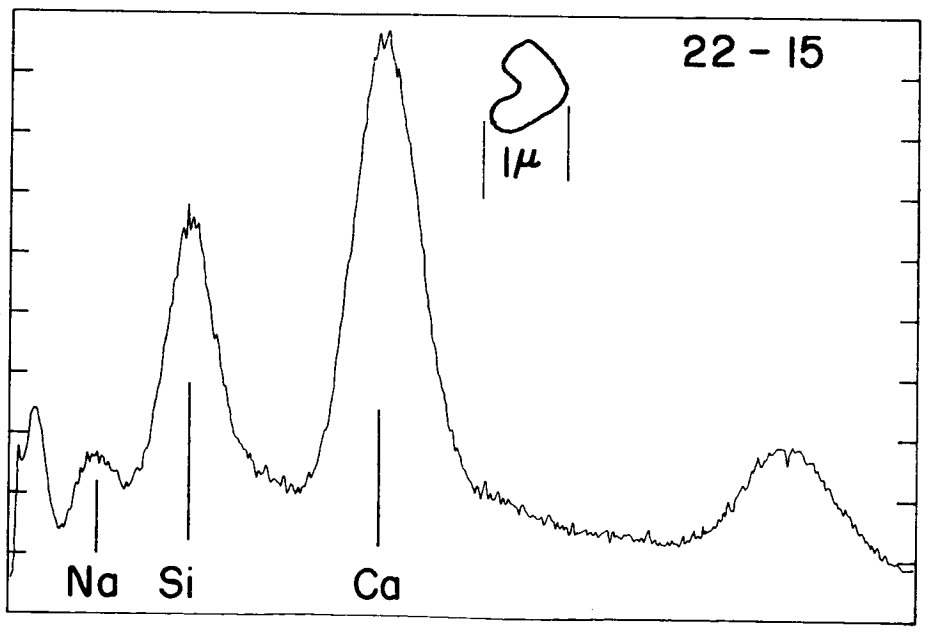

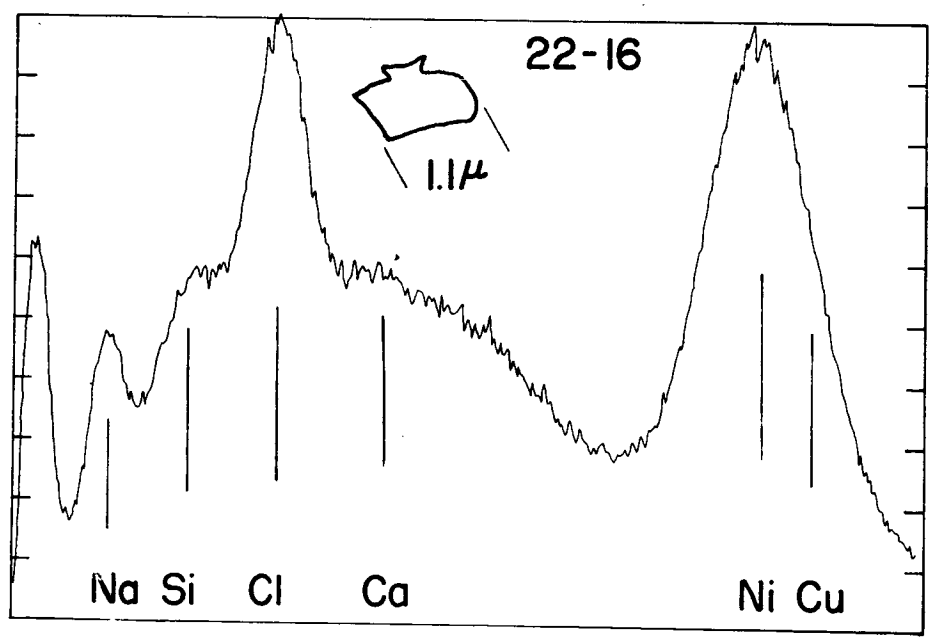

PRECEDING PAGE BLANK NOT FILMED.

FIGURE V-9 A SELECTED SPECTRA INDICATING THE COMPOSITIONAL VARIETY OBSERVED IN FLIGHT SAMPLES #21 AND 22

119-A

Fig V-9 B
119-B

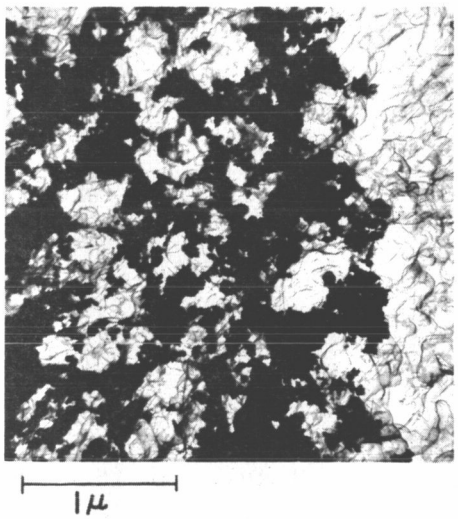

a. General area view showing relatively dense collection of sub-micron material.

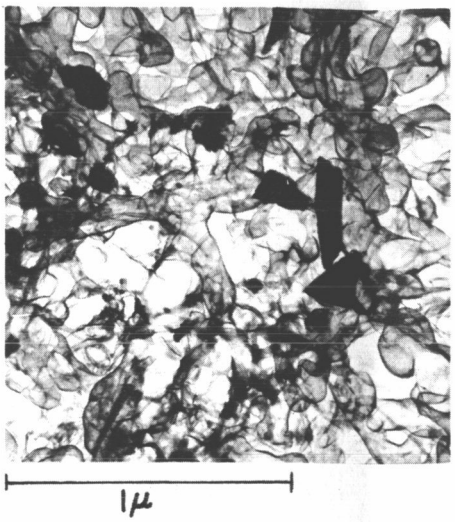

b. Shows angular structure generally observed for particles

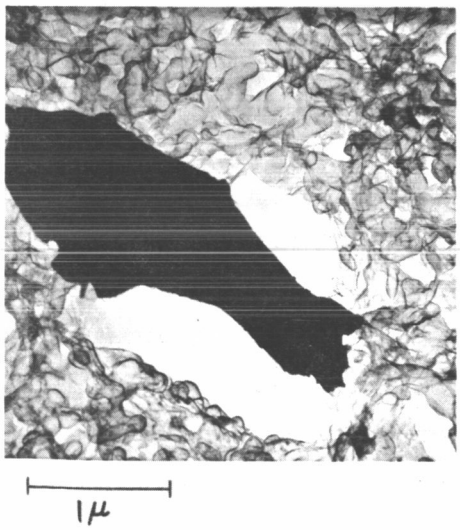

c. Large particle which has begun to melt under electron beam. Some reaction with carbon substrate indicated.

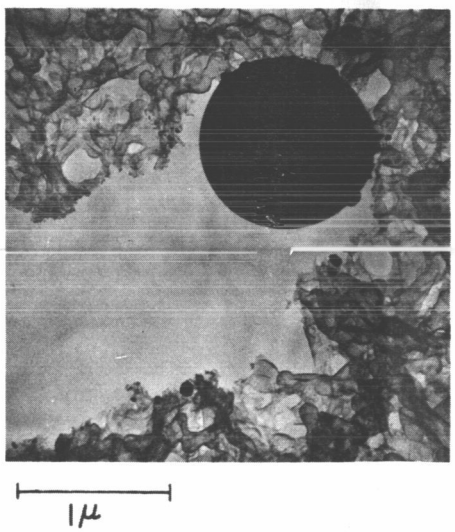

d. Final result of completely melting particle in c.

FIGURE V-10 ELECTRON MICROSCOPE PHOTOS OF SAMPLE #22

4. Discussion

The diversity of particle compositions observed must be indicative of their formation via condensation of volatiles rather than by the mechanical dispersion of the magma. Particles do vary strikingly in their composition. Several observations require discussion. We observe particles which may be categorized in terms of their major components as consisting of calcium plus silicon, chromium plus sulfur and/or chlorine, and nickel and/or iron plus chlorine. It is surprising that we appear to see nickel present more frequently than iron since in the original magma the iron is approximately 1000 times more concentrated than the nickel. It is also notable that we observe little or no magnesium compared to the calcium concentrations. Both nickel and chromium are strongly observable in the particles, but these represent only trace quantities in the magma. The fact that chromium and sulfur and/or chlorine are found together needs explanation. Are these observations in accord with our expectations based on thermochemical data and can the compositions observed tell us anything about the vaporization and condensation process? To consider these questions we will look at the available thermochemical data for volatile chlorides and hydroxides.

The volatilization of silica, alumina, and iron oxides in high pressure steam turbine applications is well recognized. However, the exact nature of the volatile species in these applications has not necessarily been established. Elliott (1952) has reported pressures of SiO_2 of 2.6×10^{-6} atm under conditions of 1 atm water and 1490°C. He reports a higher volatility of silica under reducing conditions and argues for the vapor species being $SiO \cdot H_2O$. Wendlandt and Glemser (1963) report that the species $Si(OH)_4$ is the important volatile silica species up to 180 atm and that at higher pressures more highly hydrated and polymerized species become important. In spite of the uncertainty in the volatile silica species the data of Elliott provides an order of magnitude value for silica volatility in water atmospheres.

Elliott has also examined alumina under comparable conditions at 1500°C and 1 atm water and found no evidence for alumina volatilization.

Thus he argued that the vapor pressure of the alumina hydrate was less than 10^{-6} atm at 1500°C and one atm water. Thermodynamic consideration of the effects of gaseous HCl on alumina to form either volatile AlCl or $AlCl_3$ indicates that a volatile hydroxide species is probably more important than a volatile chloride species. Based on the observations of Elliott we can expect the concentration of SiO_2 to be much greater than that of Al_2O_3 in the smoke particles as we have observed.

In Tables V-7 and V-8 we summarize some thermodynamic calculations for the formation of volatile chlorides and hydroxides of the alkaline earth and iron, cobalt, nickel trio from their oxides. Thermodynamic data for gaseous metal chlorides have been tabulated based both on experimental data and theoretical estimates from Brewer, Somayajulu and Brackett (1963). These data were used together with the data taken from standard thermodynamic tabulations to construct Table V-7. Data for volatile hydroxides have not been developed in a comparable manner. Jordan (1965) has recently reviewed some of the available data for gaseous hydroxides and has also carried out experimental studies which identified the hydroxides $Ni(OH)_2$ and $Co(OH)_2$. The thermodynamic data for the gaseous hydroxides beryllium, magnesium, iron, cobalt, and nickel were taken from the review of Jordan. The data for gaseous barium hydroxide came from the thesis of R.S. Newbury (1965).

One can see in Table V-7 that the pressure of the calcium chloride will be 2 to 3 orders of magnitude greater than that of the magnesium chloride. These pressures are calculated based on the assumption that the activity of the oxide is proportional to its mole fraction in the basalt magma and this assumption probably yields calculated pressures higher than may actually exist. We would expect that the relative ratio of calcium hydroxide to magnesium hydroxide in the vapor would be similar to that calculated for the chlorides. Thus, the data imply that the calcium content in the vapor will be relatively very much greater than the magnesium and thus the calcium content in the particles should be much greater than the magnesium as was observed. One may also note by comparing Tables V-7 and V-8 the relative metal chloride to hydroxide pressure ratios

TABLE V-7

THERMOCHEMICAL CALCULATIONS FOR THE REACTION:

$$MO(s) + 2HCl(g) = MCl_2(g) + H_2O(g)$$

Metal	ΔF_{1500}	$K \left(= \frac{P_{MCl_2} \times P_{H_2O}}{a_{MO} \times P^2_{HCl}} \right)$	$P_{MCl_2} \left(\text{at } \frac{P_{H_2O}}{P_{HCl}} = 100 \right)$
Beryllium	+ 31 kcal/mole	3×10^{-5}	
Magnesium	+ 16.1	5×10^{-3}	$\sim 5 \times 10^{-8}$ atm
Calcium	+ 0.02	1	$\sim 10^{-5}$
Strontium	- 17.6	3.6×10^{2}	
Barium	- 30.9	3.1×10^{4}	
Iron	- 0.77	1.3	$\sim 10^{-5}$
Cobalt	- 2.27	2.1	
Nickel	+ 3.43	.31	$\sim 10^{-8}$

TABLE V-8

THERMOCHEMICAL CALCULATIONS FOR THE REACTION:

$$MO(s) + H_2O(g) = M(OH)_2(g)$$

Metal	ΔF_{1500}	$K \left(= \frac{P_{M(OH)_2}}{a_{MO} \; P_{H_2O}} \right)$	$P_{M(OH)_2} \left(\text{at } P_{H_2O} = 1 \right)$
Beryllium	+ 29.2 kcal/mole	6×10^{-5}	
Magnesium	+ 46.6	1.8×10^{-7}	$\sim 2 \times 10^{-8}$ atm
Calcium			
Strontium			
Barium	+ 20.5	10^{-3}	
Iron	31.0	3.1×10^{-5}	$\sim 2.5 \times 10^{-6}$
Cobalt	34.7	0.9×10^{-5}	
Nickel	33.0	1.6×10^{-5}	$\sim 10^{-9}$

for a pressure of HCl to pressure of water equal to 0.01. These data indicate that for magnesium there will be approximately equal quantities of hydroxide and chloride species in the vapor but that for calcium and for the iron, nickel compounds the chloride species will be most important. It may be noted for the alkaline earth compounds that the beryllium hydroxide is more stable than the beryllium chloride whereas this tendency changes as one goes down the series toward barium. On the basis of these calculations we would expect to find barium chloride the more important species in the gas phase. In Table V-7 for the formation of the chloride, note that there is a consistent change in the free-energy of formation as one goes down the series from beryllium to barium. However, in Table V-8 for the formation of the hydroxide this does not seem to hold true in terms of the beryllium and magnesium data. This may indicate an error in the data for beryllium or magnesium hydroxide. The fact that we find calcium in our particles without the presence of chlorine would seem to indicate that the calcium hydroxide must be a more stable species than indicated by interpolation between the magnesium and barium data of Table V-8.

The data assembled in Tables V-7 and V-8 for the volatile chlorides and hydroxides offer no basis for understanding how nickel came to be present in quantities apparently comparable to iron in the particles while nickel concentrations in basalt magma are on the order of one thousandth that of iron. It should be recognized, however, that our calculations are based on assuming specific vapor species. These are not necessarily the species which are present. Sugden and Schofield (1966) have identified hydroxy-halide species as well as hydroxides and halides in flames. They reported that when an alkaline earth halide was added to a flame that they observed not only dihalides but also hydroxy-halides such as Ca(OH)Cl. In the absence of halide, they reported that the gaseous dihydroxide species predominated over the mono-hydroxide. The equilibrium studies from which the thermodynamic data used in Table V-8 were obtained all indicated that the dihydroxide species were the most important. However, there have been no studies in mixed water-HCl systems which would provide quantitative data on the stabilities of the hydroxy-halides. In addition, most experimental work is based on the study of a single metal.

There has been very little study of systems containing more than one metal vapor species. In this respect, the recent report of Dewing (1967) should be noted. He reports on the enhanced volatility of dichlorides in the presence of trichlorides. Both aluminum chloride and ferric chloride vapors were passed over the dichlorides of magnesium, manganese, and cobalt. The apparent vapor pressures of the dichlorides were increased by several orders of magnitude. Dewing investigated the apparent pressures of the dichlorides as functions of the pressure of the trichlorides and showed from this study that complexes containing two trichloride molecules (presumably of the type $Ca\ Al_2\ Cl_8$) exist and that in the $AlCl_3$ and not in the $FeCl_3$ systems still more complex species containing three trichloride molecules are also present. Thus the possible formation of gaseous complexes between two or more hydroxy or halide species cannot be discounted and may account for the apparently high concentrations of nickel found in the particles. One other mechanism to account for the nickel to iron ratio is to consider a condensation process which favors concentration of nickel with respect to iron. One can conceive that this might occur if on the expansion and cooling of the gases the iron is oxidized and thus a separation between nickel and iron is achieved due to the much lower condensation temperature of ferric chloride as compared to the nickel chloride.

Chromium also occurs in trace quantity in the magma. Chromium concentration in basalts is on the order of two hundred parts per million. Schafer (1964) discusses the transport of chromium as $CrCl_4$ at 400-500°C. He points out that the volatilization of chromium and Cr_2O_3 has been observed in the presence of oxygen at 1000°C or higher and that gaseous species such as CrO_2 and CrO_3 have been identified mass-spectrometrically. He also points out that it has been noted that the presence of water vapor markedly increases the transport of Cr_2O_3. Glemser and Mueller (1964) have studied the volatility of CrO_3 in the presence of water vapor at 135-185°C and have established that the gaseous species is $CrO_2(OH)_2$. Based on the equilibrium constant data of Glemser and Mueller and a 10^{-4} mole fraction of CrO_3 in the magma, we estimate a vapor pressure of the $CrO_2(OH)_2$ of 2/10 atm at 1500°K and one atm water. Thus, this species is extremely volatile and it

is easy to understand the relative concentrations of chromium observed in the particles in spite of being a trace element in the magma itself. The experimental evidence of this study would seem to indicate that chromium may exist in the gas phase as a mixed sulfo-chloride. This is not unreasonable but we have found no previous studies of such compounds.

E. CONCLUSIONS

The great variety of particle compositions observed can only be explained in terms of formation of the particles by condensation from the vapor phase; particles formed by mechanical dispersion of basalt magma during the violent eruption process would be expected to show a greater uniformity in composition.

The experimental data are in accord with volatilization of Si, Ca, and Al as hydroxy compounds. Sodium is not readily detected in the Probescope measurement techniques, but on the basis of the studies on vaporization of basalt discussed earlier in this chapter, it is believed to be an important component of the smokes.

Chromium and nickel which are trace quantities in the magma are observed frequently in the aerosol particles. The thermodynamic analysis indicates that chromium would be highly volatile as a hydroxy compound in spite of its low concentration in the magma. The Probescope data shows chromium generally in the presence of sulfur and/or chlorine, thus indicating that the volatile species may be a sulfo-chloride of chromium. This seems quite reasonable since the existence of gaseous oxy-chlorides are recognized. However, the thermodynamic analysis cannot account for the relatively high frequency of Ni observations to Fe observations in view of the approximately 1:1000 Ni to Fe concentration ratio in the magma. The only interpretation, on the basis of our present understanding of gaseous species, which seems reasonable to explain the observations is the possible oxidation in the atmosphere of volatile ferrous to even more volatile ferric compounds thus permitting the concentration of nickel with respect to iron by a condensation process in the portions of the cloud which we sampled. If nickel, through the formation of some presently

unrecognized complex vapor species is being preferentially vaporized from the magma with respect to other elements, then aerosol particles of volcanic origin will complicate measurements such as those of Brocas and Picciotto (1967). These authors have attempted to use the nickel content of antarctic snow as a measure of the influx rate of extraterrestrial matter over the entire earth's surface.

The particles obtained from the fuming vent on the island Surtsey do appear to differ somewhat in nature from those collected by flying through the volcanic cloud. Further study of aerosol samples from different volcanic situations are needed to define whether the compositions and nature of the particles will differ at different stages of volcanism.

The particle compositions obtained in this study do appear quite distinctive and should make possible the identification of dust layers which have been formed by the deposition of fume particles from volcanic activity. Plans should be made to examine particles from the lunar surface by the Probescope technique.

VI. MAGMA CHAMBER MECHANICS

It is difficult to envisage more than two ways by which material may be expelled from a primary or secondary magma chamber. The first is by way of a tensile fracture through which low viscosity material such as gas, lava, or fluidized ash, easily flows. If the effective viscosity of the chamber contents is too high to satisfy the criteria for flow through fissures discussed in the previous report, eruption can only take place by blowing a hole in the roof of the magma chamber. During this year's program we extended and experimentally tested some of our theoretical models for fissure eruptions and made some progress in our theoretical understanding of the behavior of volcanos of more explosive type.

A. FISSURE ERUPTIONS

1. Experimental Modeling of Dike Formation

In our 1965 report we developed simple numerical criteria for the factors controlling the width of dikes and for the pressures necessary to cause their formation. We have now carried out a series of experiments to test the validity of the pressure criteria and to gain some insight into a number of the less tangible factors which might control the migration of a melt through fractures to the surface.

As a model we took a spherical liquid-filled chamber imbedded in a tank of gelatin (Figure VI-1). The chamber was connected by means of a thin tube to a reservoir which could be raised or lowered in order to increase or decrease the liquid pressure in it. The gelatin was selected as a medium to simulate the behavior of rocks because of its low tensile strength and ability to fracture at easily observable speeds. It also has the advantages of being transparent so that the progress of the "eruption" can be easily observed.

In order to emplace the "magma chambers" the liquid was first frozen in the required spherical shape and then placed in the cold gelatin before it set. Thus, it was necessary to choose a liquid whose melting

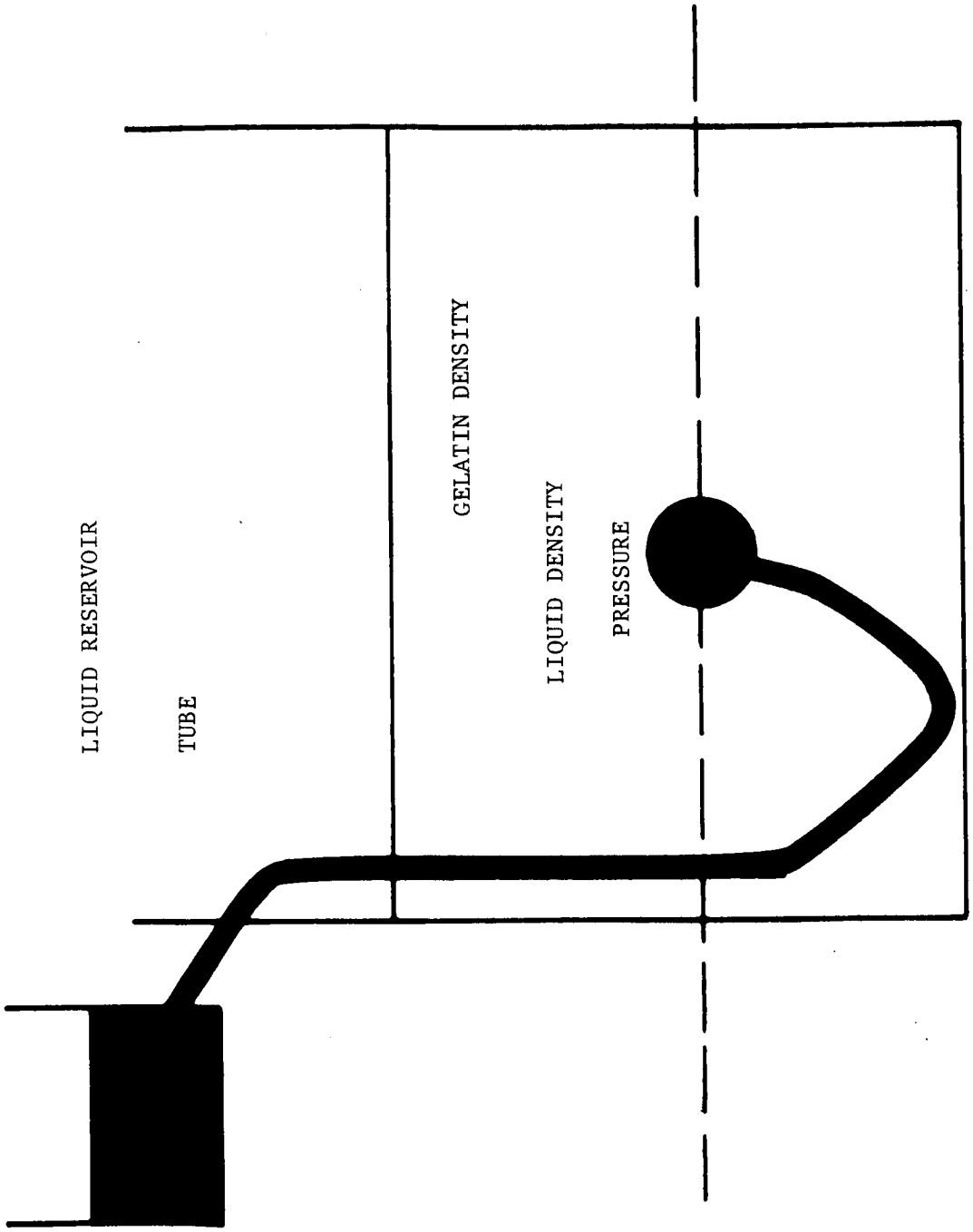

FIGURE VI-1 EXPERIMENTAL ARRANGEMENT FOR ERUPTION SIMULATION

temperature was below that required for the gelatin to set but higher than 0°C. Two liquids, paraxylene and paraldehyde, were selected because they had the required melting properties, a lower density than gelatin, and were immiscible in water. As the two liquids wet the gelatin differently they exhibited some minor differences in their eruptive behavior.

In carrying out an experiment the pressure in the chamber was first set equal to the nominal overburden pressure. The reservoir was raised very slowly, so that the pressure in the chamber could be calculated directly from the hydrostatic head. When the first fracture was formed in the gelatin, the pressure was noted. Then the reservoir was clamped in place and the entire development of the dike and the subsequent surface eruption observed.

It will be recalled from our previous report that we suggested that eruption of magma from a primary chamber took place when the pressure across the potential fault plane was reduced to zero. For a cylindrical magma chamber in a homogeneous, isotropic material, the chamber pressure necessary to fulfill these requirements would be twice the overburden pressure. It can easily be shown (see, for example, Sokolnikoff, 1955) that a similar calculation for a spherical chamber predicts a pressure of three times the overburden pressure will be necessary to produce the required tensile fracture. Neither the spherical nor the cylindrical model is necessarily realistic. If the potential chamber were extremely thin in relation to its length and width or had sharp boundaries, only a slight increase over the overburden pressure would be necessary to cause an opening.

It is possible that even during shear failure a local opening, large enough to admit the entry of magma, would be formed and if this were sufficiently sheet-like, a relatively small pressure increase might cause eruption. Brace (1966) had discussed some other criteria for the fracture of rocks in shear and shows experimental values of shear stress of failure as a function of normal stress across the fracture plane. Within the accuracy required for our models it appears that as long as the stress field is predominately compressional the shear strength is proportional to the overburden pressure.

Figure VI-2 shows the eruption pressure as a function of overburden pressure for a number of tests carried out using the gelatin model. It is clear from the diagram that while a pressure increase was necessary to cause eruption, only seldom did it approach a factor of 2 and never the factor of 3 predicted by the spherical chamber model. There are several possible explanations for this, the first and most obvious is that the theory is unsatisfactory; the second is that the high stress concentrations induced by the presence of the tube leading into the chamber caused fracture to occur prematurely. Some evidence for the latter may be the fact that eruptions frequently started along one side of the chamber and then moved progressively towards the top. Another possibility is that the initial fracture was in shear but the opening was sufficiently large that, once a crack was made, it would continue to propagate. A fourth possibility is that the strains induced in the gelatin were so large that the application of finite strain theory rather than infinitesimal strain theory would be required. Whatever the explanation, it is clear that the experiments described here have neither clearly established nor disproven the criteria we have used for opening the fracture in rocks at high pressures. On the other hand, when the physical and chemical evidence for an approximate pressure doubling, discussed in our previous report, is taken together with the geological and geophysical evidence for the episodic nature of volcanism, it appears that such a criterion may not be far from being realistic. Further investigations of this point would seem to be required.

Although our attempts to prove the pressure doubling hypothesis were somewhat inconclusive, the number of ways in which the models duplicated features observed in actual volcanic eruptions was remarkable, and the insight which they gave us was well worth the experimental difficulties involved. The first point which became apparent as the experiments progressed was that the initial fracture almost always occurred approximately parallel to the plane joining opposite corners of the reservoir. Because this plane is the one farthest from the restraining walls, it is the one across which the tensile fracture may be opened with the minimum excess pressure. Thus, the experiment illustrates how tectonic stresses

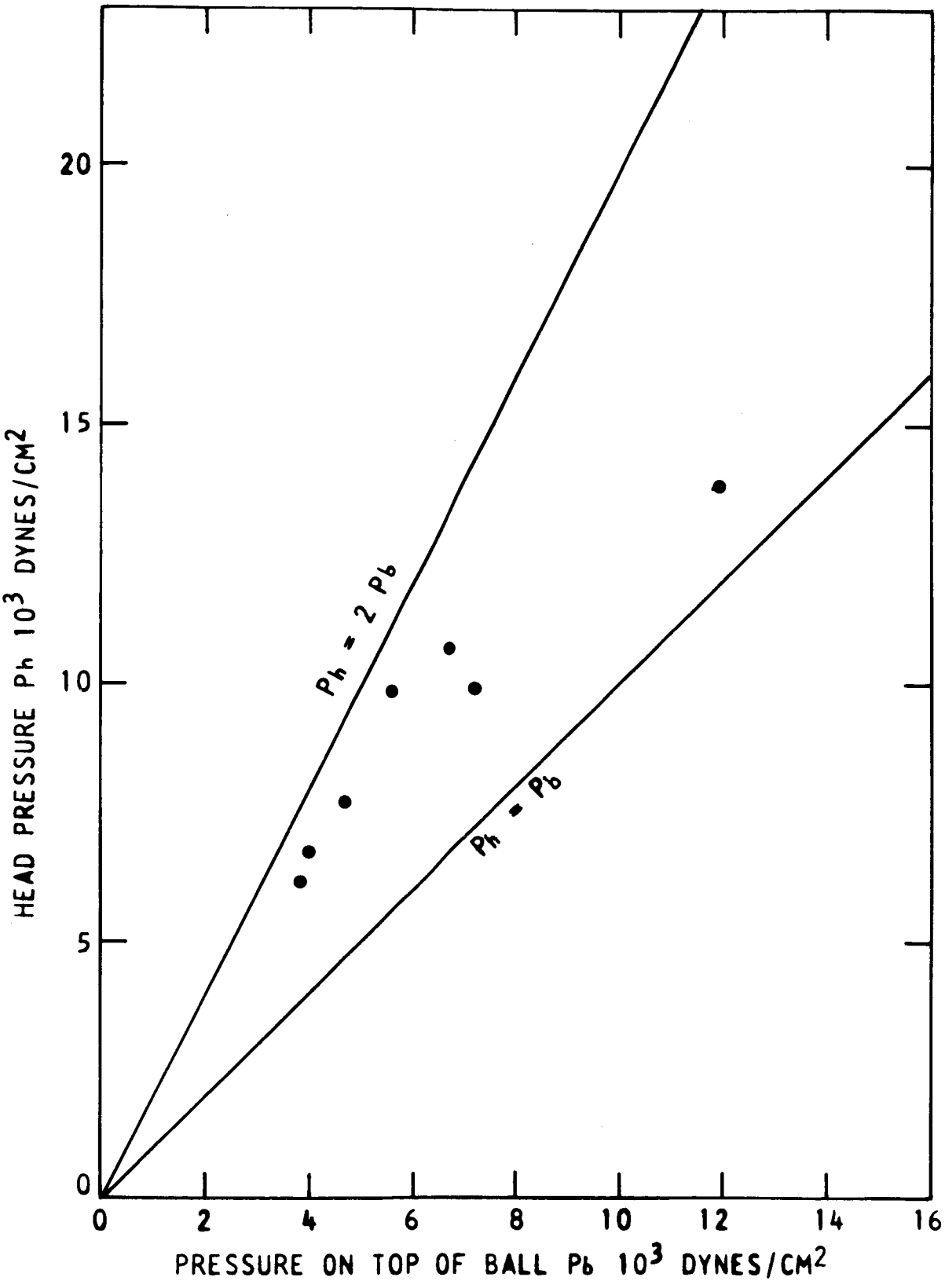

FIGURE VI-2 ERUPTION PRESSURE AS A FUNCTION OF OVERBURDEN PRESSURE FOR GELATIN MODEL

or elastic anisotropy in the rock can control the orientation of the fracture plane and points up the fact that the orientation of long dikes need not reflect orientation of the subsurface magma chambers. We believe it provides a realistic demonstration of the way in which the preferred orientation of dikes, such as those found in Iceland and in northern Scotland is controlled by tectonic stresses as predicted by Anderson (1951) and others.

Figures VI-3 and VI-4 illustrate the development of a typical dike. From the initial fracture of the chamber wall until the dike's edge approaches the surface it spreads laterally as well as upward. The initial surface eruption usually occurs along the entire length of the fracture, but very shortly after the first "fissure eruption" there is a tendency for the flow to be localized along one low impedance path with the result that later eruptions in the same sequence are concentrated at a single point. It is encouraging when considering the validity of the above model to read the description of fissure eruptions given by Rittmann (1942,p.46) who says "Linear or fissure eruptions have the character of initial perforations....Only exceptionally are eruptions repeated at the same fissure after intervals of rest, and even then they are generally first concentrated along a short section of fissure and after a while at a single favored spot."

Another point worth noting is that the linear dimensions of the fissure trace at the surface are usually a substantial fraction, i.e., 1/4 or more of the depth of burial of the source, thus the length of a single fracture zone may be used as a crude estimate of the depth of the chamber from which the melt is coming.

2. Periodicity of Primary Basaltic Eruptions

The use of liquids with different wetting properties to simulate the magma illustrates one type of factor which may act to control the periodicity of volcanic eruptions. When paraxylene, which did not wet the gelatin, was used eruptions tended to periodic in spite of the continuous, but limited, supply of liquid. This periodicity apparently resulted from

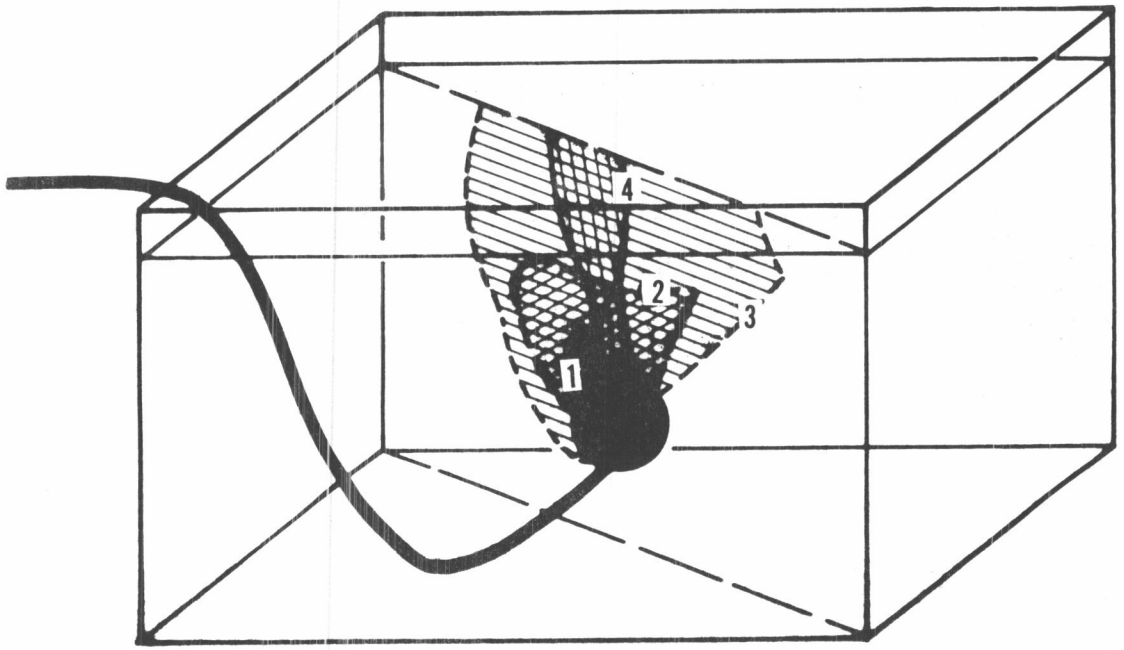

1. Initial perforation
2. Spreading toward surface
3. Initial fissure eruption
4. Localization of flow along path of least resistance

FIGURE VI-3 SKETCH OF STAGES OF DEVELOPMENT OF A TYPICAL DIKE IN GELATIN

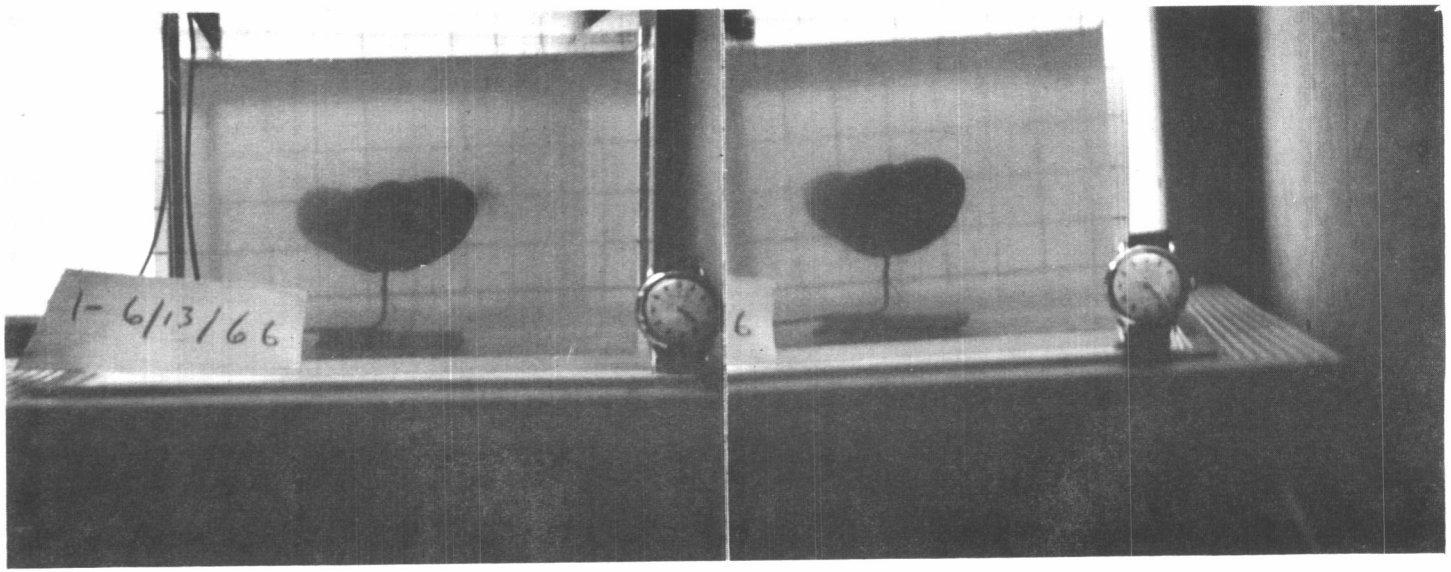

FIGURE VI-4 STEREO PAIR SHOWING DIKE APPROACHING SURFACE

the higher pressure necessary to force liquid into an already existing fracture than could be maintained by the rate at which magma was supplied to the chamber. An analogous situation appears in nature where a minimum flow rate must be maintained in order to prevent the melt from cooling. If this minimum rate is lower than the rate at which melt is generated, then the eruptions will become periodic. In contrast, when a liquid which wet the gelatin is used after the initial breakthrough, they tend to be continuous.

In principle the ratio of dormant period to eruption period can be calculated by comparing the average magma generation rate per fissure to the average flow rate in the fissure. For a fixed generation rate the minimum ratio occurs when the flow through a dike is the smallest that will sustain continuous flow without solidifying. In our 1965 report we pointed out that a peculiar characteristic of all dike swarms and of the individual dikes is their relatively uniform width. A semi-quantitative explanation of this uniform width was obtained by considering the balance between the heat generated within the dike by frictional effects and the heat lost to the walls by conduction. We suggested that if one injected a hot viscous magma into a cold rock it would start to cool, rapidly at first, more slowly later, resulting in a rapid increase in viscosity which would act to prevent flow. The detailed analysis of the heat losses associated with formation of a new fracture by a dike is a complicated one and no solutions are yet available. As a first approximation we attempted to avoid many of the complexities by postulating that dikes can only propagate when the total heat generated per unit length exceeds the heat loss shortly after the time of intrusion. It then was relatively easy to estimate the critical dimensions for such a dike.

We originally took as our model a highly oversimplified, idealized feeder dike leading from a magma chamber to some point near the surface (Figure VI-5a). The width of the dike is 2w and the densities of the wall rock and the melt are ρ_w and ρ_m, respectively. If the walls of the chamber are weak enough to maintain the pressure in the chamber as the magma is withdrawn, the effective pressure gradient driving the melt upward will be

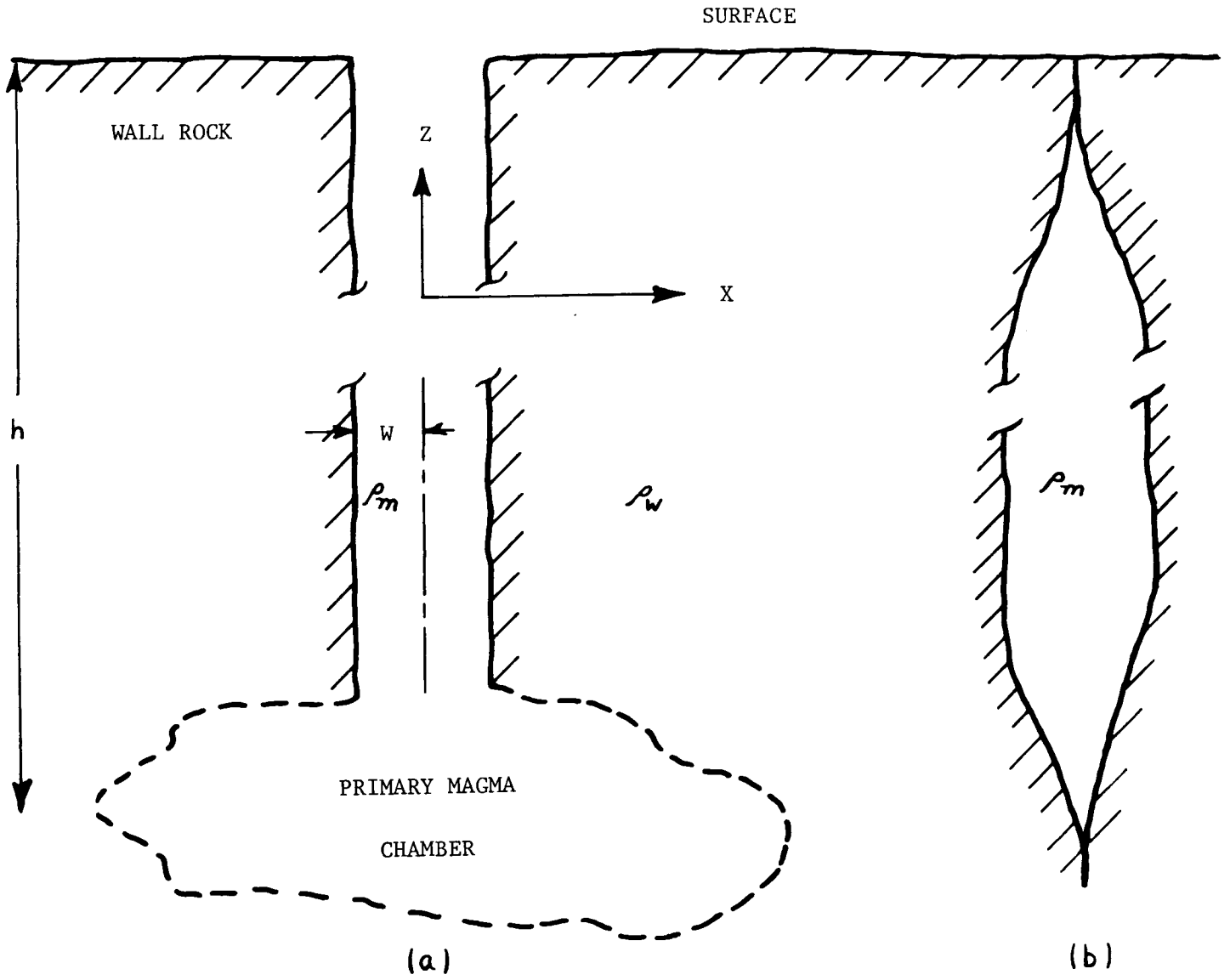

FIGURE VI-5 MODELS FOR SIMPLE DIKE PROPAGATION THEORY

$$\frac{\partial \bar{p}}{\partial z} = (\rho_w - \rho_m)g \qquad \text{(VI-1)}$$

where g is the gravitational acceleration.

While this model is convenient to illustrate the problem, it is not necessary that the dike be connected either to the primary chamber or to the surface in order to have the same effective driving pressure gradient. Consider Figure VI-5b which shows schematically a dike without such connections. The pressure gradient $\partial p/\partial z$ in the wall rock acting across the fracture plane will be roughly $\rho_w g$ and that in the melt will be $-\rho_m g$ where ρ_w and ρ_m are the densities of the wall rock and melt, respectively and g is the gravitational acceleration. The effective pressure gradient will thus be $\bar{p}_{,z} = (\rho_m - \rho_w)$ and equations of motion for the melt may be approximated by:

$$\frac{\partial}{\partial x}\left(\frac{\eta(x)\partial v}{\partial x}\right) = \bar{p}_{,z} \qquad \text{(VI-2)}$$

which was Eq.(3.21-3) of our first final report.

For a 10% density difference between the melt and the wall rock, the driving pressure gradient would be about 300 dynes per square cm.

It was relatively straightforward to show that if the viscosity η is uniform everywhere within the dike, the total frictional heat Q_η generated with the dike per unit surface area is

$$Q_\eta = \left(\frac{\partial p}{\partial z}\right)^2 \frac{w^3}{3\eta} \qquad \text{(VI-3)}$$

If we have values for the pressure gradient and viscosity, then we can determine how much heat is being generated per unit surface area. Figure VI-6, taken from our 1965 report, shows some predicted values of viscosity as a function of temperature for dry basalts compared with some experimental data from Euler and Winkler (1957), and from Shaw (1963).

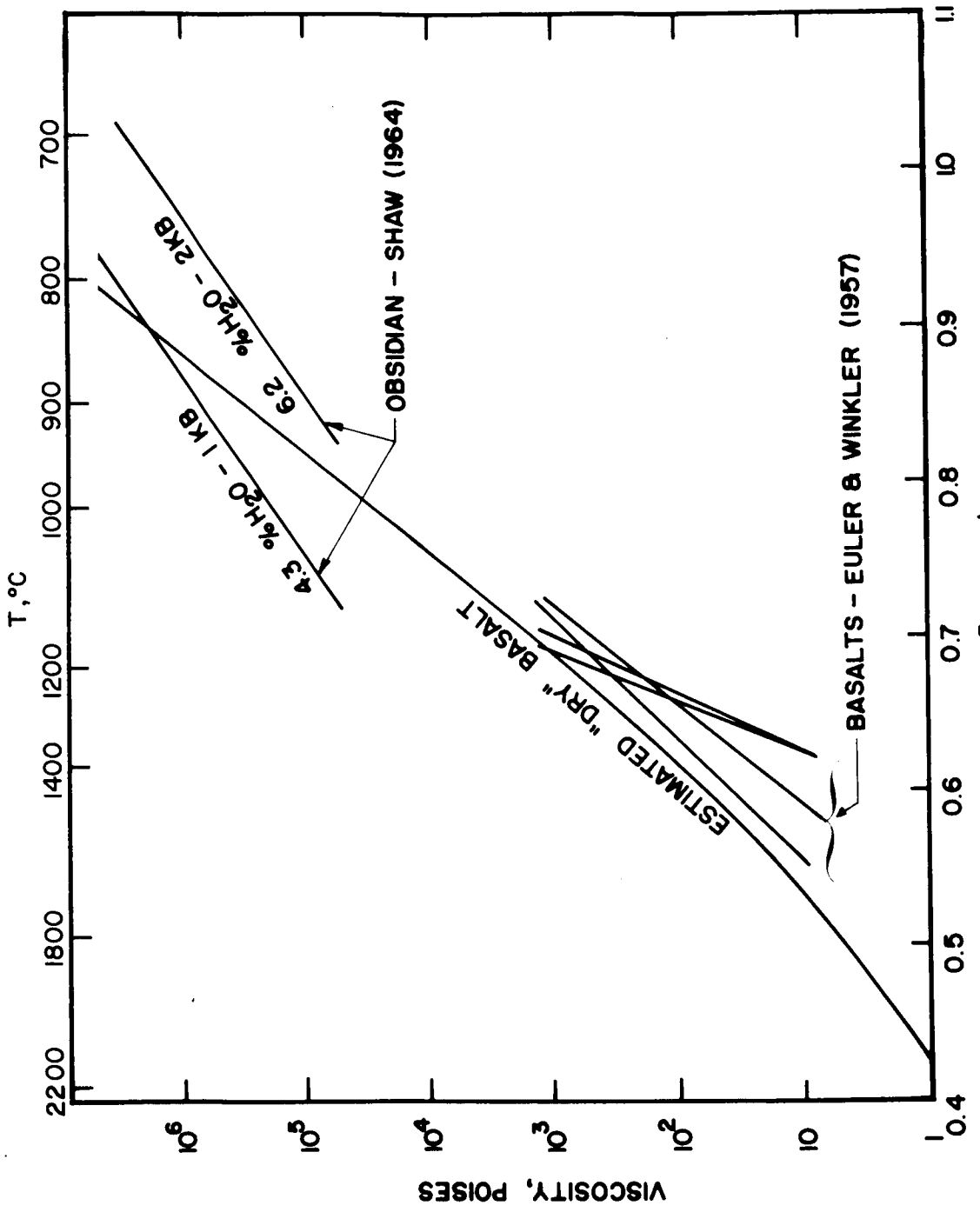

FIGURE VI-6 TYPICAL MELT VISCOSITIES AS A FUNCTION OF TEMPERATURE

In general, basalt melts extruded onto the surface of the earth are estimated to have viscosities around 10^4 poises although these may vary between 10^3 and 10^5 poises. If we substitute such typical values of viscosity into the expression(VI-3) for Q_η and choose a pressure gradient of 300 dynes per cubic cm, we can estimate the heat generated as a function of dike width. In Figure VI-7 we show the amount of heat generated per square cm of surface area calculated as a function of dike widths for three viscosities: 10^3 poises, 10^4 poises, and 10^5 poises. We see that under a fixed pressure gradient as the dike width increases, and as the viscosity decreases, the rate of heat generated increases.

Now let us consider the heat lost to the sides. Here, although it is difficult to write an exact expression for the heat loss, we have approximated it by a function of the form

$$Q_L = k\ (T_m - T_w)\ \beta(t)/w \qquad \text{(VI-4)}$$

where

k = the thermal conductivity

T_m = the magma temperature

T_w = the wall temperature

β is some parameter which varies with time.

The longer the dike has been emplaced, the lower the thermal gradient at the edges, and lower the value of $\beta(t)$. If we choose $k = 5 \times 10^{-2}$ watts/cm °C and the difference between the magma and wall temperatures to be 1000°C, all that remains in order to be able to determine the heat loss is an estimate for β.

Carslaw and Jaeger (1959) have discussed the problem of a cooling dike in which no heat is generated. From their results we can make a rough estimate of β. In Figure VI-8 we show β as a function of the fraction of the original temperature difference remaining between dike and wall rock for a dike whose thermal conductivity is high or one which is well mixed.

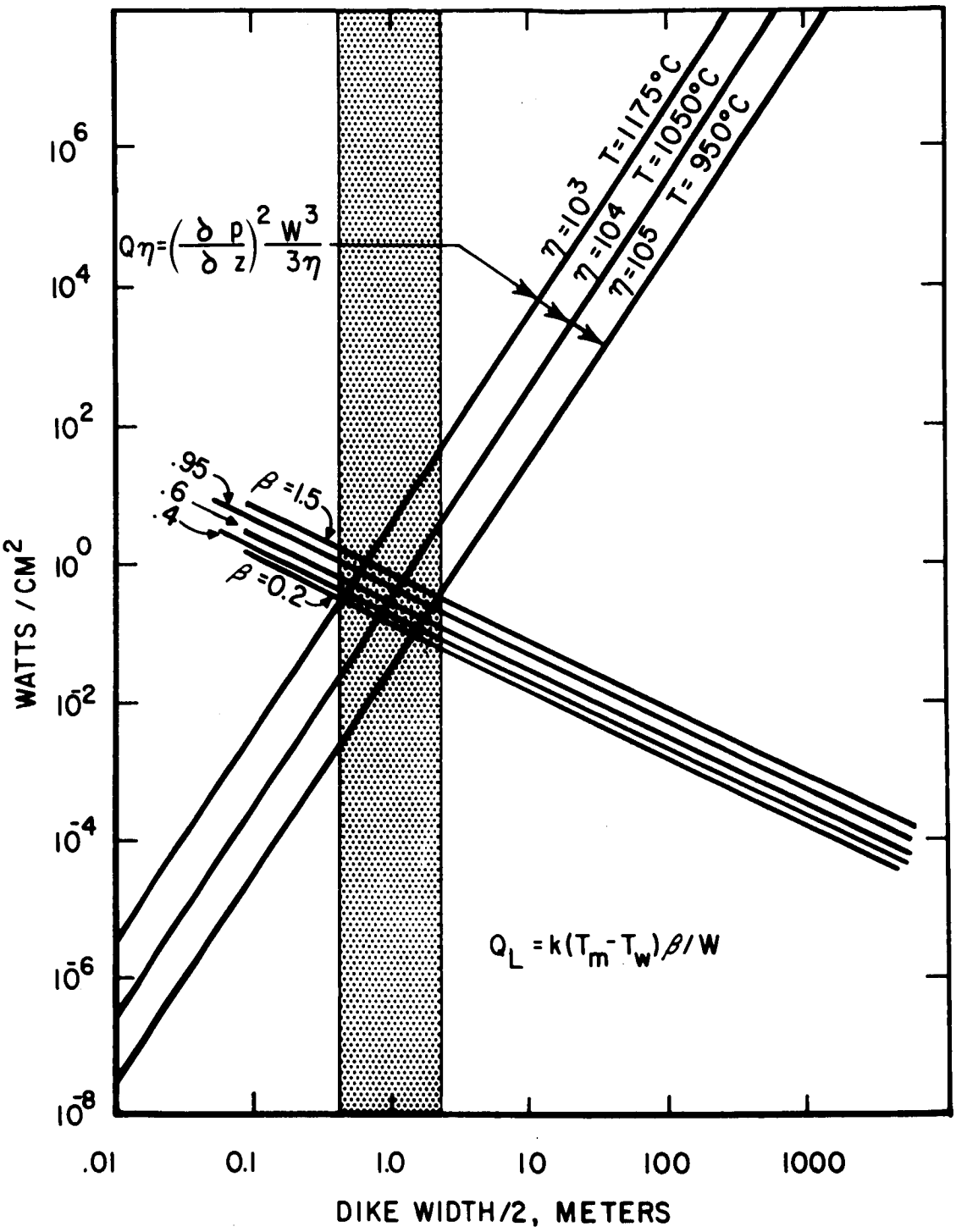

FIGURE VI-7 COMPARISON OF HEAT GENERATION WITH HEAT LOSS AS A FUNCTION OF DIKE WIDTH, HEAT CONDUCTION FACTOR β, AND VISCOSITY, FOR A PRESSURE GRADIENT OF 300 DYNES/CM^2/CM, AND INITIAL TEMPERATURE DIFFERENCE BETWEEN COUNTRY ROCK AND WALL ROCK OF 1000°C. SHADED AREA REPRESENTS MINIMUM WIDTHS MOST FAVORABLE FOR BASALTIC DIKE FORMATION UNDER THESE CONDITIONS

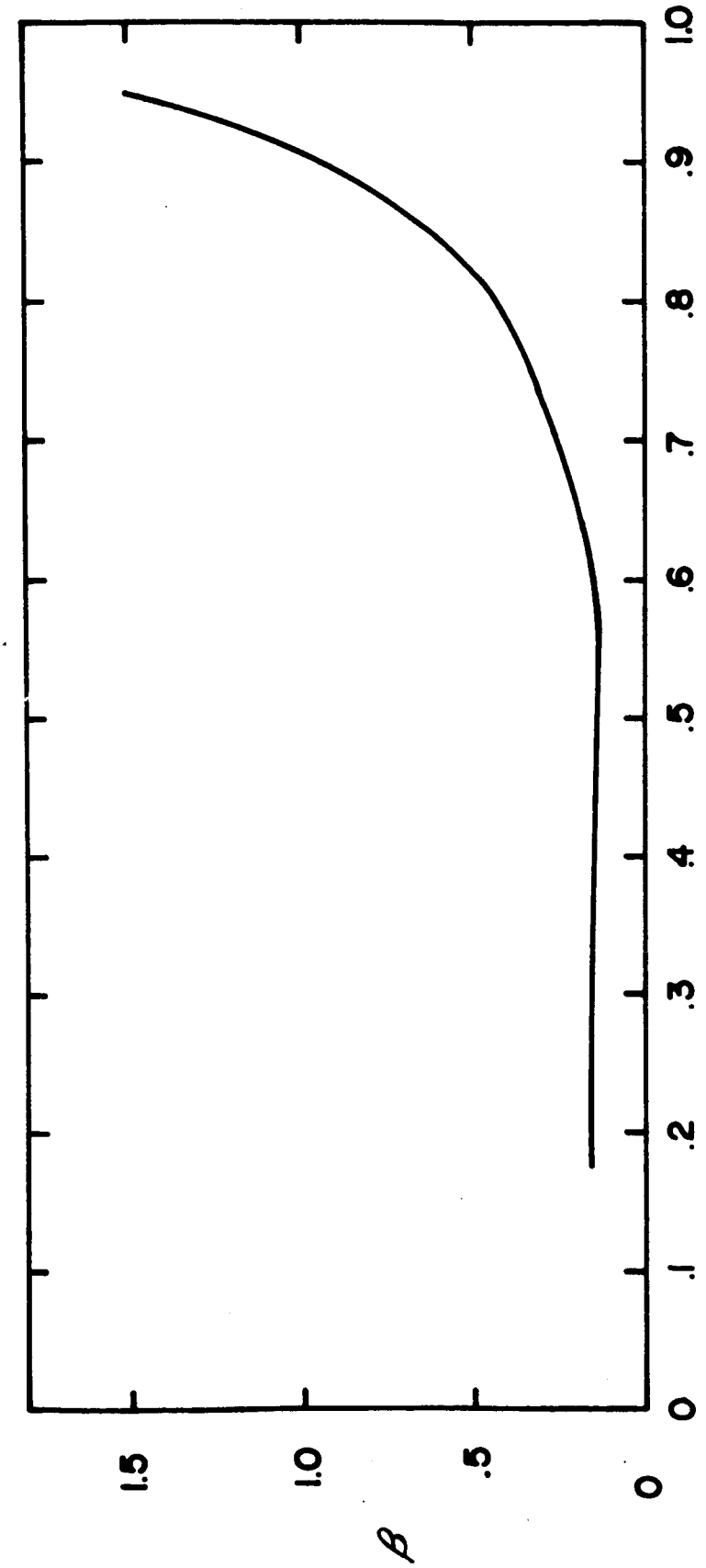

FIGURE VI-8 HEAT CONDUCTION FUNCTION β ($\Delta T/\Delta T_o$) FOR A STATIONARY DIKE WITHOUT HEAT GENERATION (after Carslaw and Jaeger, 1959)

We see that initial values of β are very high but by the time the temperature difference has dropped to 90%, β is less than 1. Figure VI-7 compares the heat loss Q_L as computed from Eq. (VI-4) with the heat generated as a function of β and w. It shows that the heat loss Q_L is far more sensitive to the width of the dike than it is to the exact value of β. In general, as the width of the dike increases, the rate of heat loss will decrease for similar values of β (i.e., the ratio of remaining heat to original heat). We previously showed that the critical half-width w, where the rate of heat loss is equal to the rate of heat generation for a temperature difference between wallrock and dike of a 1000°C is on the order of 1 meter. Narrower dikes will cool rapidly and wider ones will generate more heat than can be conducted away. In the latter case, the melt will become less viscous, resulting in a high flow rate and high heat generation, allowing even more melt to be passed through the same sized opening.

We mentioned in our 1965 report that Thorarinsson (1965) estimated 4 ± 2 meters as a reasonable width for Icelandic eruption fissures 100 meters below the surface and that Bodvarsson and Walker (1964) computed the average width of 1000 dikes in eastern Iceland to be around 3 meters and the average of 450 dikes further south to be 3.7 meters. It is interesting to note that Bailey and Wilson (1924) and Richey(1939) estimate the average width of the Tertiary tholeiitic dikes in Mull to be 1.8 meters. Translating these dike widths into half-widths one gets values of 2, 1.5, 1.6, and .9 meters, only slightly greater than the minimum predicted from the rough calculations above. In terms of our model we would estimate from Figure VI-7 that the Icelandic dikes may be somewhat above the minimum width, and hence their flow rate may be limited by the rate at which magma can be supplied from the mantle. If those in Mull are of similar viscosity then they are close to the minimum size that can be stable.

We noted in our 1965 report that by going through the same calculations for dikes on the moon where the pressure gradient is 1/6 of that on earth, that one finds, for similar melts propagating through similar type materials, the critical dike width would be about 2.6 times as wide as on the earth.

We are now in a position to test the models by estimating the periodicity of terrestrial volcanic eruptions from them and then comparing these estimates with observations.

The volume flow through each side of a dike or half-width w with viscosity η is given by

$$V = -\overline{p}_{,z} w^3/3\eta \qquad \text{(VI-5)}$$

This volume is shown in Figure VI-9 with the critical dike width region shaded. Thorarinsson (1965), in summarizing the available data on Icelandic fissure eruptions, reports

"By far the largest lava eruption in Iceland in Historical Time and the longest ever witnessed by man anywhere on the earth was the Laki eruption in 1783. A rather thorough and reliable description of this eruption, written by Reverend Jón Steingrímsson, is summarized by Thoroddsen in his Geschichte der isländischen Vulkane, together with a description of the fissure (pp.14-67). The eruption started June 8, 1783. The entire Laki fissure which erupted in 1783 is about 25 km (cf. Geol. Map of Icland, South Central portion) but the fissure is separated in two by Mt. Laki which it did not cut through. Until July 29 the lava flowed down the canyon of the river Skapta (cf. the map) but on that day explosive activity like that of the first day of the eruption began again and lava started flowing eastward towards the Hverfisfljot river. It is very likely that until July 29 only that part of the fissure which is SW of Mt. Laki was active and that the NE part of the fissure opened up July 29. After that only a small amount of lava seems to have been emitted by the fissure SW of Mt. Laki. According to Thoroddsen and verified by the new gological map (see map referenced above) the area of the lava that flowed from the SW part of the fissure is about 370 km^2 and its volume about $10^{10} m^3$. A. Hellands estimate is about 15% higher. Assuming that practically all this lava flowed during the first 50 days (until July 29) which is very likely, we have an average flow of about 2300 m^3/sec. Assuming also which is likely, that all this lava flowed from the SW part of the fissure, the lava emitting part of which has a length of about 10 km and assuming further an average fissure width of 4m,

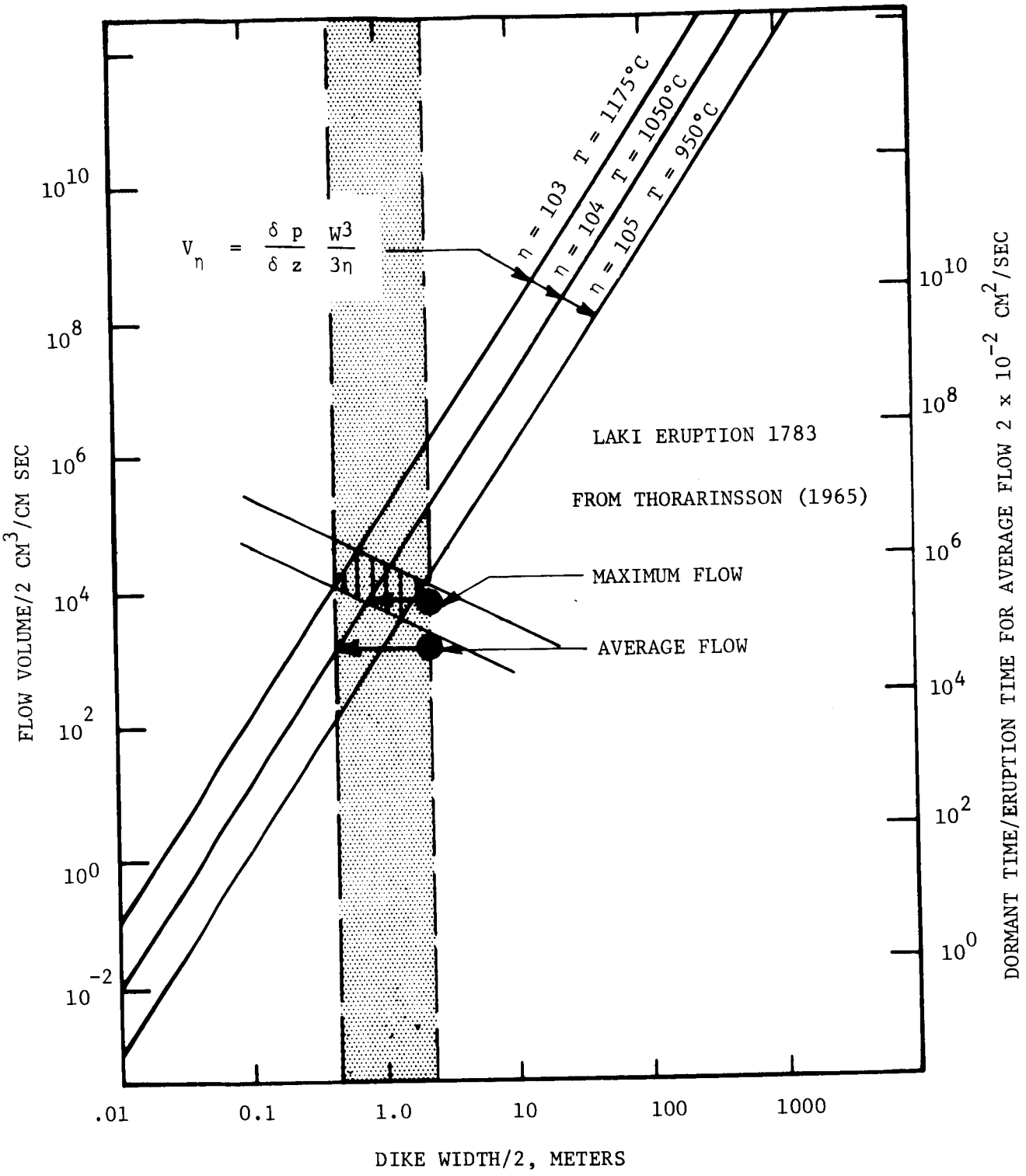

FIGURE VI-9

(a) VOLUME FLOW AS A FUNCTION OF DIKE WIDTH AND VISCOSITY FOR AN EFFECTIVE PRESSURE GRADIENT OF 300 dynes/cm²/cm

(b) RATIO OF DORMANT TIME TO ERUPTION TIME AT AVERAGE BASALT EXTRUSION RATE OF 2×10^{-2} cm²/sec

like in our former cases, we have an average upward migration for these 50 days of nearly 6 cm/sec. But no doubt the rate of flow varied a lot and we may safely assume that the maximum flow was at least 5 times that of the average flow for so long a period which brings us to figures of about 30 cm/sec for maximum upward migration. Further it should be kept in mind that hardly did the 10 km long fissure pour out lava in its entire length at the same time, which means that 30 cm/sec is in all probability a minimum figure for the maximum upward migration.

"These are the only three fissure eruptions in Iceland where we can reach some reasonable approximation as to the upward migration of the melt. The most uncertain factor in this is probably the fissure width. But the figures arrived at, assuming the same fissure width for all the eruptions are in rather a good agreement with each other, as seen from Table I [VI-1].

"In the table I have calculated with 4m width of fissures and density of melt the same as of solid lava. This is certainly too high a density for the melt, I would think at least 50% too high for the upper part of the fissure. Consequently the flow and upward migration figures in the table are at least 50% too low."

TABLE VI-1

UPWARD MIGRATION OF MAGMA IN THREE ICELANDIC ERUPTION FISSURES*

	Laki, 1784	Hekla, 1947	Askja, 1961
Length of fissure, m	10000	4000	400
Time-span, hours	1200	20	8
Average flow, m^3/sec	2300	1250	600
Avg. flow/100 m fissure, m^3/sec	23	31	150
Avg. upward migration cm/sec	6	8	35
Estimated max. flow m^3/sec	12000	5000	1000
Est. max. flow/100 m fissure, m^3/sec	120	125	250
Est. max. upward migra. cm/sec	30	30	60
SiO_2 content %	49 to 50	57 to 58	50.3
Estimated viscosity, poises	10^4	10^6 to 10^7	10^4

*From Thorarinsson (1965)

The average and maximum flow rates correspond to 200 cm^3/cm sec and 6000 cm^3/cm sec respectively. When these values are plotted on Figure VI-9 it is obvious that to make the flow volume, dike width, and viscosity estimates consistent would require either intermittent flow and a dike width at depth closer to 2 than to 4 meters, or continuous flow and a width of about one meter. While the intermittent model would seem to be the most consistent with our present minimum width criteria, a better understanding of the function β (t) is needed before this can be established with any certainty.

Assuming a mid-Atlantic ridge spreading rate of 1.25 cm/yr and an average crustal thickness of 5 km, we have estimated the rate of generation of basaltic crust to be about 2×10^{-2} cm^3/cm sec to each side. If the Laki eruption were typical of ridge fissure eruptions then the average ratio of dormant time to eruption time for any given line across the volcanic region should be $(1.3 \times 10^3) / (2 \times 10^{-2} = 6 \times 10^4$. If the eruption lasted 50 days the expected dormant time in years would be $(6 \times 10^4 \times 60) / 365 \sim 8000$ years. If all fissure eruptions were of this size and duration we could predict how often such an eruption would be expected over the entire length of Iceland. We note that as the 10 km fissure represents about 1/40 of the total length of Iceland, an eruption such as from the southwest half of the Laki fissure should take place about once every 200 years. If we consider that the eruption from the northeast fissure was of the same order of magnitude then an eruption of the size of two taken together would occur every 400 years. This does not seem to be inconsistent with observations.

All these estimates assume that fissure eruptions on Iceland are taking place at the same rate as on the rest of the mid-Atlantic ridge. If the crustal structure in Iceland is not typical of the ridge they may have to be revised.

It is also interesting to make a simple calculation on the relative frequencies of eruptions from volcanos like Surtsey. Consider a dike with half-width one meter and viscosity 10^4 poise being driven by a pressure gradient of 300 dynes/ sq cm. The flow from each side of this dike would be about 100 cm^2/cm sec. Now at a rate of basaltic crust generation

of 2 x 10^{-2} sq cm/cm sec the ratio of the dormant to eruption times would be about 5000. If we estimate the area of influence of volcanos like Surtsey to be about 5 km, then 20 such volcanos would be required for each 100 km stretch. If each eruption lasted for 5 years, the period between eruptions in each 100 km stretch would average about 1000 years. As at least 11 such submarine eruptions have been reported in historical time (Thorarinsson, 1964) it would seem that either our estimate of the minimum fissure flow rates are in error or melt has been supplied only intermittently to secondary chambers underlying Surtsey. Either or both of these explanations could be right. Once a localized eruption site develops it will tend to develop lower and lower impedance as it heats. On the other hand, the shift of the eruption site from Surtsey to Syrtlingur to Jolnir and back to Surtsey might indicate that separate episodes of secondary chamber filling have taken place.

While some further work will be necessary before the models which are evolving can be applied with confidence to the moon, it does seem that considerable progress towards estimation of maximum eruption frequencies of lunar basaltic volcanos has been made.

B. EXPLOSIVE ERUPTIONS

We now turn to the problem of what happens when pressure release cannot be obtained by loss of material in either solid or gaseous forms through fissures and the ultimate failure must take place by explosive ejection of the rock overlying the chamber. Although the details of the explosive behavior are obviously a complex function of the chamber geometry, liquid to gas ratio and a number of other factors, a great deal of insight may be gained by considering the greatly oversimplified model shown in Figure VI-10.

Consider a pocket of gas of volume V with surface projection A at pressure p sufficiently great that the strength of the rock has been overcome and it is starting to shoot a block thickness h_b and surface α A towards the surface. The energy required to lift the plug is

$$E = \rho g h_b^2 \alpha A \qquad \text{(VI-6)}$$

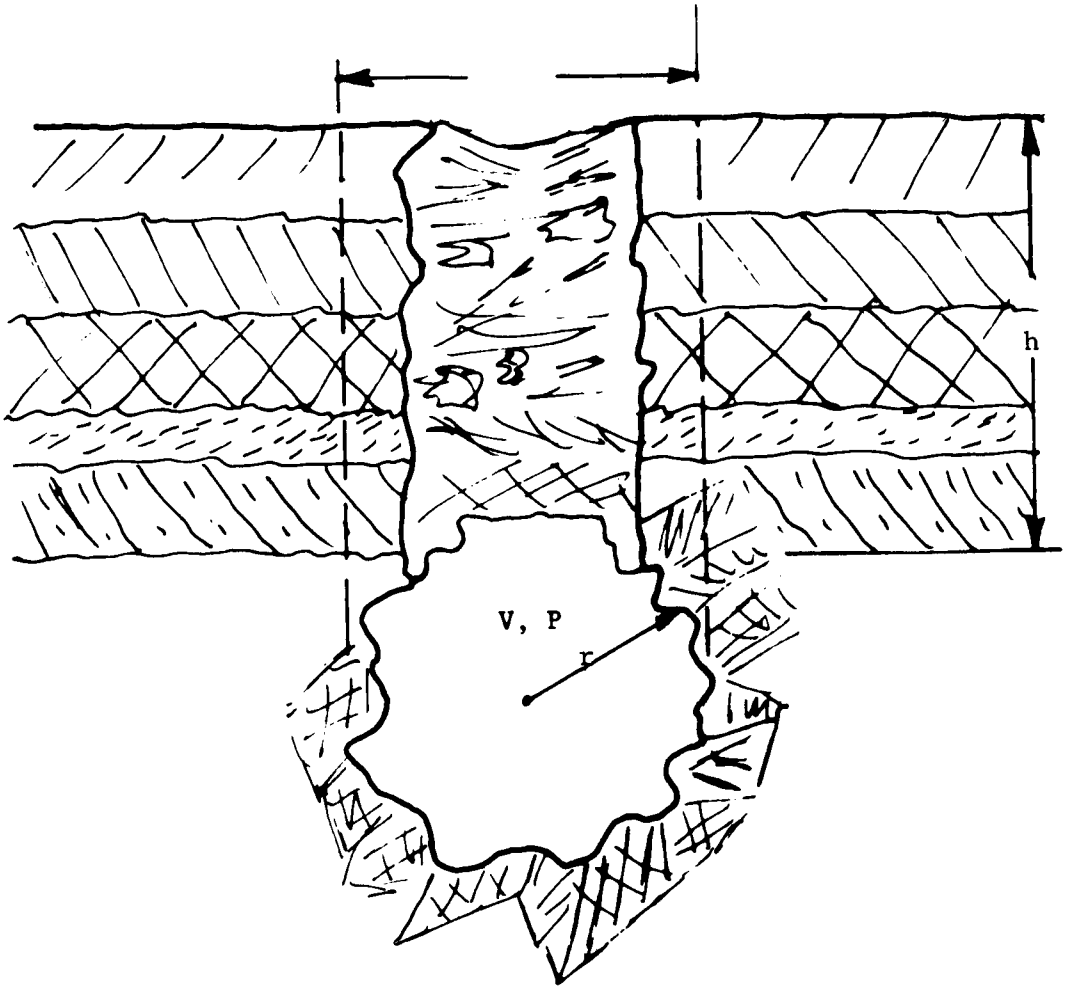

FIGURE VI-10 IDEALIZED SECONDARY MAGMA CHAMBER OF VOLUME V CONTAINING GAS AT PRESSURE P

The energy available in the chamber which could be released by adiabatic expansion of an ideal gas, would be given by

$$\frac{V}{\gamma-1}\left(p - p_o\left(\frac{p}{p_o}\right)^{1/2}\right) \qquad \text{(VI-7)}$$

where p_o is the atmospheric pressure and γ is a characteristic of the gas. If we arbitrarily define an explosive eruption to be one in which the mass of material completely clears the surface, then for such an eruption to take place the energy in the chamber would have to exceed the energy required to lift the bottom of the plug above the surface. For the purpose of our calculations it is sufficient to assume that the initial pressure in the chamber is very much greater than atmospheric pressure and Eq. (VI-6) can be reduced to

$$E = \frac{V\, p_o}{\gamma-1} \qquad \text{(VI-8)}$$

We may rewrite Eqs. (VI-6) and (VI-8) and combine them to give

$$\zeta > \frac{h\ \alpha\ A}{V}\ (\gamma-1) \qquad \text{(VI-9)}$$

where $\zeta = p/\rho gh$.

For water vapor, γ is of the order of 1.3 as long as the pressure is not too high. For a spherical chamber of radius r, the ratio A/V is $.75/r$. If failure takes place along the planes of maximum shear stress induced by the high pressure then α would equal .5. Substituting these into Eq. (VI-9) yields

$$\zeta > \frac{h}{r} \qquad \text{(VI-10)}$$

The difficulties imposed by this inequality are at once apparent. In order to obtain high pressures several conditions must be fulfilled. Among them, the fact that the depth of burial h must be considerably greater than the effective radius r of the cavity. This requires h/r values much greater

than 1. On the other hand, the weakness of the rocks makes it difficult to envisage how the ratio ζ of the pressure in the chamber to the pressure in the rocks outside (which is approximately equivalent to the overburden pressure ρgh) could ever be much greater than 2 without having the chamber fail in tension.

Several possible ways to avoid the above complications seem evident. These involve decreasing the mass to be ejected without decreasing the overburden pressure. It is clear that once a small crater exists or a cone is built up some of the weight of the pile of material beside will be transmitted laterally toward the center of the chamber. This may explain why violent explosive eruptions are not likely to occur in a region where there is no pre-existing cone or crater. Thorarinsson (1966) describes two purely explosive eruptions in which all the material expelled from the volcano was broken from the solid ground and not primary magmatic material: the eruptions of Bandai-san in Japan, 1888, and eruption Nilahue in Chile, 1955. The Bandai-san eruption was from a pre-existing andesitic cone and hence the geometry necessary for explosive eruptions was already present. This volcano had been quiet for nearly 11 centuries. Thorarinsson says "On that day, July 15, detonations were heard in nearby villages at 07h, an earthquake was felt at 07 h 30 m lasting about 20 seconds. The eruption started at 07 h 45 m. Then 15 to 20 violent explosions were heard. The blasts were directed, the last ones were nearly horizontal, directed towards north. Within an hour from its start the eruption was over. The summit area of the volcano - a mountain body of 12×10^9 m^3 - had been blasted away. No primary magma seems to have been involved, and all the material erupted or blasted away was accessory. No part of it was heated to the melting point."

In contrast to this the Nilahue eruption in Chile, July 27 - Nov. 10, 1955, which was otherwise similar to the Bandai-san eruption was from a new volcano on the western bank of the Andes chain in Chile. A marked increase in tremors preceded the eruption and two days before it was noted that the ground was hot in certain spots 2-3 km from the future vent. Thorarinsson speculates that this was probably being heated by escaping gas.

Thorarinsson says "The eruption started visibly on July 27, 1955, at about 07 h. It does not seem to have been violent in the beginning yet at 10 h the eruption column had reached 7000 m height. On the second day of the eruption a real crater had not yet been formed, the gases and tephravapor columns rose from two separate vents and not until five days after that had the crater reached its present oval shape through the merging of the two vents. Approximately 520 x 10^6 tons of tephra was ejected, roughly corresponding to the weight of the rock originally occupying the eruption pit (518 x 10^6 tons). It has been estimated by volcanologists examining this crater that 2400 km^3 of gases were released in the eruption."

"It is worth noting that even such a purely explosive eruption as this did not start with a great violence but increased gradually in vigor."

While the examples given above represent only a very small sample of the available data, they do represent two of the best observed explosive eruptions. If the observations reported are characteristic of most explosive eruptions, then they would be entirely consistent with the predictions of our model which requires that the plug of potential ejecta be relatively thin compared to the depth of the chamber if an explosive eruption is to take place. Conversely, when an explosive crater, as opposed to a collapse caldera, is found it would seem that the depth to the source can be estimated from the width, depth, and/or amount of ejecta.

The model described above is appropriate only for an ideal gas and eruptions in which the amount of gas is large compared to the amount of melt. When the two amounts are comparable or the pressure is high enough that the gas does not behave ideally, the model must be refined. As the necessary data on the gas-liquid relationships did not become available until near the end of the current program, the necessary refinement was left for future work. If, as discussed in Chapter IV, the moon contains more volatiles than the earth's mantle, then explosive eruptions of its primary magmas may be relatively more important.

VII MECHANICS OF ASH FLOWS

A. REVIEW OF PAST WORK

As the importance of ash flows as the source of many tuffs has become recognized, a great deal of attention has been paid to the mechanics of their mobilization on the earth and on the moon, mostly treating them as fluidized beds. Although it is clear that the individual cooling units vary greatly in thickness, from less than a meter to many tens of meters thick, eyewitness accounts of their emplacement are so sparce that the velocities and thickness of these flows when they are in motion is largely a matter of conjecture; Rittmann (1962) mentions only two examples. The flow resulting from the eruption of Mt. Pelée in Martinique on May 8, 1902, which destroyed the town of St. Pierre with its 29,000 inhabitants, was reported to have attained a velocity of at least 150 meters per second. A similar eruption a few months later on December 19 was estimated to have come down the mountainside, averaging about 20 meters per second, but it is not clear whether this velocity refers to the ash flow or the accompanying cloud.

The question of how such large masses of material become so mobile has been a target for several theoretical studies. It has long been known that when gas is passed through beds of particulate material with a high enough velocity, the individual particles become separated, fluidizing the entire mass so that it behaves like a low viscosity liquid. Most theoretical studies, such as those of McTaggart (1960), O'Keefe and Adams (1965), have assumed that a similar phenomenon is responsible for the mobilization of nueés ardentes.

Two sources for the gas necessary for this type of mobilization have been postulated (Figure VII-1). The first originally suggested by Anderson and Flett (1903) and later developed in more detail by O'Keefe and Adams (1965), assumes that the gas is emitted by the individual particles in sufficient abundance and causes fluidization. O'Keefe and

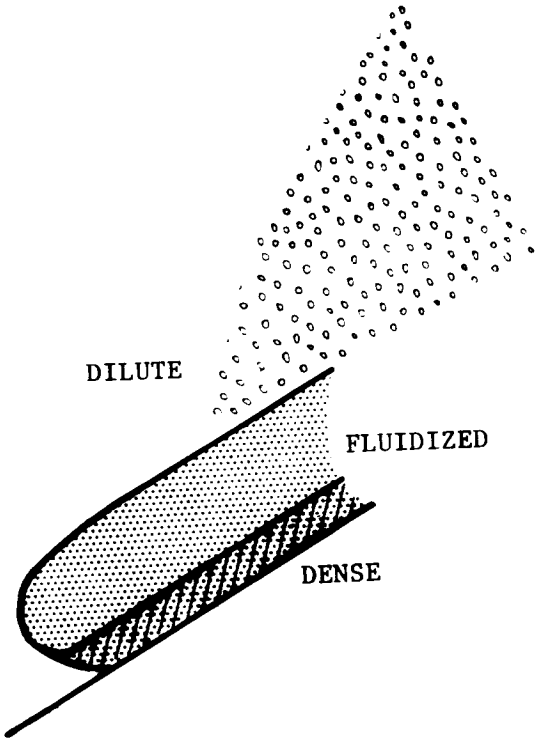

FLUIDIZATION BY GAS EMISSION

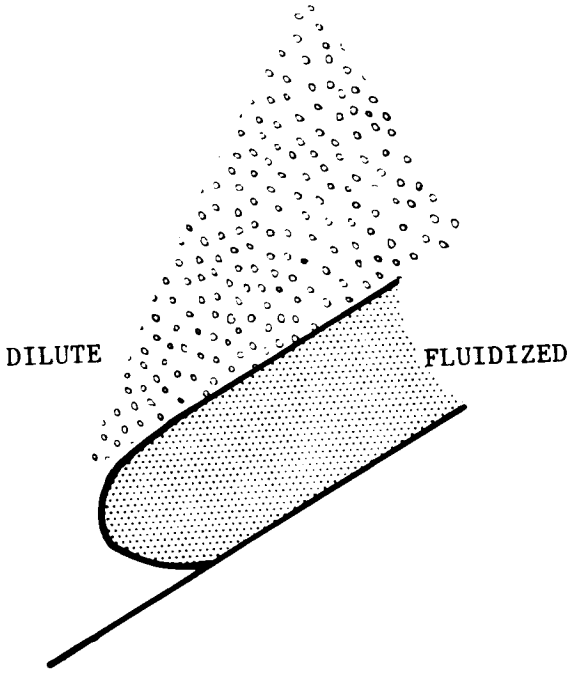

FLUIDIZATION BY HEATED AIR

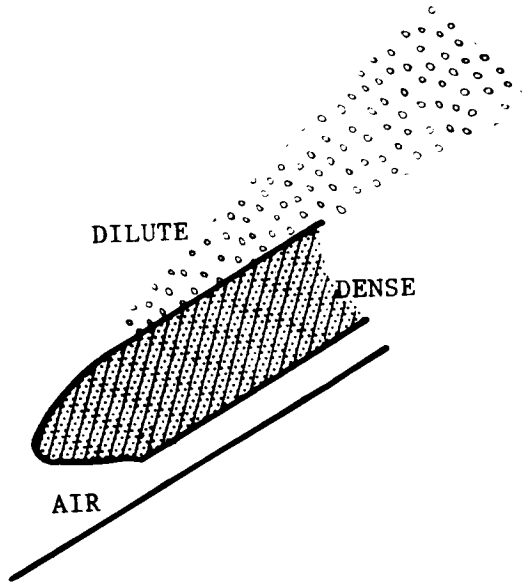

AIR CUSHION MODEL

FIGURE VII-1 COMPARISON OF VARIOUS MODELS FOR MOBILIZATION OF ASH FLOWS

Adams' analyses show clearly that each bed fluidized by this mechanism will consist of three phases: a nonfluidized phase at the base, a dense fluidized phase in the middle, and an upper disperse phase with only a few percent isolated particles rising from the top.

The second model for mobilization proposed by McTaggert (1960) involves fluidization by heating of gas entrapped by the flow while it is in motion. The theory for this has not been developed in as much detail as that for the gas emission hypothesis, but it would seem that if the gas were entrapped near the base of the flow the dense, nonfluidized, basal phase might not be necessary. While both these phenomena may be important, we would like to suggest a third phenomenon which may play a dominant role in high velocity ash flows of the type that destroyed St. Pierre, which requires neither gas emission nor gas heating.

B. LEVITATION MODEL FOR TERRESTRIAL FLOWS

Consider a mass of material of surface density of grams per square centimeter moving rapidly over the ground at a velocity v at some small height above the ground, so that part of the air in front of it becomes entrapped beneath the flow while the remainder is pushed up over the top (Figure VII-2). If we note that the air trying to flow backward under the flow will require higher pressure to overcome the increased resistance of the narrow channel, this increased resistance will force the line of separation downward from the center of the flow probably resulting in a higher velocity and lower pressure over the top of the flow, and as a result some lift may develop, i.e., the system is forced to become airfoil-like because of the presence of the lower constriction due to the ground. This can be readily demonstrated on the laboratory scale. Near the front of the flow we may define this lift in the form of a pressure difference $\Delta\rho$ between the top and bottom of the flow such that

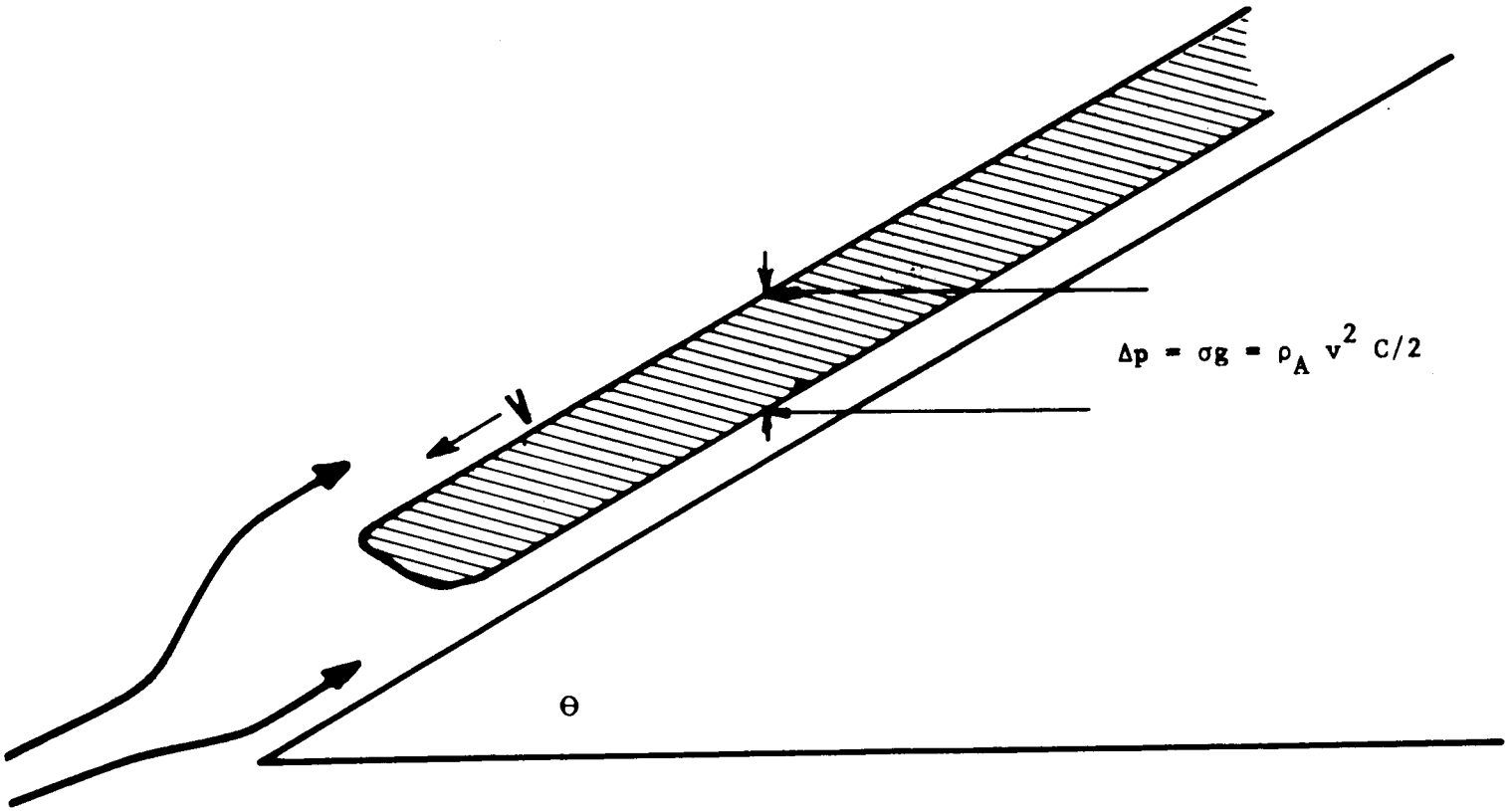

FIGURE VII-2 MODEL FOR FLOW LEVITATED BY LIFT OVER FRONT

$$\Delta\rho \equiv (1/2)\ \rho v^2\ C_L \qquad \text{(VII-1)}$$

where v is the velocity of the flow

ρ is the density of the air, and

C_L is some lift coefficient which will undoubtedly be a function of the size and shape of the flow and might even be negative in some special cases. Now we know that if the pressure difference $\Delta\rho$ becomes as great as the weight of the flow σg, the flow will become airborne, i.e., at

$$v = \sqrt{\frac{2\sigma g}{\rho C_L}} \qquad \text{(VII-2)}$$

To see at what velocities this might happen, we may take ρ to be the density of air 1.2×10^{-3} grams/cm^3 and g the gravitational acceleration to be 980 cm/sec^2 and substitute these into equation VII-1 along with appropriate lift coefficients and rearrange it to yield

$$v = 1.28 \times 10^3 \sqrt{\sigma/C_L} \qquad \text{(VII-3)}$$

Figure VII-3 shows a plot of velocity necessary for mobilization as a function of surface density for several different lift coefficients.

Quantitative experimental evidence for levitation may be readily obtained in the laboratory by flicking laminas such as playing cards, file cards, or business cards across a table or allowing them to fall down an inclined plane. In all cases the laminas develop lift and become airborne.

Similarly blowing air along a plane will levitate a stationary lamina lying on the plane. Our first experiments using the table showed that the velocity necessary for sufficient lift to be developed to make the flow essentially frictionless were of the order of 1 meter per second, indicating a lift coefficient of about 2. A similar phenomenon appears in tilted sedimentation of sand down the wall of a glass tube filled with water (Figure VII-4). The flow remains composite, exhibits lift at the front and achieves much higher velocities than in vertical

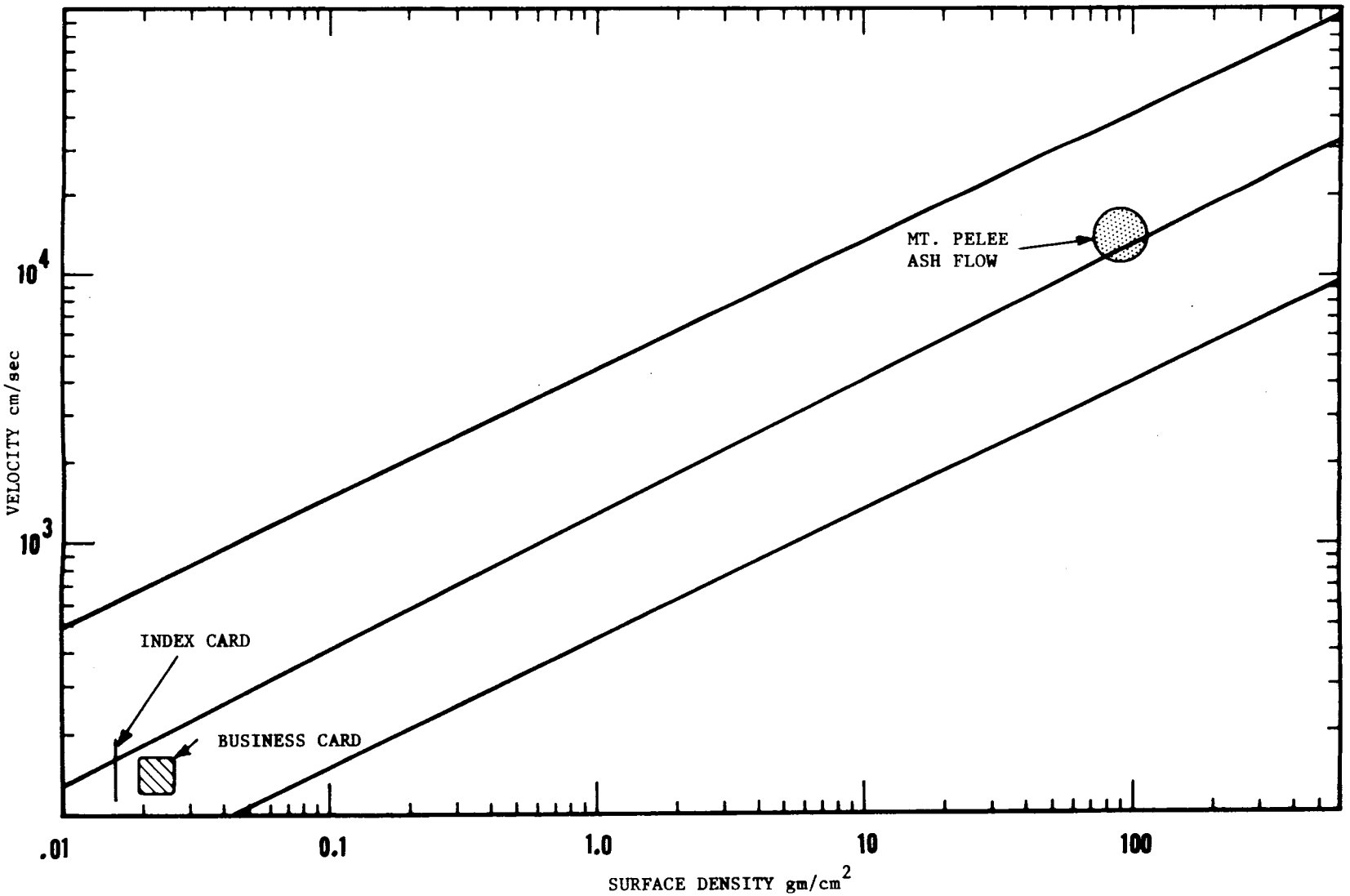

FIGURE VII-3 VELOCITY REQUIRED FOR LEVITATION IN AIR AS A FUNCTION OF SURFACE DENSITY AND LIFT COEFFICIENT. COMPARISON OF OBSERVATIONS WITH THEORETICAL CURVES.

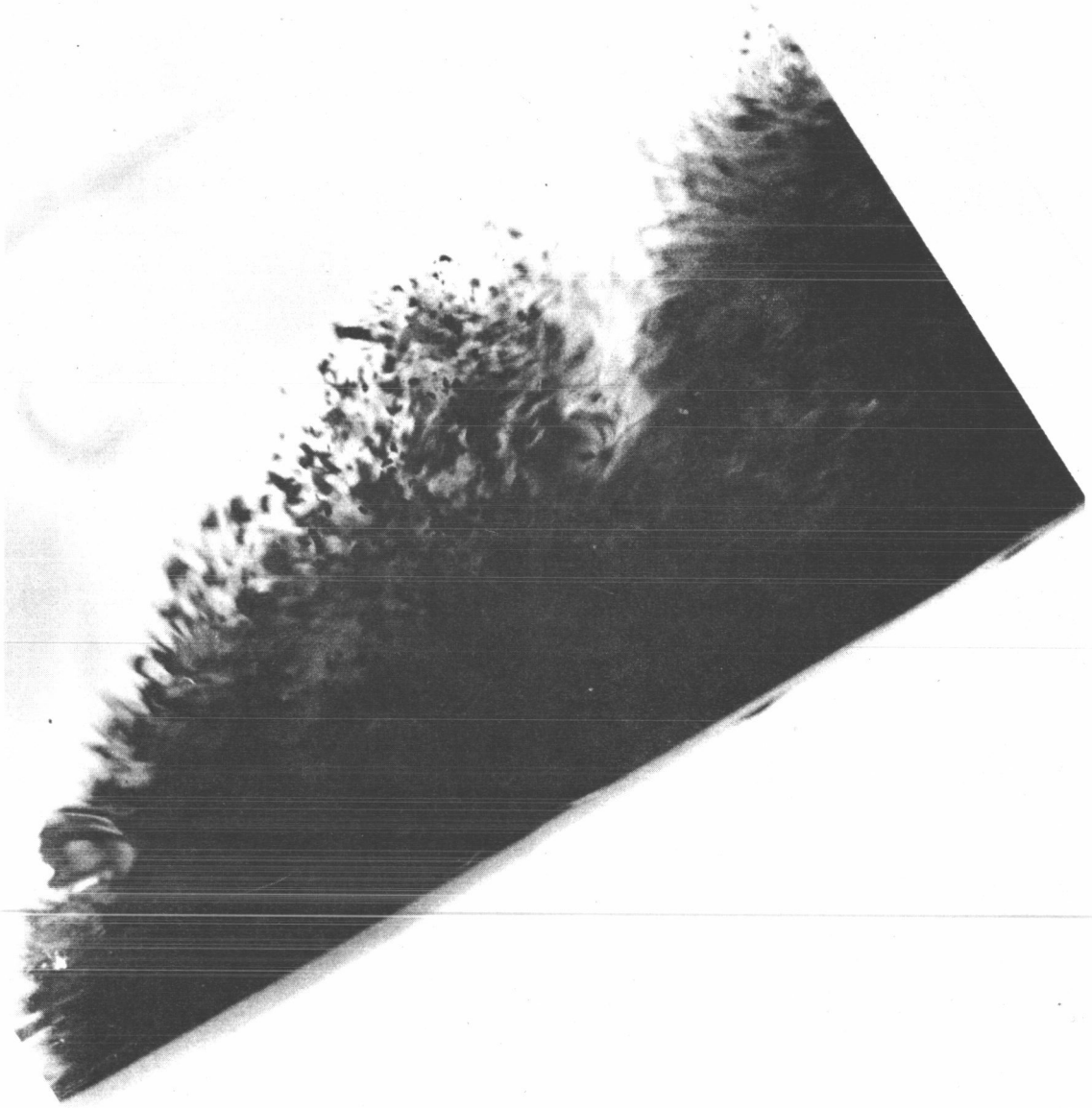

FIGURE VII-4 TILTED SEDIMENTATION OF SAND DOWN WALL OF GLASS TUBE FILLED WITH WATER SIMULATING ASH FLOW

sedimentation.

Although the concept of avalanches traveling on a cushion of air has been suggested by Shreve (1967), some circumstantial evidence that this phenomenon may also be involved in the mobilization of some thinner ash flows may be obtained by estimating the lift coefficient which might be necessary to levitate the flow which destroyed St. Pierre. The thickest deposits were of the order of .5 meters (O'Keefe and Adams, 1965). If we assume a surface density of about 100 grams/cm^2, and take the reported velocity 150 meters per second and substitute these into Eq. (VII-3), we arrive at a lift coefficient near unity (Figure VII-3). Thus at the reporced velocity a lift coefficient only half that developed in the laboratory experiment would have been sufficient for levitation suggesting that it is quite probable that the nuée ardente from Mt. Pelée was riding on a cushion of air.

C. CONCLUSIONS

If some or all ash flows of the Peléean type move on a cushion of air constricted or entrapped beneath them by the lift over the front of the flow, this would seem to have a number of implications:

1. Rather than being fluidized, the flow may move as a dense phase allowing it to easily support large boulders which are commonly observed.

2. There is no necessity for gas emission once high enough velocities are attained.

3. There is no necessity to have an immobile phase in contact with the ground.

4. The velocities observed would seem to be enough to develop a lift which would in turn explain the apparent mobilities.

5. The drag may be reduced further because of motion of the particles at the boundaries, in particular the upper boundary in the direction of the air flow. This would constitute a sort of boundary layer control analogous to the flow past a rotating cylinder which exhibits low drag and Magnus effect left.

6. The common association of nuées ardentes with horizontal explosions from the volcanic vent is consistent with the hypothesis in that the explosion provides an initial high velocity which is necessary for mobilization.

7. It is clear that this particular mechanism of mobilization requires relatively dense atmospheres and is not likely to occur on the moon.

Prediction of the likelihood of terrestrial-type ash flow occurrence on the moon requires an understanding of the relative importance of the various mobilization mechanisms on earth. For quantitative evaluation of O'Keefe's mechanism, one needs to know the rate at which volatiles are liberated from a magma. We have obtained some data which is necessary for this type of evaluation and reported in in Chapter V.

McTaggart's mechanism cannot operate on the moon but could be important on earth; however, we believe that for thin flows it may be overshadowed by the mechanism we propose. Further data and calculations along the lines indicated above are required before one can hope to predict which, if any, of the above mechanisms dominate. Conversely, we expect that if ash flows are found to occur on the moon and the significant parameters describing the distribution of material can be obtained, this will help in understanding what causes their highly destructive terrestrial counterparts.

VIII. CONCLUSIONS

A. IMPLICATIONS FOR LUNAR EXPLORATION

Although some of our studies are incomplete, they have already indicated a number of ways in which the nature of volcanism on the moon should be considerably different from that on the earth. These differences have scientifically important implications since they suggest where studies of particular lunar features can contribute enormously to understanding volcanic activity on the earth by providing tests for currently proposed mechanisms of such activity. Thus from measurements on features whose controlling mechanisms we understand, or are attempting to understand, we will learn more about the thermal and volcanic history of both the moon and the earth.

In the course of our work to date we have generated a number of definite ideas about specific lunar samples and observations which we believe will be scientifically rewarding. Although initial opportunities for sample selection and geological observations will be limited, we feel that NASA should be aware of the implications of suggested measurements so that when opportunities to choose among different samples and observations present themselves, those which will be most scientifically significant will be selected.

There are four types of material that the astronauts might be expected to encounter: lava flows, ash flows, unsorted lunar debris, and gas or vapor emissions. We will consider them in turn.

1. Lava Flows

By the time the landing site for the Apollo missions has been selected, data obtained from orbiters and unmanned landers will have provided a good idea of the morphological features to be encountered. If extensive lava flows appear to be present, the following parameters should be obtained.

a. The relative areal extent of each individual flow should be noted as well as the thickness, length of the fissure from which it came, the type of terrain over which it moved, and its stratigraphic position relative to the other flows. Most of this can probably be accomplished before a manned landing.

b. Compositional information about hugh lava flows is most important for determining the composition of the moon's interior, its thermal history, and the depth of melting; the massive lava flows are most likely to have come directly from the deep interior. Thus, in selecting samples it is important to choose representative ones from massive lava flows. An exception would be a sample from such flows that contain xenoliths; these could be particularly valuable for the purpose of providing information on the mantle composition in view of the studies discussed in Chapter III.

The volume of the large flows compared with the rate of magma generation calculated from compositional data will enable an estimation of the frequency of flows in much the way we treated the mid-Atlantic ridge in Chapter VI. Conversely, if samples are obtained from two nearby flows of large dimensions, it should be possible to make age determinations on them and thus infer the rate of magma generation. As the rate of generation, the flow frequency, and the internal composition are related quantities, the observations and compositional data must fit a self-consistent model.

On the basis of our discussion in Chapter III on the origin of magmas and our estimates of the depth of melting on the moon in Chapter IV, we have predicted that lunar magmas will be most similar to submarine basalts or basaltic achondrites in composition. The compositions found for lunar magmas will test this model.

c. If one can estimate the width of dikes from which the flows are coming one can derive the duration of a flow and its viscosity in a manner analogous to that used for the Laki eruption in Chapter VI.

d. Smaller lava flows, particularly those erupted from central volcanos, are more likely to have been derived from secondary chambers than the larger ones. We consider sampling of these flows of secondary importance.

However, when samples from these can also be obtained and compared with those from the larger flows, the degree of differentiation and the mineral assemblages found will provide an estimate of the importance of secondary chambers in lunar volcanic activity.

2. Ash Flows

We now turn to the problem of ash flows. If lunar deposits are found which are similar to terrestrial ash flows, they can provide important information both on the mechanism of terrestrial ash flows and on the composition of the lunar interior.

We have pointed out in Chapter VII that two proposed mechanisms of ash flow mobilization depend on the presence of an atmosphere while one mechanism requires only gas emission from the ash itself. Any ash flows observed on the moon can only have been mobilized by the gas emission. Their existence should provide a measure of the relative significance of the different mechanisms on the earth. Although further theoretical work along these lines is still required, we believe that even if it is impossible to sample the flow, its thickness, length, and the slope down which it traveled contains useful information on eruption conditions.

If the composition of the flow material turns out to be considerably more basic than terrestrial ash flows, it may be evidence that the volatile content of the lunar interior is higher than that of the earth's mantle or alternatively, it may simply be an effect of the lower lunar pressure. A better theoretical understanding of the relative importance of these two possibilities would seem to be the only way to separate them.

3. Debris Sampling

Initial astronaut landings are likely to be in regions containing only unsorted debris resulting from continual reworking of underlying rocks by meteorite bombardment. Even in the absence of volcanic rocks we believe that if volcanic activity has occurred, evidence for it will be present in the debris.

We have shown in Chapter V that vapor condensates make up a large fraction of smoke particles produced by volcanos. On the moon we expect that, to a degree, similar particles will be produced in the throats of lunar volcanos, but because of the lack of an atmosphere condensation of a portion of the lava vapors would also occur on the moon's surface hundreds of km from the vent. Because of the apparently diagnostic characteristics of the vapor condensates, they should be clearly identifiable even when mixed with large amounts of fragmentary material. If the rate of meteorite impacts is low enough, a thin layer of condensates might exist at this moment on the surface. We believe special effort should be made to look for this evidence of volcanic activity.

4. Atmospheric Sampling

If volcanic activity is taking place on the moon today, it will undoubtedly contribute to the formation of a tenuous atmosphere. From analysis of such an atmosphere one could, in principle, put limits on the intensity of the activity. In the unlikely event that the astronaut lands near an active fumarole, it would be of advantage to obtain samples of any gases being emitted. If this is not possible, either through difficulties in gas sampling or because the vent is inactive, a careful search should be made to find particulate matter which might represent vapor condensates. Such condensates would probably provide important information on the nature of the underlying magma and thus on the stage of lunar evolution.

B. SUGGESTIONS FOR FURTHER WORK

We believe that theoretical studies together with directed experimental work such as described in this report can provide valuable insights into the type of observations and samplings which the astronauts should complete on the moon. In addition, such detailed studies will ensure a more rapid interpretation of unexpected findings. Thus, studies of this nature will make more certain a scientifically profitable exploration of the moon within the extreme time and equipment limitations prevailing. In our opinion a number of additional investigations in various areas of the problem of magma generation, migration, and crystallization are required at this time.

1. Magma Generation

It is extremely important to carry out an experimental study of distribution constants as a function of pressure in order to confirm or deny the hypothesis developed in Chapter III to explain the observed terrestrial variations in magma compositions. At the same time, theoretical studies should be extended to determine whether the existing lead and strontium isotope data are consistent with the model developed in Chapter III.

If the above studies confirm our present hypothesis, it will be possible to uniquely establish the pressures at which magmas originate, whether on the earth or on the moon. In addition, the trace element distribution and content in ultramafic zenoliths will provide clues as to their depth of origin and thus increase our understanding of mantle composition. We believe that the Manned Spacecraft Center has facilities for the high pressure and analytical work required to carry out this experimental program, and we feel that they should give serious consideration to making these measurements. Because of our background in the study to date we would propose to complete the theoretical work ourselves.

During this year's program we have presented evidence for the necessity of revising the model of the earth's mantle based on the expected change in distribution constants with depth. The present computer programs

for the thermal history of the moon should be altered to test implications of this revised composition for the quantity and rate of magma generation, and their consistence with terrestrial heat flow.

In addition, the hypothesis that the moon is more like carbonaceous chondrites in composition should be tested by examining the implications for thermal history and magma generation.

To properly carry out the thermal history calculations the radiative transfer study should be completed to provide needed data on olivine and other mantle materials. These studies have already provided strong evidence that the increase in absorption coefficient with temperature in silicates will act to decrease the radiative conduction substantially below that predicted from room temperature spectra (Aronson, et al. (1967a, b).

2. Magma Migration

Further study is required on the break-out mechanism and the mechanics of secondary magma chamber formation. By combining the data on volatiles that we have obtained this year with the models which we have been developing for magma chamber mechanics we expect to be able to determine to what extent subsurface structure can be inferred from surface ejecta. This work will involve further development of the quantitative models for the break-out mechanism and further study of the factors controlling the formation of sills, secondary magma chamber, and calderas. Successful completion of this work should result in our being able to put limits on the ratio of extrusive to intrusive igneous activity from the composition of surface flows.

3. Magma Crystallization

During the present contract period we have collected and developed much of the background information on gas content and vaporization behavior required for quantitatively describing volcanic behavior as magma reaches the surface. We have not had time to resolve the question of electrical effects associated with volcanism. This work should be completed and the quantitative model developed.

The work during this period indicated that the fume particles derived from volcanism contained relatively large quantities of chromium and nickel, which occur as trace quantities in magma. In addition, the particles had surprisingly unique compositions. We feel that the particle analysis program should be continued to determine to what extent the particles formed may differ at different stages of volcanism; the particle compositions may prove useful as a measure of the state of the magma from which they are derived. Finally, this program should be continued to clearly establish to what extent lunar surface particles can be used as a criteria of volcanic activity.

ACKNOWLEDGMENTS

This report was prepared by the Research and Development Division of Arthur D. Little, Inc., and covers work carried out under Contract NAS9-5839 during the period March 25, 1966 to June 30, 1967. The work was administered by the National Aeronautics and Space Administration, Manned Spacecraft Center with Dr. David S. McKay as Contract Monitor. In addition to those listed as authors, the following persons made invaluable contributions to the study: J. R. Aronson, M. Bowden, F. Eden, B. Peatie, and N. F. Surprenant. Dr. S. Thorarinsson of the Museum of Natural History, Reykjavik, Iceland provided much data, published and unpublished, on the quantitative behavior of volcanos.

REFERENCES

Aki, K (1967), personal communication.

Anderson, D.L. (1964), Universal Dispersion Tables 1. Love Waves Across Oceans and Continents on a Spherical Earth: Bull Seism. Soc. Am. 54, pp. 681-726.

Anderson, D.L. and O'Connell, R. (1966),"Viscosity of the Earth,"Geophys. J.Roy. Astron. Soc. 13.

Anderson, D.L., and Toksöz, M.N. (1963),"Surface Waves on a Spherical Earth. I. Upper Mantle Structure from Love Waves,"J. Geophys. Res. 68, pp. 3483-3500.

Anderson, E.M. (1951),"The Dynamics of Faulting and Dyke Formation with Applications to Britain,"Ediburgh, Oliver and Boyd.

Anderson, Tempest, and Flett, J.S. (1903), Report on the Eruptions of the Soufrière in St. Vincent in 1902, and on a Visit to Montagne Pelée in Martinique, Part 1, Royal Soc. (London) Philos. Trans. Ser. A, 200, pp. 353-553.

Aronson,J.R., Emslie, A.G., McConnell, R.K., Eckroad, S.W., von Thüna,P.C., (1967a),"The Application of High Temperature Radiative Thermal Conductivity of Minerals and Rocks to a Model of Lunar Volcanism," Final Report to NASA, Manned Spacecraft Center, Houston,Tex.,May 1967.

Aronson, J.R., Eckroad, S.W., Emslie, A.G., McConnell, R.K., Jr., and von Thüna, P.C. (1967b)," Radiative Thermal Conductivity in Planetary Interiors,"to be published.

Bailey, (Sir) E.B., and Wilson, G.V. (1924), Tertiary and Post-Tertiary Geology of Mull, Loch Aline and Oban, Mem. Geol. Surv. p.360.

Bergsten, F. (1930), Changes of Level on the Coasts of Sweden, Geografiska Annaler, pp. 21-55.

Bikerman, J.J. (1953), Foams, Reinhold, New York.

Billings, M.P. (1954), Structural Geology, Prentice-Hall.

Bjornsson, S. (1966), Surtsey Progress Report II, p. 97.

Bodvarsson, G., and Walker, G.P.L. (1964),"Crustal Drift in Iceland," Geophys. J. Roy. Astron. Soc. 8, pp. 285-300.

Brace, W.F., Paulding, B.W., Jr., and Scholtz, C. (1966),"Dilatancy in the Fracture of Crystalline Rocks,"J. Geophys. Res. 71, #16, pp. 3939-3953.

Bradley, R.S. (1963), High Pressure Physics and Chemistry, 2, Chapter 2, "Applications of High Pressure Studies to the Earth Sciences," by Peter J. Wyllie, Academic Press.

Brewer, L., Somayajulu, and Brackett, E. (1963), "Thermodynamic Properties of Gaseous Metal Dihalides," Chem. Rev. 63, pp. 111-121.

Brocas, J. and Picciotto, E. (1967), "Nickel Content of Antarctic Snow: Implications of the Influx Rate of Extraterrestrial Dust," J. Geophys. Res. 72, pp. 2229-2236.

Cable, M. (1966),"Kinetics and Mechanisms of Fining Glasses,"J. Am. Ceram. Soc. 49, p. 436.

Carslaw, H.S., and Jaeger, J.C. (1959), Conduction of Heat in Solids, Oxford, Clarendon Press.

Centolanzi, F.J., and Chapman, D.R. (1966)," Vapor Pressure of Tektite Glass and its Bearing on Tektite Trajectories Determined from Aerodynamic Analysis,"J. Geophys. Res. 71, p. 1735.

Clark, S.P., Jr. (1966), Handbook of Physical Constants, Geolog.Soc. Am.

Dewing, E.W. (1967) "Gaseous Complexes between Dichlorides and Trichlorides of Aluminum and Iron," Nature 214, p. 483.

Drickamer, H.G., Lynch, R.W., Clendemen, R.L., and Perez-Albuerne (1966), Solid State Physics, "X-Ray Diffraction Studies of the Lattice Parameters of Solids Under Very High Pressures," 19, p. 135, Academic Press.

Eaton, J.P. and Murata, K.J. (1960),"How Volcanoes Grow,"Science 132, p.925.

Elliott, G.R.B. (1952), "Gaseous Hydrated Oxides, Hydroxides, and Other Hydrated Molecules," Thesis submitted to Univ. of California, Berkeley and issued as Report UCRL-1831, by the Radiation Lab of the Univ. of Calif.

Ellis, A.J. (1957), Chemical Equilibrium in Magmatic Gases, Am. J. of Sci. 255, pp. 416-431.

Engel, A.E.J., Engel, C.G., and Havens, R.G. (1965), Chemical Characteristics of Oceanic Basalts and the Upper Mantle, Geolog. Soc. Am. Bull. 76, pp. 719-734.

Erlank, A.J., and Hofmeyer, P.K. (1966), K/Rb and K/Cs Ratios in Karroo Dolerites from South Africa, J. Geophys. Res. 71, pp. 5439-5445.

Euler, R., and Winkler, H.G.F. (1957),"Viscosity of Rock and Silicate Melts,"Glastech. Ber. 30, pp. 325-332.

Faile, S.P., and Roy, D.M. (1966),"Solubilities of Ar, N_2, CO_2 and He in Glasses at Pressures to 10 Kbars,"J. Am. Ceram. Soc. 49, pp.638-643.

Flint, R.F. (1957), Glacial and Pleistocene Geology, John Wiley & Sons, New York.

Fotheringham, J. (1920),"Secular Accelerations of Sun and Moon as Determined from Ancient Lunar and Solar Eclipses, Occultations, and Equinox Observations," Monthly Notices, Roy. Astron. Soc. 80,p.578.

Frey, F.A., and Haskin, L.A. (1964),"Rare Earths in Oceanic Basalts," J. Geophys. Res. 69, pp. 775-780.

Gast, P.W. (1965),"Limitations on the Composition of the Upper Mantle," Science 147, pp. 858-860.

Glemser, O., and Mueller, A. (1964), "Gaseous Hydroxides VIII, Gaseous Chromium Hydroxide," Z. Anorg. Allgem. Chem. 334, pp. 150-154.

Gordon, R.B. (1965),"Diffusion Creep in the Earth's Mantle," J. Geophys. Res. 70, pp. 2413-2418.

Green, D.H., and Ringwood, A.E. (1963),"Mineral Assemblages in a Model Mantle Composition,"J. Geophys. Res. 68, pp. 937-945.

Grove, C.S., Jr., Wise, G.E., Jr., Marsh, W.C., and Gray, J.B. (1951), "Viscosity of Fire-Fighting Foam," Ind. Eng. Chem. 43, pp.1120-1122.

Gunn, B.M. (1965), "K/Rb and K/Ba Ratios in Antarctic and New Zealand Tholeiites and Alkali Basalts," J. Geophys. Res. 70, pp. 6241-6247.

Gutenberg, B. (1941),"Changes in Sea Level, Postglacial Uplift, and Mobility of the Earth's Interior," Geolog. Soc. Am. Bull. 52, pp. 721-772.

Hamilton, D.L., Burnham, C.W., and Osborn, E.F. (1964), "The Solubility of Water and Effects of Oxygen Fugacity and Water Content on Crystallization in Mafic Magmas," J. Petrol. 5, pp. 21-29.

Haskell, W.A. (1937), "The Viscosity of the Asthenosphere," Am. J. Sci. 33, pp. 22-28.

Haskin, L.A., and Gehl, M.A. (1962), "The Rare-Earth Distribution in Sediments," J. Geophys. Res. 67, pp. 2537-2541.

Hayward, A.T.J. (1962), "The Viscosity of Bubbly Oil," J. Inst. Petrol. 48, p. 156.

Heiskanen, W.A., and Vening Meinesz, F.A. (1958), "The Earth and its Gravity Field," McGraw-Hill, New York.

Heir, K.S., Compston, W., and McDougall, I. (1965), "Thorium and Uranium Concentrations, and the Isotopic Composition of Strontium in the Differentiated Gasmanian Dolerites," Geochimica et Cosmochimica Acta 29, pp. 643-659.

Hier, K.S., McDougall, I., and Adams, J.A.S. (1964), "Thorium, Uranium, and Potassium Concentrations in Hawaiian Lavas," Nature 201, pp. 254-256.

Hier, K.S., and Rogers, J.J.W. (1963), "Radiometric Determination of Thorium, Uranium, and Potassium in Basalts and in Two Magmatic Differentiation Series," Geochimica et Cosmochimica Acta 27, pp. 137-154.

Jacobs, J.A., Russell, R.D., and Wilson, J. T. (1959), Physics and Geology, McGraw-Hill, New York.

Jeffreys, H. (1963), "On the Hydrostatic Theory of the Figure of the Earth," Geophys. J. 8, pp. 196-202.

Jordan, A.S. (1965), "Some Volatile Hydroxides of Molybdenum, Cobalt, and Nickel," Thesis submitted to the Univ. of Pennsylvania.

Kääriäinen, E. (1949), "Beitrage zur Landhebung in Finnland," Veroff. des Finn. Geod. Instit. Nr. 36, pp. 91-94.

Kääriäinen, E. (1953), "On the Recent Uplift of the Earth's Crust in Finland," Publ. Finn. Geod. Instit. 42.

Kaula, W.M. (1966), "Teseral Harmonics of the Earth's Gravitational Field from Camera Tracking of Satellites," J. Geophys. Res. 71, pp. 4377-4388.

Kuno, H. (1960), "High Alumina Basalt," J. Petrol. 1, pp. 121-145.

Kushiro, I, and Kuno, H. (1963), "Origin of Primary Basalt Magmas and Classification of Basaltic Rocks," J. Petrol. 4, pp. 75-89.

Kushiro, I. (1965), "The Liquidus Relations in the Systems Forsterite-$CaAl_2SiO_6$-Silica and Forsterite-Nepheline-Silica at High Pressures," Yearbook 64, Carnegie Insti., Washington, p.103.

Langseth, M.G.,Jr., LePichon, X, and Ewing, M. (1966), "Crustal Structure of the Mid-Ocean Ridges," J. Geophys. Res. 71, #22, pp. 5321-5355.

Lessing, P., Decker, R.W., and Reynolds, R.C., Jr. (1963), "Potassium and Rubidium Distribution in Hawaiian Lavas," J. Geophys. Res. 68, pp. 5851-5855.

MacDonald, G.J.F. (1959), "Calculations on the Thermal History of the Earth," J. Geophys. Res. 64, pp. 1967-2000.

MacDonald, G.J.F. (1963), "The Deep Structure of Oceans and Continents," Rev. Geophys. I, pp. 587-665.

MacDonald, G.J.F. (1964), "Dependence of the Surface Heat Flow on the Radioactivity of the Earth," J. Geophys. Res. 69, pp. 2933-2946.

MacDonald, G.J.F. (1966), "The Figure and Long Term Mechanical Properties of the Earth," in Advances in Earth Science, P.M. Hurley, editor, M.I.T. Press, Cambridge.

Mason, B. (1962), Meteorites, John Wiley & Sons, New York.

McConnell, R.K., Jr.(1963), "The Viscoelastic Response of a Layered Earth to the Removal of the Fennoscandian Ice Sheet," Ph.D. Thesis, University of Toronto.

McConnell, R.K., Jr.(1965), "Isostatic Adjustment in a Layered Earth," J. Geophys. Res. 70, pp. 5171-5188.

McConnell, R.K., Jr.(1967), "Viscosity of the Earth's Mantle," in Proceedings of the Conference on the History of the Earth's Crust, in Press.

McConnell, R.K., Jr., McCaline, L.A., Lee, D.W., Aronson, J.R., and Allen, R.V. (1967), "A Model for Planetary Igneous Differentiation," Rev. Geophys. 5, pp. 121-172.

McKenzie, D.P. (1966), "The Viscosity of the Lower Mantle," J. Geophys. Res. 71, pp. 3995-4010.

McTaggart, K.C. (1960), "The Mobility of Nuées Ardentes," Am. J. Sci. 258, pp. 369-382.

Moore, J.G. (1965), "Petrology of Deep-Sea Basalt Near Hawaii," Am. J. Sci. 263, pp. 40-52.

Morgan, J.W., and Lovering, J.F. (1965), "Uranium and Thorium Abundances in the Basalt Cored in Mohole Project (Guadalupe Site)," J. Geophys. Res. 70, pp. 4724-4725.

Morgan, J.W., and Lovering, J.F. (1967), "Uranium and Thorium Abundances in Carbonaceous Chondrites," Nature 213, pp. 873-875.

Muir, I.D., and Tilley, C.E. (1964), "Basalts from the Northern Part of the Rift Zone of the Mid-Atlantic Ridge," J. Petrol. 5, pp.409-434.

Muir, I.D., and Tilley, C.E. (1966), "Basalts from the Northern Partof the Mid-Atlantic Ridge. II. The Atlantis Collections Near 30°N," J. Petrol. 7, pp. 193-201.

Munk, W.H., and MacDonald, G.J.F. (1960), The Rotation of the Earth, Cambridge University Press, New York.

Naughton, J.J. (1953), "Solubility of H_2 in Pyrex Glass," J. Appl. Phys. 24, pp. 499-500.

Newbury, R.S. (1965), "Vapor Species of the Barium-Oxygen-Hydrogen System," Thesis submitted to the Univ. of California, Berkeley.

Niskanen, E. (1939), "On the Upheaval of Land in Fennoscandia," Annales Academiae Scientiarum Fennicae, Ser. A, 53, No. 10, pp. 1-30.

O'Keefe, J.A., and Adams, E.W. (1965), "Tektite Structure and Lunar Ash Flows," J. Geophys. Res. 70, pp. 3819-3829.

Orowan, E. (1965), "Convection in a Non-Newtonian Mantle, Continental Drift, and Mountain Building," Philos. Trans., Roy. Soc. London, Ser. A, 258, pp. 284-313.

Richey, J.E. (1939), "The Dykes of Scotland," Trans. Edin. Geol. Soc. 13, p. 393.

Ringwood, A.E. (1966), "Genesis of Chondritic Meteorites," Rev. Geophys. 4, pp. 113-175.

Rittmann, A. (1962), "Volcanoes and Their Activity," Interscience, New York.

Sauramo, Matti (1955), "Land Uplift with Hinge Lines in Fennoscandia," Suom. Tiedeakat. Toimit., Series A, III , Geol.-Geog. 44, 22 pp.illus.

Sauramo, Matti (1958),"Die Geschichte Der Ostsee," Suom. Tiedeakat. Toimit., Series A, III, Geol.-Geog. 51.

Schäfer, H. (1964), "Chemical Transport Reactions," Academic Press, New York and London.

Schilling, J.G. (1966), Rare Earth Fractionation in Hawaiian Volcanic Rocks, Ph.D. Thesis submitted to Mass. Institute of Technology.

Schilling, J.G. and Winchester, J.W. (1966), "Rare Earths in Hawaiian Basalts," Science 153, pp. 867-869.

Schmidt, R.A., Smith, R.H., Lasch, J.E., Mosen, A.W., Olehy, D.A., and Vasilevskis, J. (1963), "Abundances of the Fourteen Rare-Earth Elements, Scandium, and Yttrium in Meteoritic and Terrestrial Matter," Geochim. et Cosmochim. Acta 27, pp. 577-622.

Schmidt, R.A., Smith, R.H., and Olchy, D.A. (1964), "Rare-Earth, Yttrium, and Scandium Abundances in Meteoritic and Terrestrial Matter - II," Geochim. et Cosmochim. Acta 28, pp. 67-86.

Shaw, Herbert R. (1963), "Obsidian - H_2O Viscosities at 1000 and 2000 bars in the Temperature Range 700°-900°C," J. Geophys. Res. 68, pp.6337-6343.

Shoemaker, E.M. (1966), "The Lunar Surface," U.S.Geological Survey, presented at AIAA 3rd Annual Meeting and Technical Dislay, Boston, Mass., Nov. 30, 1966.

Sigvaldson, G.E., and Elisson, G. (1966), Surtsey Progress Report II, p.93.

Sirén, A. (1951), "On Computing the Land Uplift from the Lake Water Level Records in Finland,"Hydrografisen Toimiston Tiedonantoja XIV, p.1-182.

Steuber, A.M., and Murthy, V.R. (1966), "Strontium Isotope and Alkali Element Abundances in Ultramafic Rocks," Geochim. et Cosmochim. Acta 30, pp. 1243-1259.

Sugden, T.M., and Schofield, K. (1965), "Heats of Dissociation of Gaseous Alkaline Earth Dihydroxides," Trans. Faraday Soc. 62, pp. 566-575.

Takeuchi, H., and Hasegawa, Y. (1965), "Viscosity Distribution within the Earth," Roy. Astron. Soc. Geophys. J. 9, No. 5, pp. 503-508.

Tatsumoto, M, Hedge, C.E., and Engel, A.E.J.(1965), "Potassium, Rubidium, Strontium, Thorium, Uranium, and the Ratio of Strontium-87 to Strontium-86 in Oceanic Tholeiitic Basalt," Science 150, pp.886-888.

Thorarinsson, Sigurdur (1964), Surtsey, The New Island in the North Atlantic, Almenna bókafilagio.

Thorarinsson, Sigurdur (1965), Personal communication.

Tilton, G.R., and Reed, G.W. (1963) in Earth Sciences and Meteorites, J. Geiss and E. D. Goldberg, Eds. (Interscience) New York.

Toksoz, M. Nafi, Chinnery, Michael A., and Anderson, Don L. (1967), "Inhomogenieties in the Earth's Mantle," Geophys. J., in press.

Vine, F.J. (1966), "Spreading of the Ocean Floor, New Evidence," Science 154, pp. 1405-1415.

Vonnegut, B., McConnell, R.K.,Jr., and Allen, R.V. (1966), "Evaporation of Lava and its Condensation from the Vapor Phase in Terrestrial and Lunar Volcanism," Nature 209, pp. 445-448.

Wang, C.Y. (1966), "Earth's Zonal Deformations," J. Geophys. Res. 71, pp. 1713-1720.

Wells, A.F. (1962), Structural Inorganic Chemistry, Oxford Univ. Press.

Wendlandt, H.G., and Glemser, O. (1963), "Reaction of Oxides with Water at High Pressures and Temperatures," Angew. Chem. 75, pp. 949.

Weyl, W. (1931), "Reactions of CO_2 with Silicates Under High Pressure," Glastech. Ber. 9, pp. 641-660.

White, D.E., and Waring, G.A. (1963), Chapter K, "Volcanic Emanations," in Data of Geochemistry, published by U.S.Govt. Printing Office, Washington.

Wollard, G.P. (1962), "The Land of the Antarctic," Sci. Am. 207, No. 3 pp. 151-166.